GEMBEDDING INTEGRATED RFID SENSORS INTO FIBER REINFORCED PLASTICS DURING THE MANUFACTURING PROCESS

by

BILLY JOE GRAY

Presented to the Faculty of the Graduate School of

The University of Texas at Arlington in Partial Fulfillment

of the Requirements

for the Degree of

DOCTOR OF PHILOSOPHY

THE UNIVERSITY OF TEXAS AT ARLINGTON

August 2015

Acknowledgements

“At the end of the day, you got to be able to look yourself in the mirror and know that you led a life worth living. That you gave more than you took. That you actually added something to society, to humanity, to our country based on the time that you’re on this planet.” – Larry Vickers 26 MAR 2015

To all who have helped me, counseled me, shared my burdens, given me inspiration, or just provided an encouraging remark, thank you!

Late at night, the most patient ear I had was God’s. I never heard a reply, simply the urge to continue on the path.

To my wife, Tisha Gray, thank you for taking care of me. Even though I think you questioned my sanity and that of my advisor, you stood by me and tried to keep me focused.

To my advisor and friend Dr. Erick Jones, I think you are insane. I know you kept saying, “When you’re around crazy all of the time, you think crazy.” You kept me crazy. Thank you for mentoring me and pushing down the path, even when it wasn’t one I necessarily wanted to go down. To my committee members, Dr. Jaime Rogers, Dr. Gloria Fragoso, and Dr. John Priest, thank you for agreeing to serve on my committee and providing feedback on my work.

To my children, Anna and Joseph (Bailey), you’ve had to do the best without a father there all of the time. I hope this makes you proud and helps see that you can achieve your dreams. To my parents Mary and Jerry Gray, thanks for always being there.

For my co-workers at Tarleton, you’ve been the most understanding since you’ve been there or are there with me. Especially I’d like to thank Dr. George Mollick, who has dealt with my lack of understanding and who has helped me cope with the Ph.D. process.

To my students, thanks for understanding that there is something strange going on while I've been on this journey.

For my co-workers at S-TEC, thanks for your support and for being my guinea pigs and letting me work ideas out. I'm a better professor for it and I understood much more because of it.

To my fellow Ph.D. students, Dr. Maurice Cavitt, Dr. Vettri Gnaneswaren, Dr. Ida Lumintu, Dr. Restu Sunarto-Bussey, Dr. Shernette Kydd, Jairo de Jesus, Sam Okate, Soma Sekar Balasubmaranian, and Shalini Gupta, thanks for showing me the ropes and walking the path with me.

For all of my friends, thanks for hanging out with me when I needed it and checking in on me. And especially thanks for understanding why I haven't always been around. There is huge party coming.

And for anyone that feels left out, thank you too. Like I said at the beginning, there is no way that this is truly an individual accomplishment. And I know I couldn't have gotten here without help from others.

June 29, 2015

Abstract

EMBEDDING INTEGRATED RFID SENSORS INTO

FIBER REINFORCED PLASTICS DURING

THE MANUFACTURING PROCESS

Billy Joe Gray, PhD

The University of Texas at Arlington, 2015

Supervising Professor: Erick C. Jones

This research evaluates the impact of embedding a Radio Frequency Identification (RFID) tag into the structure of a fiber reinforced polymer (FRP). The first portion of the research evaluates the mechanical impacts of embedding the tag through simulation of the stresses that the polymer will be exposed to and then comparing with compression and shear testing of the polymer parts. The second portion of the research evaluates the impact of the reinforcement materials on the transmission of radio frequency to and from the tag. The last portion of the research looks at how the costs of RFID compare to the current use of the FRP materials as well as other sensors that are used in industry.

The expected outcome of this research is that the inclusion of the RFID tag adds to the value of the parts that it is included in. This is from the sensing capabilities that are possible, the identification capabilities to aide automation, and the design improvements that can be made to both products as well as manufacturing processes.

Table of Contents

List of Illustrations

List of Tables

Chapter 1

Introduction

The introduction begins the discussion of the topics of embedding electronic sensors into fiber reinforced polymers (FRP) and the use of radio frequency identification (RFID) in order to satisfy wireless communication with these sensors. The chapter discusses the reasons why material sensing is necessary, how wireless sensing falls back into manufacturing, how sensing would be used in manufacturing, and how sensing enables smart materials. The research purpose, executive summary, and the organization of the dissertation are all setup in the introduction.

1.1 Sensing in Materials

There are several reasons why researchers and engineers are interested in sensing capabilities inside of materials. First, in the manufacture of fiber reinforced polymers, many designs utilize material structures that are larger than necessary due to known deficiencies in the manufacturing process. These deficiencies include voids in the resin from entrapped air pockets, inconsistencies in the catalyst resin mix, incomplete saturation between the resin and the fiber reinforcement, and a list of other possible defects (Strong, 2008; Mason, 2006; Loyola, Zhao, Loh, & La Saponara, 2013; Phillip, Winkler, & Reinhart, 2013). Sensing in the material during the manufacturing processes allows the researchers and engineers to understand what types of stresses occur during these processes and what physical properties are in a specific batch (Merilampi, Björninen, Ukkonen, Ruuskanen, & Sydänheimo, 2011). The inclusion of sensing can lead to higher quality manufacturing processes that create better materials and the ability for designers and manufacturers to reduce weight and thickness. According to Mason (2006), most engineers add extra thicknesses to FRP designs to allow for these defects in the manufacturing process. These thicker parts cause higher material costs for the

manufacturer and increased weight in the part, and possibly passes cost inefficiencies on to the consumer of the part.

A second reason for researchers and engineers to want to sense material conditions falls back to manufacturing. Manufacturers know what the intended cure rates are supposed to be in composite manufacturing. They also know that parts do not always cure evenly throughout the part which can cause built up stresses in the part (Strong, 2005; Strong, 2008). Many of these stresses can affect the bond between the resin and the reinforcement resulting in loads that are translated through the resin onto the reinforcement in an optimal manner. Once the parts are manufactured, they are often tested to ensure that the material will meet the design requirements. With embedded sensing, manufacturers will be able to tell what stresses the part experiences during manufacturing and whether the part cured correctly. Because this can be performed real time, extra materials may not have to be manufactured for testing thereby reducing costs in manufacturing. Coupled with the designer's improved efficiencies mentioned before, composite manufacturing can become more cost efficient, which aides in making composites a more economically viable option. The more efficient costs also play into more possible adoptions of composites over other material types.

A third reason why researchers and engineers are interested in the ability to sense inside of materials is for the development of cyber physical sensing. Dumstorff, Paul, and Lang explained cyber physical sensing as "… computational elements (cyber) collaborate and even merge with the physical elements" (2014). The integration of sensing into materials leads researchers back in to cybernetics and smart materials where the sensors embedded into the material can feedback information about what physical properties the structure is being exposed to. The sensing capabilities allows for materials to identify damage and provide input about their condition (Arronche, La

Saponara, Yesil, & Bayram, 2013). An example of this approach can be viewed from the perspective of damage control from catastrophic events where the structure can only provide further use in a limited capacity such as limiting an aircraft's maneuverability based on a damaged wing structure. Another view of this approach can be from a maintenance perspective where the sensor enabled material identifies when it needs to serviced based on its actual use instead of based on a specified time interval.

1.2 Why is there a Need for Integrated Sensing

The need for integrated sensing is so large that the Department of Energy listed it as one of their four key technologies in the Enabling Technologies category at their Fiber Reinforced Polymer Composite Manufacturing Workshop in January 2014. This need was identified from the standpoint that "Sensors are not well integrated with data or manufacturing processes" ("Fiber Reinforced Polymer Composite Manufacturing Workshop: Summary Report" 2014). The workshop also noted the lack of use of intelligent sensors. From the workshop's perspective, the necessary "distributed sensors linked to data and physics, integrated with manufacturing and embedded in structures is an area of opportunity" ("Fiber Reinforced Polymer Composite Manufacturing Workshop: Summary Report," 2014). Included in these areas of opportunity are self-diagnostic materials, "sensing technologies, especially for joints", "nondestructive testing at the point of manufacture", and data informatics and data mining at the material level of manufacturing ("Fiber Reinforced Polymer Composite Manufacturing Workshop: Summary Report," 2014). One of the outcomes from the workshop was to identify the need of using actual processing data to produce design data needed to design new structures. The Department of Energy viewed the design data as a manner in which designers could reduce the need for models and simulations that they currently build in order to determine the strength and behavior of structures built with these materials. They

also noted the belief that the use of integrated sensors would lead to being able to predict the life of composite parts and components which would advance the use of composites in different applications ("Fiber Reinforced Polymer Composite Manufacturing Workshop: Summary Report," 2014). This includes using the sensor and nondestructive tools to monitor the materials life.

1.3 Purpose for this Research

Unfortunately, researchers and engineers typically only measure the first few products to ensure that the process will yield what they believe is an acceptable product. Sensing is discontinued after the first few products, usually because the first products would have to be destroyed in order to determine material strength. Most sensors currently in use need an interface to the outside world in order to communicate sensor data. This is often in the form of leads or wires. It would also be useful for a number of reasons to be able to sense in the material during their end use. Wired sensors would be somewhat prohibitive in these applications. RFID, however, enables the ability to wirelessly communicate information and its use is the focus of this study.

1.4 Polymers During Cure Processes

Though an older concept, the monitoring of the cure process of high value FRP components has traditionally relied on wired leads to provide power and feedback to computers so that the process can be monitored. This results in the measurements being taken in a cutout or on a scarf edge, locations that will be removed from the final product. This also yields stress points in these areas due to the protrusion of the electrical leads that lead from the sensors back to the computer equipment. By utilizing RFID tags, it is postulated that the sensing of the cure cycle could be easily monitored without inducing defects in the areas of the part that they are embedded in.

One of the methods engineers utilize when designing FRP parts is to increase the thickness of the part by a safety margin. They make the parts thicker than they may need to be in order to offset any inconsistencies in the materials that cause weakness or premature fatigue. This is done primarily because of variation and difficulties in monitoring every part that is manufactured. Variations in conditions, including temperature and humidity, can affect the stress in the part. Too high of a temperature can lead to creep in the resin. Too low of a temperature inhibits the polymer's crosslinking. Both feed into the quality and strength of the FRP (Jeon, Muliana, and La Saponara, 2014; Miyano, Nakada, and Cai, 2008; Nakada and Miyano, 2009). In order to know how the FRP part is processed, researchers have developed techniques and equipment that will allow them to monitor the cure process in real time.

In order to monitor FRP development, sensors are embedded into the layers of reinforcement of the FRP. Some sensors include fiber optics, which are woven into the fiber reinforcements and act as a part of the reinforcement matrix as well as sense stress throughout the part. Other sensors include dielectric sensing which utilizes electric current flow to detect when crosslinking occurs in the resin. Current will flow while the resin remains viscous, but will decrease as the resin continues to crosslink. This allows the observer to know the precise time that the part is actually done. Though there are other methods, all have the same recurring theme of having to have wired leads that run from the sensor to a multiplexer or industrial computer to actually interpret the sensor and record the data. Even in the case of fiber optics, where the fiber optic sensor can remain in the FRP, the leads that run to the computer create a defect resulting in that part of the FRP to be removed from the final part. In some instances this is acceptable if the leads protrude in a cut out region, but it may be that extra material has to be added to the part to attach the sensor to the leads. Mason states: "During part development, cure can be

reliably characterized, in general terms, using these variables. Cure rates, however, vary from part to part, even when parts are meant to be identical" (2006).

Mason continues:

> "Without a way to directly measure the progress of crosslinking, fabricators of thermoset composites traditionally have had to build a safety margin into cure times in order to avoid the damage that premature demolding can do to tools and undercured parts. While this ensures that sufficient crosslinking occurs, it lengthens cycle time and processing costs beyond what might otherwise be required. Additionally, there is the risk of overcuring, which can reduce ductility, making a part brittle (2006)."

1.5 Research Objectives

The objective of this research is to develop a methodology, test the results, and evaluate the use of the sensor enabled RFID tags to wirelessly monitor and communicate the physical stresses that an FRP part sees during the manufacturing and end use of that part. This portion of the research evaluates how the RFID tag affects the mechanical structure of the FRP part. The research objectives associated with this project are shown in Table 2 and are defined below. The outline of the research is shown in Figure 1-1.

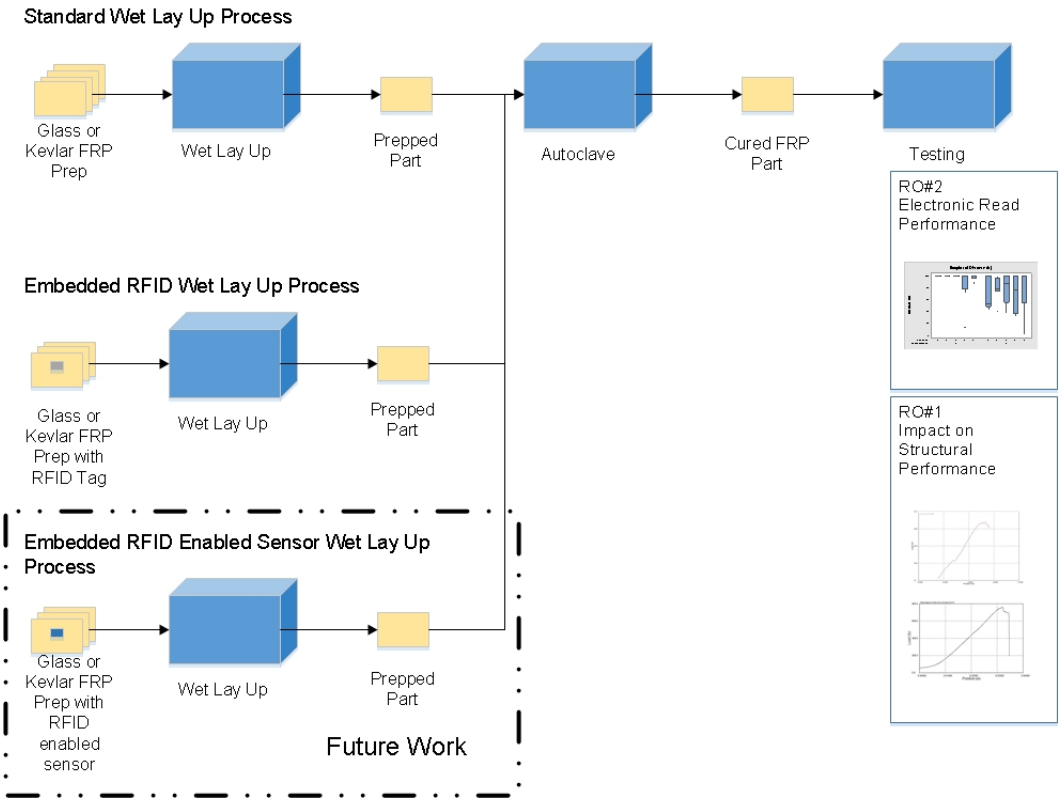

Figure 1-1: RFID Enabled Sensing In Fiber Reinforced Polymers

Research Objective 1: Evaluate the impact of embedded RFID tags on the mechanical properties of a composite structure. The methods and approach to be used for this research is to evaluate which factors are necessary to measure a structure's mechanical properties, determine the feasibility of finite element methodology (FEM) as a modeling tool to predict the stresses on a structure, test and evaluate the necessary factors using finite element analysis, perform visual inspection on composite parts to validate materials are free from defects, and test parts to the applicable ASTM specifications.

Research Objective 2: Evaluate the impact of embedded RFID tags on electronic transmission readability performance. The methods and approach to for this component

of the research is to look at how to determine the performance factors for measuring the electronic transmission readability performance factors of the embedded RFID tags, test and evaluate the embedded RFID tag performance factors on electronic transmission readability, and determine the economic viability of embedding RFID tags into a composite material.

Research Objective 3: Evaluate the impact of embedded RFID tags on life cycle analysis sustainability parameters. The methods and approach envisioned in this portion of the research is to determine the Life Cycle Analysis sustainability parameters and test and evaluate the Life Cycle Analysis sustainability parameters.

The intellectual merit of this research is that it yields a wireless tool that can be used to measure real time conditions of an FRP's physical characteristics during the cure process. Current techniques require that the sensors are physically tethered to the computer. The broader impact of this research is an embedded method that allows for monitoring an FRP during further processing and use.

1.6 Organization of this Dissertation

The dissertation follows a five point engineering format of introduction, background, methodology, results, and conclusion.

In this chapter the information regarding why this research is being performed is introduced. The section describes the topic of physical sensing in FRPs and why there is a need in FRPs for wireless sensing. It also explains the purpose of this dissertation and the need for mechanical testing of embedded electronics.

Chapter 2 discusses the literature review of RFID technologies, FRPs, and embedded sensing. The background also discusses recent, relevant funded research.

Chapter 3 defines the methodology used in this research. This includes the specific objectives, the research methodology, and the tools used to validate or dispute the hypotheses.

Chapter 4 discusses and interprets the results of the experiments. Computer simulations, statistical data, and economic expectations are included in the chapter.

Chapter 5 is the conclusion of the research and provides a summary of the experiments conducted. It includes the limitations of the research and describes the next steps in the sequence of the research.

Chapter 2

Background

In the background, definitions used in the research along with others' work that influenced this line of research are defined. Similar research that was previous funded through the National Science Foundation (NSF), the Department of Energy (DoE), and through industry are identified and discussed. The chapter concludes with information on life cycle costing and life cycle analysis.

2.1 RFID as a Technology

2.1.1 Radio Frequency Identification (RFID)

Radio Frequency Identification is a technology that has been in existence in some form since the 1930's. One of the earliest practical uses of utilizing radio frequency to identify an object was in the form of radio detection and ranging (RADAR) (Jones, Gray, & Armstrong, 2014; Jones & Chung, 2011; Jones & Chung, 2008). Further advances led to RFID becoming more commonplace. The Dallas North Toll Road opened up in the 1960's and utilized RFID tags to identify the different vehicles on the toll road (Jones, Gray, & Armstrong, 2014; Jones & Chung, 2011; Jones & Chung, 2008). RFID tags started being used in cattle ear tags to track cattle as they moved from lot to lot. Further advances continued as electronics became smaller. RFID tags are small enough now that can be implanted in a human or swallowed in a pill (Jones, Gray, & Armstrong, 2014).

2.1.2 RFID Theory of Operation

RFID works on the principles of electromagnetic frequencies. An electromagnetic wave is emitted from an antenna. Tags in range of the transmissions are energized and transmit back their recorded data. The antenna sends the tag signals to a reader that interprets the signal into data. Figure 2-1 shows a diagram of how RFID works.

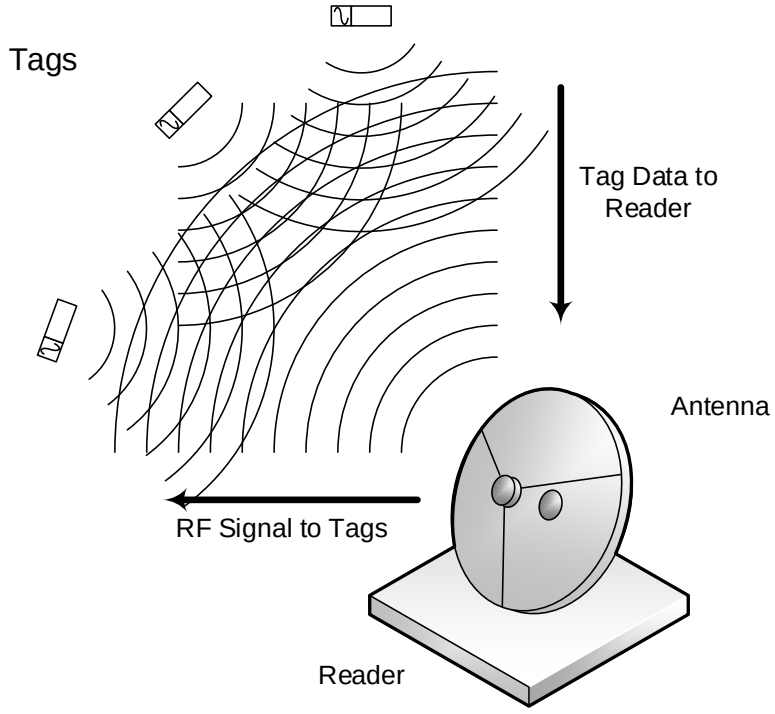

Figure 2-1: RFID Theory of Operation

The distance that a tag will operate at is impacted by the environment, the frequency, the power of the original signal, and the type of tag that is being used. There are several environmental factors to consider due to how radio frequency (RF) signals are transmitted. Liquids and metallic objects can shield or block the RF transmissions. Many materials may reduce the signal strength but do not block it.

There are also several RF frequencies that can be used. These range from the high frequency 13.57 MHz up to the ultrahigh frequency 2.4 GHz. The signal strength can also be varied by changing the power of the signal (Jones, Gray, & Armstrong, 2014). There are two main types of tags that are used; passive and active.

2.1.3 Passive Tags

A Passive RFID Tag is a tag that does not contain an integrated power source such as a battery. Passive tags are able to harvest the electrical energy they need to operate from the radio frequencies transmitted from the reader's antenna. Because these tags do not need an integrated power source, they have a more simplistic design that entails of the RFID chip, the RFID antenna, and a backing material that the antenna and chip are adhered to.

One of the biggest advantages the passive tag holds is the unlimited shelf life of the tag. Unless the tag is damaged through mechanical or environmental abuse, it should be able to respond to interrogation from a reader for an indefinite time period. Another advantage is the cost of the tag. Depending on volume, these tags can run as low as $0.05 per tag. It is still somewhat more expensive than printing on a barcode, but the additional benefits over barcodes make this tag economically attractive. Table 1shows some of the advantages and disadvantages between RFID and barcode technologies. One of the drawbacks with passive tags is their read range. Compared to active tags, passive tags have a much smaller read range and can only reflect the energy that they receive from the reader antenna.

Table 2-1: Advantages and Disadvantages of Barcode and RFID Technologies (Jones, Gray, and Armstrong, 2014)

	Barcode	RFID
Advantages	Indefinite lifespan depending on environment Inexpensive to produce	Indefinite lifespan Readable through different materials Read many tags at once Reuseable Can integrate with other devices
Disadvantages	Requires line of sight to operate Readable one at a time Sensitive to handling Sensitive to environment Degrade over time	Costs are comparably higher

2.1.4 Active Tags

Active tags differ from passive tags in that they contain an integrated power source, normally a battery. The battery is used to operate the circuitry of the tag as well as provide a power source for the antenna. Active tags can also be connected with other devices such as global positioning systems (GPS) or sensors in order to provide communication and input into a multimodal system. Active tags are larger and more expensive than passive tags. Their main advantage is the distances that they can transmit and receive signals.

2.1.5 Semi-Active Tags

Semi-active tags use technologies from both active and passive tags. They utilize an internal power source to operate internal circuitry and sensors. The communication of the tag still occurs through scavenged energy from the RF signal from the reader antenna. This allows for a tag that operates even after the battery dies on the sensors.

2.2 Fiber Reinforced Polymers

2.2.1 Manufacturing Processes

2.2.1.1. Wet Layup

The wet layup process is a method commonly used to build composite materials. (Strong, 2005) (Strong, 2008) This process allows for a variety of shapes and sizes to be built though it is commonly utilized more in large volume manufacturing of engineering composites than in advanced composites. (Strong, 2008) One aspect of this method that is similar to many processes is that because of its manual nature it is a good solution for small production runs where it would not be feasible to incorporate an automated solution.

The wet layup process lends itself to many types of resins that can be utilized. Most resins are shipped to the end user in the “neat” form where the end user will add any fillers or reinforcements that they desire in the end product. This results in resins from the low cost polyesters up to the more expensive epoxies and bismaleimides as possible resin solutions.

The initiators and catalysts used in wet layup are typically chosen based on two criteria: cure temperature and resin type. (Strong, 2008) Some resin/catalyst mixes can completely cure at room temperature (i.e. polyester/MEKP) while others need to be cured in an oven or autoclave. This affects the pot life of the mixes and the amount that can be

mixed at one time. Depending on the accuracy of the measurements of the two components, the ratios and temperatures can induce variations from part to part.

Wet layup can utilize a variety of forms of reinforcement. These reinforcements can be anything from “mats, woven cloths, knits, or any other kind of common textile goods.” (Strong, 2008) Reinforcements that lend themselves to this type of process include glass fiber, aramid fiber (Kevlar^{TM}), and carbon fiber. The reinforcements are laid upon the tool and the resin/catalyst mix is applied and worked into the reinforcement. Depending on the strengths and mechanical properties that are to be attained, the reinforcements may be applied in different orientations. This assures that the final part will function in a manner according to the engineering specifications.

Though wet layup is a valid solution, it can potentially contribute problems to the part being manufactured. The problems, as defined by Strong (2008), include:

- difficulty in aligning the fibers in exactly the directions desired
- difficulty in optimizing the amount of fibers to achieve the highest properties possible
- difficulty in controlling the fiber/resin ratio
- difficulty in getting full fiber wet-out
- difficulty in reducing the void content
- potential problems in mixing the resin and hardener (including emission and toxicity problems

(p. 389)

2.3 Embedded Sensing

There have been multiple instances where sensors have been embedded into materials. The common goal is the ability to sense what the materials are exposed to in terms of stress or temperatures. In some cases the sensor is a part of the structure in the

material such as in the use of fiber optics. In other cases the sensor is a defect in the material's structure, thereby degrading the strength of the material. In most of these implementations, a major problem has been the protrusion of electrical leads through the surface of the material. As a result manufacturers can only sense in areas of the material that will be removed or do not factor in to the load on the structure.

Some newer developments in the sensing embedded into materials is the use of carbon nanotubes to determine impact and stress. The University of California at Davis has used this methodology in their labs over the past several years. What they have done involves using a matrix of Multi-Walled Carbon Nanotubes (MWCN). They measure the electrical resistance and how it changes upon being influenced by an outside force. This allows them to measure the effects of stress on the surface of a material. One of the drawbacks is again the need for electrical leads that protrude from the part.

Another method of sensing is to embed fiber optic filaments into the structure. With fiber reinforced composites, the filament is included in the reinforcement. Researchers measure how the light is distorted while a stress is applied to the part in order to determine how the part is loaded. Again, this method requires that the filament is physically connected to leads in order to interface with the sensor.

Schaaf (2008) evaluated the use of embedded electronics into fiber reinforced composites for her dissertation. She utilized piezoelectronics but established a test protocol that was similar to that used in this research. What her research found is that depending on the variation of the sensor embedded into the composite that some sensors worked with little difference in the structural strength of the part while other sensors negatively affected the structure of the material.

In work by La Saponara, Horsley, & Lestari (2011), piezoelectric materials have been embedded into load bearing composite structures in order to determine the stresses

enacted upon that material. The electronic devices have been embedded into monolithic and sandwich structures as well as surface mounted onto the structures in order to monitor the structural health of those structures. This method is one of the methods envisioned as a nondestructive testing of finished materials by allowing the physical properties of the material to be known without destroying the part. In their series of research, La Saponara, Horsley, & Lestari (2011) utilized fatigue testing to cause failures in their test specimens. This allowed them to determine how the part would read and fail over time.

Tang, Winkelmann, Lestari, & La Saponara (2011) worked on fatigue testing of piezoelectronics in fiberglass. They utilized a control part absent of any electronics and compared it against the specimens that they built with electronics embedded into different layers in the part. They loaded the part at different frequencies in order to induce and evaluate the stresses put on tot the parts over different simulated loads. What they found was that their embedded specimens broke where the leads protruded through the materials while the specimen that had surface mount sensor broke in an area away from the sensors.

Joen, Muliana, & La Saponara (2014) continued the use of piezoelectronics to determine mechanical and thermal stresses that are enacted upon a fiber reinforced polymer. In this research the authors are utilizing the electronics to read stress applied to the material due to changes in temperature. Their use of the piezoelectronics is geared more towards an indirect measurement of the temperature through mechanical stress. Their research utilized their models that were developed and tracked the models' performance against the known coefficient of thermal expansion and the measured stresses.

One of the concerns with most of the embedded sensors used to determine stresses on a part is the need for power. There has been some investigation into the use of RFID as a method to monitor fiber reinforced composites. Early work started with utilizing active tags inside of concrete structures to measure stresses on the structure.

Pille (2010) discusses integrating sensing into cast parts. One comment made by Pille that specifically shows the need for embedded sensing is “Integrated sensors detect mechanical and thermal stress or deformation as well as vibration inside the casting…” . He further mentions the ability to use the sensor data to monitor real time and provide information regard stresses that have or could cause damage to a part or assembly. Pille promotes the idea of utilizing the sensors to also aid in the manufacturing process by self-identifying and instructing where that casting should be routed (Pille, 2010). Though Pille’s work was with cast metals, he did identify methods that may be useful when other RFID prohibitive materials such as carbon fiber need to be used. These methods included the frequency type of RFID tags to use, the placement of the tags in the material versus on the surface of the material, and insulation of the tag from the prohibitive material.

Dumstorff, Paul, & Lang (2014) evaluated the challenge of integrating the inlay of the RFID tag into the resin/reinforcement matrix of an FRP. They performed finite element analysis (FEA) and simulated what stresses the tag would create in the part. They simulated with the tag being a harder structure than the matrix and they simulated the matrix being a harder structure than the tag. Their simulations included tensile and bending stresses than were applied to the part and the effects that occurred between the part and the tag. Dumstorff and Paul identified that the RFID tag does alleviate many of the problems typically seen with embedded sensing, predominately the problem of wired leads protruding through the part. They also noted the need for investigation of whether

the electronics in the RFID tag would survive the manufacturing process for the FRP. Though their investigation did not address a solution, they identified the need to determine how to introduce the electronic into the layers of the FRP without causing delamination in the material.

2.4 Life Cycle Analysis

Life Cycle Analysis (LCA) is the estimation of the costs of the environmental impacts from a product's life cycle. These include refinement of the base materials needed to manufacture the subcomponents, the transportation costs, the assembly costs, the distribution costs, and the disposal costs along with traditional processes necessary to manufacture the product (USEPA, 2006; EEA, 2014). The main components when developing a life cycle analysis include the Life Cycle Inventory (LCI) and the Life Cycle Impact Assessment (LCIA). The LCI quantifies energy and raw material requirements as well as atmospheric and waterborne emissions, solid wastes, and other releases that occur over the life of the product, process, or activity (USEPA, 2006). LCIA evaluates the potential impacts on human health and the environment based on the resources and emissions identified in the LCI (USEPA, 2006).

Life cycle analysis is a widely used tool to evaluate environmental impacts. It has been performed by a number of people and organizations going back to the 1970's (Williams, 2004). There are differing frameworks that exist through the different organizations that look at different concepts such as cradle to cradle and cradle to grave. Some approaches look at economic input-output while others look at process sum, or the energy consumption. Formalized standards exist within the Environmental Protection Agency, the International Standards Organization, and through various research groups.

Though there are numerous variations, the idea is that there is a framework that is followed that identifies areas to evaluate for the different products. In this research,

three areas are identified in life cycle analysis: material production and manufacturing, useful life, and end of life. The different components in each of these areas are evaluated for their impact on the environment.

2.5 Life Cycle Costing

Life cycle costing is an analysis tool used to assign costs to the different components determined in the life cycle analysis. It looks at initial production costs as well as the in use and the end of life costs associated with the life cycle of the product. With some extra effort, the tool can include the costs associated with environmental damage from chemicals, greenhouse gasses, etc. This allows the toll to more encompassing of the complete system instead of just evaluating the products value stream. (Kendall, Keoleian, & Lepech, 2008)

Life cycle costing has not been around as long as life cycle analysis. The first appearances seem to be in the 1990's. Since then, it has been swept up into the ISO 14040 series of standards that address Environmental Management.

Life cycle costing follows along the same lines as the life cycle assessment. Costs are associated with the different processes and activities needed to manufacture a product, the impact that the product has on society and the environment during its useful life and at its end of life.

The life cycle analysis is important because it evaluates the impact of adding electronics to the composite. The research goal is to become more efficient in our design and manufacturing processes but the efficiency does need to offset the material consumption in traditional design and manufacturing processes.

Multiple methods can be used to perform LCA and LCC. The Tiered Hybrid Analysis model as defined by Suh and Huppes (2005), requires data for the commodity items used in manufacturing the product and evaluates the environmental costs for each

process and during the three phases that will be evaluated: material production and manufacturing, useful life, and end of life.

There are other methods that can be used. Life cycle analysis based on process analysis can be performed using the Process Flow Diagram approach or the Matrix Representation approach. Life cycle analysis can also be performed using the Input-Output approach. These three methods can give environmental impacts (Process Flow and Matrix) or economic impacts (Input-Output) but they do not provide both. Hybrid approaches have been developed that allow for both environmental and economic impacts to be evaluated. The three approaches are the Tiered Hybrid Analysis, IO-based Hybrid Analysis, and Integrated Hybrid Analysis. The main differences between the approaches are tied to the availability of data and the geographical system boundaries. According to Suh and Huppes (2005), the Tiered Hybrid Analysis is not as complex as the other two and most analysis can be performed in Excel.

The analysis of the data can be performed locally using a laptop computer, the internet, and Microsoft Excel. The chief concern and costs will be centered on the databases that will need to be accessed. These databases define the impacts costs associated with the subcomponents and end products that make up the product that is under analysis.

2.6 Previous Relevant Funded Research

2.6.1 National Science Foundation

The original work behind this research began in response to the National Science Foundation (NSF) Division of Civil, Mechanical and Manufacturing Innovation (CMMI), in the Advanced Manufacturing Cluster, Manufacturing Machines and Equipment (MME) Program, PD 13-1468.

2.6.2 Department of Energy

In January, 2014 the Department of Energy (DoE) out of their Advanced Manufacturing Office hosted the Fiber Reinforced Polymer Composite Manufacturing Workshop with the goal of working towards low cost fiber reinforced polymers. The workshop focused on identifying concerns with the manufacturing process technologies, enabling technologies and approaches, and recycled and emerging materials. The three agencies that presented to the workshop were the Advanced Manufacturing National Program Office, the Defense Advanced Research Projects Agency (DARPA), and the National Aeronautics and Space Agency (NASA). Some of the chief concerns were "building confidence in materials through a technology insertion program" and "increasing bonded composite confidence". Though the focus of material selection for designs has been predominately carbon fiber, the workshop indicated that, "other fibers reinforced materials and integrated approaches that can meet the performance and cost targets could be acceptable." (Department of Energy, 2014)

One of the comments out of the enabling technologies and approaches group was the discussion of sensing and measurement. The group commented heavily on intelligent sensing from self-diagnosis and testing of materials to lifetime analysis of the material. Their comments showed that they believed that this may be one of the only manner in which the proliferation of FRP's could occur.

2.6.3 Industry

Bernhard, Dräger, Grabowski, Sotriffer, & Philipp (2011) evaluated embedding RFID tags into FRP's in order to track the materials through a company's production, inspection, and shipping processes. They evaluated the impact of readability of RFID in different types of FRP's, predominately in glass and carbon based FRP's. They found that they could read easily through glass FRP's but that the low frequency RFID tags

would work at a reduced distance through carbon FRP's. They also experimented with where in the composite layers they placed the RFID tags. One of their main concerns with embedding RFID into the composites was how it would affect the mechanical properties of the FRP's structure.

Research performed by Dumstorff, Paul, and Lang (2014) evaluated FRP and the impact that an embedded RFID tag would have of the mechanical properties of the materials. Their evaluation centered on Finite Element Methodology (FEM) simulation to determine how the tag and FRP would respond to different types of loads (shear, tensile, and compression). Their research showed that the polymer exhibited greater flexibility in the matrix than what the RFID tag was capable of. Though the research helps to show how the material would behave under different loads, all work was performed through the simulation software. There is not a follow on study that shows physical mechanical testing and the results of a production part.

Chapter 3

Methodology

The Research Objectives are expanded upon in the methodology section in order to define the specific tasks that were performed in the research. The specific methods, actions, and equipment that were taken to build, test, and evaluate the embedded RFID tags are outlined along with the methods used to collect the data from the tests.

3.1 Research Objectives and Specific Tasks

Table 2 shows the research objectives and tasks used in this research. The following sections will define the methodology used for each research objective and the corresponding tasks with each objective.

Table 3-1: Research Objectives and Tasks

Research Objective 1: Evaluate the impact of embedded RFID tags on the mechanical properties of a composite structure.
Task 1 – Evaluate the necessary factors to measure a structure's mechanical properties.
Task 2 – Determine the feasibility of FEM as a modeling tool to predict the stresses on a structure.
Task 3 – Test and evaluate factors using FEM.
Task 4 – Perform visual inspection on composite parts to validate materials are free from defects.
Task 5 – Test composite parts per ASTM D-2344 for short beam test and ASTM D695-02 for the compression test
Research Objective 2: Evaluate the impact of embedded RFID tags on electronic transmission readability performance.
Task 6 – Determine the performance factors for measuring the electronic transmission readability performance factors of the embedded RFID tags.
Task 7 – Test and evaluate the embedded RFID tag performance factors on electronic transmission readability.
Task 8 – Determine the economic viability of embedding RFID tags into a composite material.
Research Objective 3: Evaluate the impact of embedded RFID tags on life cycle analysis sustainability parameters.
Task 9 – Determine the Life Cycle Analysis sustainability parameters.
Task 10 – Test and evaluate the Life Cycle Analysis sustainability parameters.

Research Objective 1: Evaluate the impact of embedded RFID tags on the mechanical properties of a composite structure

Task 1 – Evaluate the necessary factors to measure a structure's mechanical properties.

The first step was to identify the necessary tests and criteria to ensure that the materials' structures can be tested to determine what impact embedding the RFID tags would have.

Literature review identified several methods that others have used to valid structural integrity. Many of the researchers utilized the ASTM (American Society for Testing and Materials) specifications as a basis for testing materials. The three most common test specifications used were the compression test (ASTM D695-02), the tensile test (ASTM D638-14), and the short beam shear test (ASTM D2344/D2344M-13). The original proposal for this research called for tensile testing but because the tensile test is predominately utilized to identify the strength of the fiber and not the bond between the fiber and the resin, it was decided that the test was not necessary for the research.

Loads and stresses are commonly subjected onto a part to determine if embedding a device results in a defect. Common measurements on the parts include their width, length, and thickness. These measurements were used to determine the part's volume. Once the part was loaded up and a failure occurred, the load was divided by the volume to determine the stress on the part.

Task 2 – Determine the feasibility of FEM as a modeling tool to predict the stresses on a structure.

FEM was evaluated as a tool for identifying potential problems with embedding RFID into FRP's.

In order to model the composite parts for FEM, a software package needed to be identified that could perform the calculations necessary for the FEM. Based on availability, AutoDesk's Mechanical Simulation 2015 package was used. This package included the correct materials for the composites and the RFID tags that were to be used in the simulation. The output of the software provided both mechanical movement of the part while under stress as well as a simulated stress depending on the load that was applied to the simulation.

Task 3 – Test and evaluate factors using FEM.

Once the simulation software was determined, the next step was to build the FEM models in the simulation package and determine where the parts would break and under what stresses the parts would break.

Parts were modeled in AutoDesk's AutoCAD Inventor 2015. Because of how the laminations behave once they are bonded with the epoxy resin, the layers of 15 plies and 5 plies were modeled as two separate pieces instead of 20 separate pieces. This is allowable under lamination theory which theorizes that because the parts are bonded, they will behave mechanically as a whole piece instead of separate pieces. The reason behind the 15 plies and 5 plies is that the shear stresses would build up in the middle of the part, or between 10 plies and 10 plies. If the tags were placed there, then it would be unclear if the part failed naturally at that point or if the part failed due to the inclusion of the tag. By offsetting which layers the tags are placed in, the failure would be more likely attributed to the tag instead of the material. The interest in the calculations is the bond between the composite material and the RFID tag. The use of lamination theory also simplifies the calculations that need to be made and speeds the simulation up without sacrificing the accuracy of the calculations. Once the separate pieces of the composite

materials and the RFID tag are modeled and assembled in Inventor, the model can be passed to the Mechanical Simulation package in order to perform the FEM.

Simulations of the parts in compression and in shear were run. The outputs of the simulations contain multiple scenarios of how the parts will be stressed under load. In these simulations a load of 1200 pounds was specified. All parts were constrained in the manner in which they would be during actual testing. The simulations provided different results based on which scenarios were most probable. The outputs also show the stresses and movements of the parts in a color spectrum along with numerical readouts of the stress in pounds per square inch (psi) and movement in inches. Animations of the simulations are also available so that the load up of stresses and movements in part can be seen over a defined time period.

Task 4 – Perform visual inspection on composite parts to validate materials are free from defects

Upon manufacture of the FRP parts with and without embedded electronics, the parts were inspected to ensure that there were no visible or known defects in the parts prior to testing.

Parts were manufactured using the wet layup method. This is a manual process that is commonly used for prototyping and low volume production. The process is applicable for both glass fiber and Kevlar fiber. The following are the processes used for each material type.

3.1.1 Manufacturing Methods for Glass Fiber Reinforced Polymers

The Glass parts were manufactured on an 18” x 18” x ¼” aluminum plate layup tool. The parts had sets of tags embedded in them, arranged in a manner that allowed for the test specimens defined in the test methodology to be cut of the parts. The glass parts were manufactured at a thickness of approximately 1/8”. This allowed the specimens for

all tests to be produced. Each part built contained at least one of each of the tag types as well as allowed space for an untagged test specimen. The parts were built using 20 plies with a $[0/45/90/-45/0]_4$ orientation. The tags are embedded in between the first two layers (or plies 5 and 6) closest to the tool side.

The specific manufacturing process is as follows:

a) Clean the layup tool to remove any residual materials from previous use. Cleaning processes may include scraping, steel wool, and/or wiping down with acetone.

b) Treat the surface of the layup tool with a non-silicone based wax. Apply one coat of wax. Once the wax has setup, buff off the wax using a cloth rag. Ensure that all wax is removed as failing to do so will result in surface defects.

c) Spray the tool with a polyvinyl alcohol (PVA). Wipe off a 1” perimeter on the tool to allow for the bagging tape to adhere later. Wait for the PVA to dry.

d) For the glass part, a volume of 8 cubic inches (8” x 8” x 1/8”) will need to filled. Part of this volume will be fabric and part will be the epoxy resin. The void volume is assumed to be zero.

e) Cut out three pieces of peel ply at a size of 15” x 15”.

f) Cut out three pieces of breather material at a size of 15” x 18” a one piece at a size of 4” x 12”.

g) Cut out one piece of bagging at a size of 22” x 26”.

h) Cut out 12 pieces of glass fabric at a size of 8” x 8” with a fiber orientation of 0°.

i) Cut out eight pieces of Glass fabric at a size of 8” x 8” with a fiber orientation of 45°.

j) Pour out 220 grams of epoxy resin and 60 grams of hardener.

k) Mix the epoxy and resin. Try to not entrain air into the mixture but make sure that the mixture is evenly mixed. The hardener is a darker color than the resin so it will be somewhat evident in regards to the mixture. The final solution should be an amber/honey color. Streaks of the hardener in the resin should not be present in the mixture. Once the resin and hardener have been mixed there will be approximately 2 hours until the resin begins to harden.

l) Apply resin to the tool surface. Cover an area approximately 10” x 10”. This will be the tool side of the part.

m) Add in a layer of glass with a fiber orientation of 0°. Using a brush, press the Glass into the resin so that the fabric lays flat onto the resin. Add additional resin to the Glass, working it in from the middle of the part to the outside edges. Add in a second piece of the Glass fabric with a 45° orientation. Repeat adding resin and fabric until the next 0° ply is added.

n) Add in the RFID tags onto the part. One of each tag type is to be added with a 1” space between each tag. All tags should lie in the 90° orientation plane.

o) Repeat adding glass in the following orientations: $[0/45/90/-45/0]_3$.

p) After the last layer is added, add the bagging tape around the edges of the tool. Do not remove the protection from the top of the bagging tape.

q) Add the peel ply layers to the top of the part. Make sure that the peel ply covers the resin.

r) Add the three pieces of 15” x 18” breather material. Any excess breather should be folded under to help manage the material.

s) Fold the 4” x 12” piece of breather into thirds and place it on the edge of the tool. Set the base of the vacuum port onto this piece of breather.

t) Peel off the protective tape from the tape on one edge of the tool. Apply the edge of the vacuum bag to the tape.

u) Peel the protection from the bagging tape on the two adjacent sides approximately ¾ of the length of the tape. Apply the edges of the vacuum bag to the tape.

v) Peel off the protection from the tape on opposite side and apply the vacuum bag. There will be excess bag on both adjacent sides of the tool.

w) Measure out approximately 4” of bagging tape. Apply it to the folds in the vacuum bag to create pleats. Peel off the rest of the protection from the tape and attach the last open parts of the vacuum bag.

x) Cut a slit into the center of the port and attach the other half of the vacuum port.

y) Place the tool into the oven and attach the vacuum line.

z) Start the vacuum. Check for leaks in the bagging and seal with bagging tape.

aa) Start the oven. The temperature ramp rate is 5°F per minute. The cure temperature is 300°F for one hour. The cooling temperature rate is 5°F per minute.

bb) Once the part is cooled it can be removed from the tool for further processing.

3.1.2 Manufacturing Methods for Kevlar Fiber Reinforced Polymers

The Kevlar parts were manufactured on an 18” x 18” x ¼” aluminum plate layup tool. The parts had sets of tags embedded in them, arranged in a manner that allowed for the test specimens defined in the test methodology to be cut of the parts. The Kevlar parts were manufactured at a thickness of approximately ¼”. This allowed the specimens for all tests to be produced. Each part built contained at least one of each of the tag types as well as allow space for an untagged test specimen. The part was built using 20 plies with a $[0/45/90/-45/0]_4$ orientation. The tags were embedded in between the first two layers closest to the tool side.

The specific process is as follows:

a) Clean the layup tool to remove any residual materials from previous use. Cleaning processes may include scraping, steel wool, and/or wiping down with acetone.
b) Treat the surface of the layup tool with a non-silicone based wax. Apply one coat of wax. Once the wax has setup, buff off the wax using a cloth rag. Ensure that all wax is removed as failing to do so will result in surface defects.
c) Spray the tool with a polyvinyl alcohol (PVA). Wipe off a 1” perimeter on the tool to allow for the bagging tape to adhere later. Wait for the PVA to dry.
d) For the Kevlar part, a volume of 16 cubic inches (8” x 8” x ¼”) will need to filled. Part of this volume will be fabric and part will be the epoxy resin. The void volume is assumed to be zero.
e) Cut out three pieces of peel ply at a size of 15” x 15”.

f) Cut out three pieces of breather material at a size of 15” x 18” a one piece at a size of 4” x 12”.

g) Cut out one piece of bagging at a size of 22” x 26”.

h) Cut out 12 pieces of Kevlar fabric at a size of 8” x 8” with a fiber orientation of 0°.

i) Cut out eight pieces of Kevlar at a size of 8” x 8” with a fiber orientation of 45°.

j) Pour out 220 grams of epoxy resin and 60 grams of hardener.

k) Mix the epoxy and resin. Try to not entrain air into the mixture but make sure that the mixture is evenly mixed. The hardener is a darker color than the resin so it will be somewhat evident in regards to the mixture. The final solution should be an amber/honey color. Streaks of the hardener in the resin should not be prevalent in the mixture. Once the resin and hardener have been mixed there will be approximately 2 hours until the resin begins to harden.

l) Apply resin to the tool surface. Cover an area approximately 10” x 10”. This will be the tool side of the part.

m) Add in a layer of Kevlar with a fiber orientation of 0°. Using a brush, press the Kevlar into the resin so that the fabric lays flat onto the resin. Add additional resin to the Kevlar, working it in from the middle of the part to the outside edges. Add in the a second piece of the Kevlar fabric with a 45° orientation. Repeat adding resin and fabric until the next 0° ply is added.

n) Add in the RFID tags onto the part. One of each tag type is to be added with a 1” space between each tag. All tags should lie in the 90° orientation plain.

o) Repeat adding Kevlar in the following orientations: $[0/45/90/-45/0]_3$.

p) After the last layer is added, add in the bagging tape around the edges of the tool. Do not remove the protection from the top of the tape.

q) Add the peel ply layers to the top of the part. Make sure that the peel ply covers the resin.

r) Add the three pieces of 15” x 18” breather material. Any excess breather should be folded under to help manage the material.

s) Fold the 4” x 12” piece of breather into thirds and place it on the edge of the tool. Set the base of the vacuum port onto this piece of breather.

t) Peel off the protective tape from the tape on one edge of the tool. Apply the edge of the vacuum bag to the tape.

u) Peel the protection from the tape on the two adjacent sides approximately ¾ of the length of the bagging tape. Apply the edges of the vacuum bag to the tape.

v) Peel off the protection from the tape on opposite side and apply the vacuum bag. There will be excess bag on both adjacent sides of the tool.

w) Measure out approximately 4” of bagging tape. Apply it to the folds in the vacuum bag to create pleats. Peel off the rest of the protection from the tape and attach the last open parts of the vacuum bag.

x) Cut a slit into the center of the port and attach the other half of the vacuum port.

y) Place the tool into the oven and attach the vacuum line.

z) Start the vacuum. Check for leaks in the bagging and seal with bagging tape.

aa) Start the oven. The temperature ramp rate is 5°F per minute. The cure temperature is 300°F for one hour. The cooling temperature rate is 5°F per minute.

bb) Once the part is cooled it can be removed from the tool for further processing.

3.1.3 Modification of the RFID tags

There were 6 variations of the RFID tags used in the experiments. All tags used were made from Alien's Higgs-3 part number ALN-9640. These modifications are listed as:

0 = no tag included (control)

1 = perforated tag – holes were punched into the inlay of the RFID tag to try and allow the resin to bond through the tag

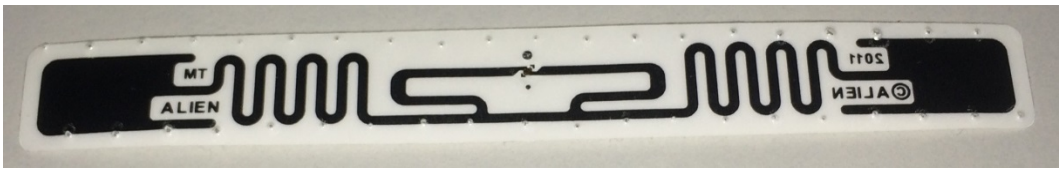

Figure 3-1: Perforated RFID Tag

2 = complete tag – off the shelf RFID tag

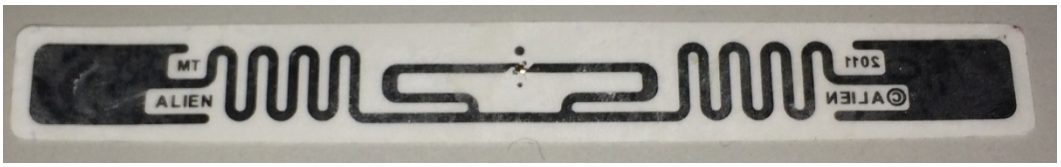

Figure 3-2: Complete RFID Tag

3 = skeletonized tag – The inlay of the tag is cut down to reduce the footprint of the tag

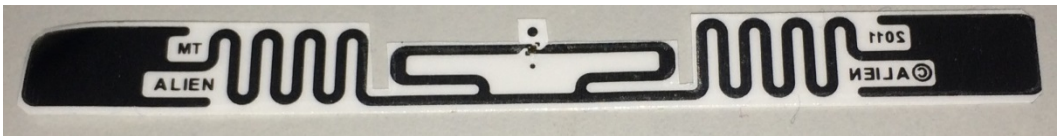

Figure 3-3: Skeletonized RFID Tag

4 = feathered tag – slits were cut into the inlay of the tag to try and allow resin to bond through the tag

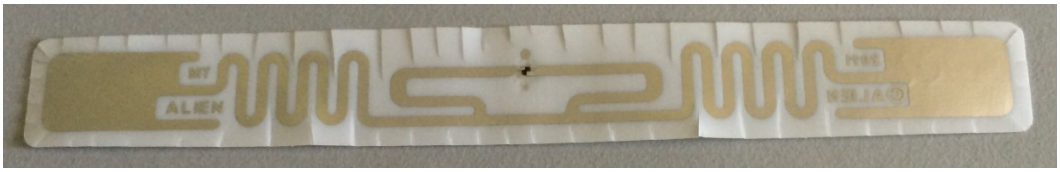

Figure 3-4: Feathered RFID Tag

5 = abraded tag – the complete tag was sanded to try and increase the surface area that the epoxy could bond to.

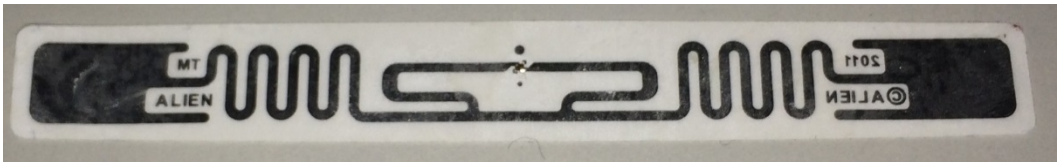

Figure 3-5: Abraded RFID Tag

Visual inspection of the parts helped ensures that the parts would fail based on the inclusion of the RFID tag and not because of a known manufacturing defect. Defects that were inspected for were voids caused by entrained air in the resin, incomplete bonds between the resin and the fibers due to contamination, and defects in the surface of the parts caused by the presence of silicon on the mold surface.

Task 5 – Test composite parts per ASTM D-2344 for short beam test and ASTM D695-02 for the compression test

Mechanical testing of the FRP test specimens determined the impact of the tag on the structure of the part.

For the compression and shear tests, a 2 x 2 factorial Design of Experiments (DoE) were setup for each test. The following sections define the DoE for each test.

3.1.4 Design of Experiments for Compression Testing

Problem Description

In the compression test, the objective was to determine how the fibers of the reinforcement buckle with a given load. This test helped define the strength between resin and the fiber and if there are any voids and defects in the resin. (Strong, 2008) In this research, the RFID tag that was embedded in the layers of the composite is viewed as a defect. The purpose of using this test was to see if the RFID tag caused the part being tested to fail at a lower load than the control part that does not contain a tag.

The same Alien ALN-9640 Higgs 3 tag was used in the same configurations as before. The materials are again Kevlar and Glass fiber reinforcement with an epoxy resin.

The experimental design is a 2 x 2 factorial with 2 factors for material and 6 factors for tags.

Experimental Units

5 samples of Kevlar reinforced polymer for each tag type

5 samples of glass reinforced polymer for each tag type

Factor A: Tag modification with levels

0 = no tag included (control)

1 = perforated tag

2 = complete tag

3 = skeletonized tag

4 = feathered tag

5 = abraded tag

Factor B: Reinforcement type with levels

K = Kevlar

G = Glass

Treatments

The treatments are the factor level combinations. In this section of the experiments, the sets of treatments are K0, K1, K2, K3, K4, K5 and G0, G1, G2, G3, G4, G5. K and G correspond to Factor B: Reinforcement Types and 0, 1, 2, 3, 4, and 5 correspond to Factor A: Tag Types.

Response

Compression strength (in psi)

Goal

To determine at each tag level for each material type if the failure of the samples with embedded tags is significantly different than the control.

Design

The total number of treatments is 6 * 2 = 12. We performed 5 replications for each treatment for a total of 60 parts that needed to be run. The 5 replications

requirement was based on the test specifications. Each specimen was numbered in order to maintain traceability of the part.

Data was collected off of the test specimen. All dimensional measurements were taken in inches and all loads were measured in pounds. The stress on the specimen were then calculated using the average width and thickness measurements and the observed peak load at failure. The calculation used to determine shear stress is:

$F^{compress} = \frac{P_m}{b \times h}$ as defined by the ASTM specification D695-02a

where:

$F^{compress}$ = short-beam strength, MPa (psi)

P_m = maximum load observed during the test, N (lbf)

b = measured specimen width, mm (in)

h =measured specimen thickness, mm (in)

Parts are manufactured with 5 tags in each part, one of each tag type, and room for a control part to be cut from the part. After the material was cured, the test specimens were cut from the parts and measured. The test specimens were determined randomly so that there were 5 of each type of tag the test. The randomization occurred through the randomization function =randbetween(0, 100000) in Excel. The numbers as assigned to the treatments were sorted least to greatest in order to randomize the treatments. Randomization of the parts is included in the appendix.

The first set of statistics calculated were the mean, standard deviations, coefficient of variation, and the number of specimens for each material type and each tag type. In addition to the descriptive statistics, the ANOVA, time series plot, normal

probability plot, and residuals versus fitted value plots will be performed. Any abnormal data points were explored in order to define the abnormality.

3.1.5 Test Method for Compression Testing

The compression test was run based on the ASTM D695-02a Standard Test Method for Compressive Properties for Rigid Plastics. Test specimen were prepared to achieve width x thickness x length dimensions of 0.50” x 0.20” x 1.50” for the Kevlar parts and 0.50” x 0.12” x 1.50” for the glass parts. Conditions at the time of test were at 67°F $\pm$ 10°F and at 50% $\pm$ 10% relative humidity. Test specimens were conditioned at this temperature and humidity for 24 hours prior to testing. The compressive strength was calculated from the tests. The stress-strain calculations in the test procedure will be omitted due to the lack of a compressometer. The following steps are based on section 10 and 11 of ASTM D695-02a.

10.1 Measure the width and thickness of the specimen to the nearest 0.01 mm (0.001 in.) at several points along its length. Calculate and record the average value of the cross sectional area. Measure the length of the specimen and record the value.

10.2 Place the test specimen between the surfaces of the compression tool, taking care to align the center line of the plunger and to ensure that the ends of the specimen are parallel with the surface of the compression tool. Adjust the crosshead of the testing machine until it just contacts the top of the compression tool plunger.

10.3 Place the specimens in the fixture so that they are flush with the base and centered. The screws in the fixture are to be tightened finger tight.

10.4 Set the speed control at 0.050 in/min

10.5 Record the maximum load carried by the specimen during the test. This should be the load at the moment of rupture.

11.1 Calculate compressive strength by dividing the maximum compressive load carried by the specimen during the test by the original average cross-sectional area of the specimen. Express the result in pounds-force per square inch and report out to three significant digits.

3.1.6 Design of Experiments for Shear Testing

Problem Description

In the shear test, the objective is to determine if the layers of the matrix and reinforcement would shear in between the layers. This test helps define the strength between resin and the fiber. (Strong, 2008) In this research, the RFID tag embedded in the layers of the composite is viewed as a defect. The purpose of using this test is to see if the RFID tag caused the part being tested to fail at a lower load than the control part that did not contain a tag.

The same Alien ALN-9640 Higgs 3 tag was used in the same configurations as before. The materials are again Kevlar and Glass fiber reinforcement with an epoxy resin.

The experimental design is a 2 x 2 factorial with 2 factors for material and 6 factors for tags

Experimental Units

5 samples of Kevlar reinforced polymer for each tag type

5 samples of glass reinforced polymer for each tag type

Factor A: Tag modification with levels

0 = no tag included (control)

1 = perforated tag

2 = complete tag

3 = skeletonized tag

4 = feathered tag

5 = abraded tag

Factor B: Reinforcement type with levels

K = Kevlar

G = Glass

Treatments

The treatments are the factor level combinations. In this section of the experiments, the sets of treatments are K0, K1, K2, K3, K4, K5 and G0, G1, G2, G3, G4, G5. K and G correspond to Factor B: Reinforcement Types and 0, 1, 2, 3, 4, and 5 correspond to Factor A: Tag Types.

Response

Shear strength (in psi)

Goal

To determine at each tag level for each material type if the failure of the samples with embedded tags is significantly different than the controls.

Design

The total number of treatments is 6 * 2 = 12. 5 replications were performed for each treatment for a total of 60 parts that needed to be run. The 5 replications requirement is based on the test specifications. Each specimen was numbered in order to maintain traceability of the part.

Data was collected off of the test specimen. All dimensional measurements were taken in inches and all loads were measured in pounds. The stress on the specimen was then calculated using the average width and thickness measurements and the observed peak load at failure. The calculation used to determine shear stress is:

$F^{sbs} = 0.75 \times \frac{P_m}{b \times h}$ as defined by the ASTM specification D2344/D2344M-13

Where:

F^{sbs} = short-beam strength, MPa (psi)

P_m = maximum load observed during the test, N (lbf)

b = measured specimen width, mm (in)

h =measured specimen thickness, mm (in)

Parts were manufactured with 5 tags in each part, one of each tag type, and room to for a control part to be cut from the part. After the material was cured, the test specimens were cut from the parts and measured. The test specimens were determined randomly so that there are 5 of each type of tag the test. The randomization occurred through the randomization function =randbetween(0, 100000) in Excel. The numbers as assigned to the treatments were sorted least to greatest in order to randomize the treatments. Randomization of the parts is included in the appendix.

The first set of statistics calculated were the mean, standard deviations, coefficient of variation, and the number of specimens for each material type and each tag type. In addition to the descriptive statistics, the ANOVA, time series plot, normal probability plot, and residuals versus fitted value plots were performed. Any abnormal data points were explored in order to define the abnormality.

3.1.7 Test Method for Short Beam Strength

The short beam shear test was run based on the ASTM D2344/D2344M-13 Standard Test Method for Short-Beam Strength of Polymer Matrix Composite Materials and Their Laminates. Test specimen were prepared to achieve width x thickness x length dimensions of 0.50” x 0.12” x 1.50” for the glass parts and 0.50” x 0.20” x 1.50” for the Kevlar parts. Conditions at the time of test shall be at 67°F $\pm$ 10°F and at 50% $\pm$ 10% relative humidity. Test specimens are conditioned at this temperature and humidity for 24 hours prior to testing. The short-beam (shear) strength was calculated from the tests. The following procedure is based on section 11 and 12 of ASTM D2344/2344M-13.

11.1 Measure the width and thickness of the specimen to the nearest 0.01 mm (0.001 in.) at several points along its length. Calculate and record the average value of the cross sectional area. Measure the length of the specimen and record the value.

11.2 Set the speed control at 0.050 in/min

11.3 Insert the test specimen into the test fixture as shown in Figure 3-6. Align and center the specimen so that the edges are equally supported and that the longitudinal axis is perpendicular to the loading nose and side supports. The loading nose should be equidistant between the supports. The span length should be approximately 0.80” for the Kevlar and 0.48” for the glass to meet the 4:1 ratio when compared to the thickness of the parts. Because of this ratio requirement and the thicknesses of the glass

and Kevlar parts being different thicknesses, the two material types must be run during two separate setups.

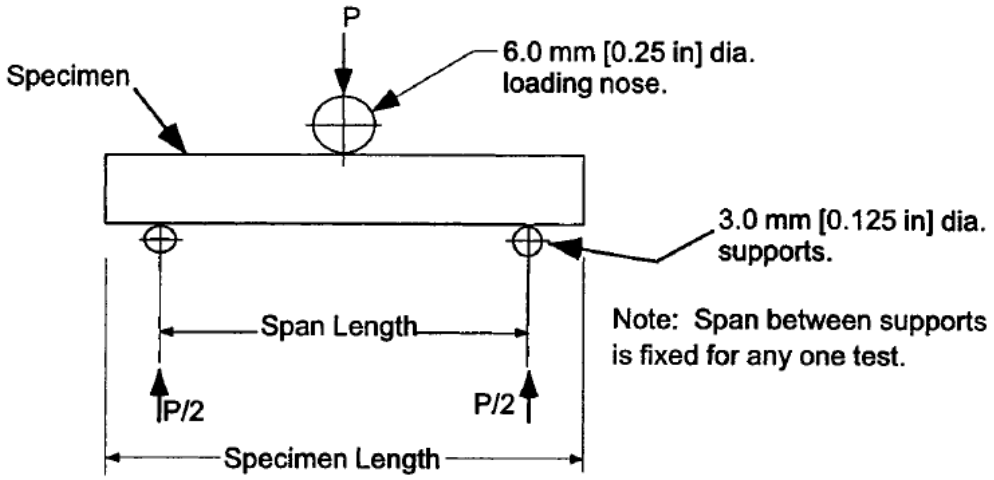

Figure 3-6: Horizontal Shear Load Diagram (ASTM D2344-13, 2013)

11.4 Apply the load to the specimen until a load drop-off of 30% occurs, there is a two piece specimen failure, or the head travel exceeds the specimen nominal thickness.

11.5 Record the load versus crosshead displacement data throughout the test method. Record the maximum load, final load, and the load at any obvious discontinuities in the load-displacement data.

11.6 Record the failure mode and location of failure. Failure modes are visually depicted in Figure 3-7.

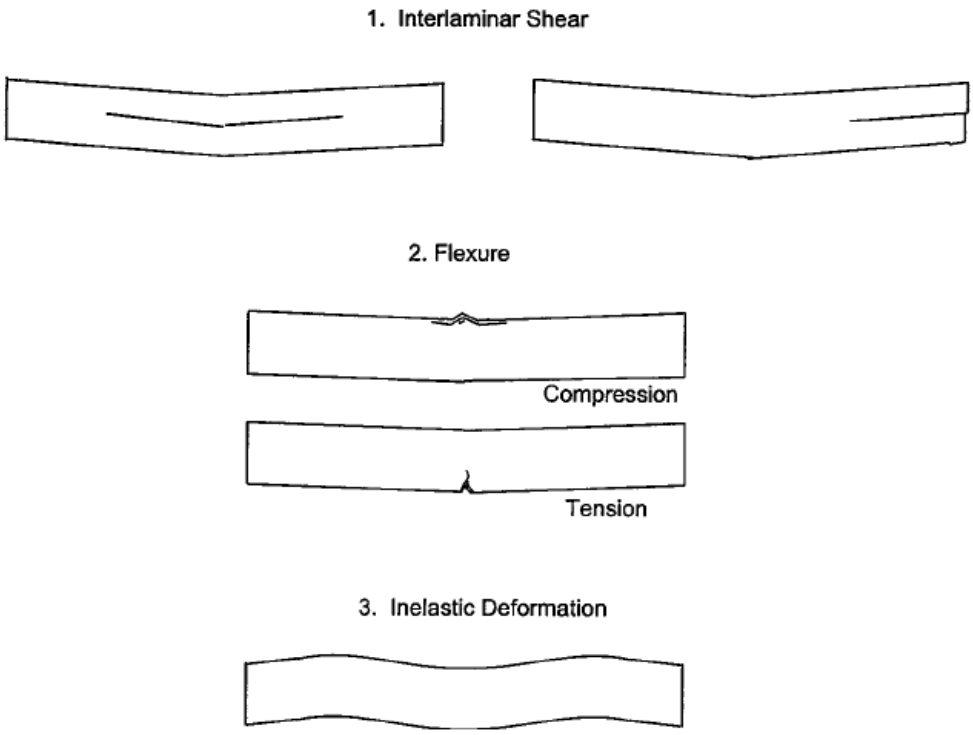

Figure 3-7: Typical Failure Modes in the Short Beam Test (ASTM D2344-13, 2013)

12.1 Calculate the short-beam strength using the equation

$$F^{sbs} = 0.75 \times \frac{P_m}{b \times h}$$

Where

F^{sbs} = short-beam strength (psi)

P_m = maximum load observed during the test (lbf)

b = measured specimen width, (in)

h = measured specimen thickness (in)

Research Objective 2: Evaluate the impact of embedded RFID tags on electronic transmission readability performance.

Task 6 – Determine the performance factors for measuring the electronic transmission readability performance factors of the embedded RFID tags.

Determine which read distances to perform the electronic readability transmission tests at.

The area was constrained to 100 feet in distance. The area was cleared of any obstructions and marked off from 0 to 100 feet in 10 foot increments.

Task 7 – Test and evaluate the embedded RFID tag performance factors on electronic transmission readability.

Perform the readability tests for the glass and Kevlar materials for all tag types.

Tags were moved away from the reader's antenna until the tags reached 100 feet or the tag had zero reads over a 5 second period.

3.1.8 Design of Experiments for Read Distance Testing

Problem Description

In the read distance test, the objective was to determine if the RFID tags can be read by the reader after the manufacturing process has occurred. This test helps define the ability to utilize RFID tags in composite material manufacturing. The RFID tag embedded in the layers of the composite was activated in order to determine how far away the tag can be read. The purpose of using this test was to see if the RFID tag is damaged by the modification or manufacturing processes.

The same Alien ALN-9640 Higgs 3 tag is used in the same configurations as before. The materials are again Kevlar and Glass fiber reinforcement with an epoxy resin.

The experimental design is a 2 x 2 factorial with 2 factors for material and 5 factors for tags.

Experimental Units

5 samples of Kevlar reinforced polymer for each tag type

5 samples of glass reinforced polymer for each tag type

Factor A: Tag modification with levels

1 = perforated tag

2 = complete tag

3 = skeletonized tag

4 = feathered tag

5 = abraded tag

Factor B: Reinforcement type with levels

K = Kevlar

G = Glass

Treatments

The treatments are the factor level combinations. In this section of the experiments, the sets of treatments are K1, K2, K3, K4, K5 and G1, G2, G3, G4, G5. K and G correspond to Factor B: Reinforcement Types and 0, 1, 2, 3, 4, and 5 correspond to Factor A: Tag Types.

Response

Read Distance (in ft)

Goal

To determine at each tag level for each material type if the read distance of the samples with embedded tags are significantly different from each other.

Design

The total number of treatments is 5 * 2 = 10. 8 replications were performed for each treatment for a total of 80 parts that need to be run. The 8 replications were determined because of the number of samples that were available to be run. Each specimen was numbered in order to maintain traceability of the part.

Data was collected off from the RFID tag in the test specimen. The only recorded data was the RFID tag read distance based on one successful read within 5 seconds at each distance.

The test specimen come from the parts made for the compression and shear tests before they are destroyed.

The first set of statistics calculated were the mean, standard deviations, coefficient of variation, and the number of specimens for each material type and each tag type. In addition to the descriptive statistics, the ANOVA, time series plot, normal probability plot, and residuals versus fitted value plots were performed. Any abnormal data points were explored in order to define the abnormality.

Task 8 – Determine the economic viability of embedding RFID tags into a composite material.

Determine the costs incurred to setup an RFID enabled system to monitor the tags embedded into the FRP parts.

Costs are accumulated in the project in order to determine how much costs would be incurred to replicate the setup for this project. Major cost items include the readers, antennas, and tags. Other costs that are accounted for include the programming time for the reader and the programming of the tags.

Research Objective 3: Evaluate the impact of embedded RFID tags on life cycle analysis sustainability parameters.

Task 9 – Determine the Life Cycle Analysis sustainability parameters.

Determine the appropriate Life Cycle Analysis tools and understand the various aspects necessary to perform Life Cycle Analysis.

Utilizing literature and previous studies on composites and on electronics, the aspects needed to perform this type of analysis were better understood. The first step was to determine which type of analysis needed to be performed. Out of the several types of analyses available, the Tiered Hybrid method was selected due to the complexity it would allow for and the ability to include not only environmental costs (environmental and energy impact) but also costs of the entire supply chain and costs during useful life. Most of these costs fall into three main areas. Material Production and Manufacturing contains all information regarding the origination of the base materials, the manufacturing and assembly of the products, and all transportation and energy associated with the manufacture of these products. The Use contains the energy and costs associated with deploying the products, the costs of operating those products, and transportation of those products to their end use stations. The End of Life associates the energies and costs of transporting, disposing, recycling, or reusing the products once they've completed their initial useful life.

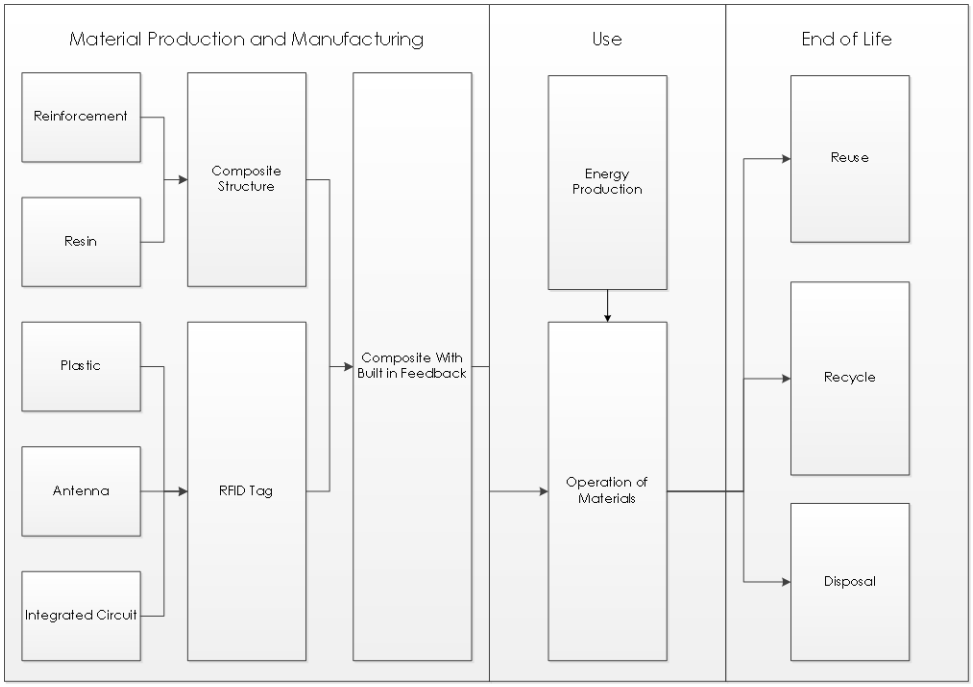

Figure 3-8: Material Layout for Life Cycle Analysis

Task 10 – Test and evaluate the Life Cycle Analysis sustainability parameters.

Perform Life Cycle Analysis on the glass and Kevlar FRP's and on the glass and Kevlar FRP's with embedded RFID tags.

For this project the open source program openLCA was utilized to build the life cycle analysis. Free databases were also utilized to cover items in the analysis such as transportation and for some of the materials. Other sources of data were estimated due to the lack of available and existing data needed for the full analysis.

All base materials are built into the LCA program. This includes defining the materials, their origination, their destination, the method of transportation, the energy needed to convert the material from one step to the next, the quantities produced and transported, the energy consumed during each process, and the environmental costs of

the materials and processes. Because most of this data is not readily available, the interactions between the different parts of the life cycle and their costs were defined.

3.2 Location of Experiments and Equipment Used

All manufacturing and testing of parts occurred at Tarleton State University in the Engineering Technology labs. The labs used were the composites lab, where the manufacturing of the test parts occurred, the materials lab, where the curing and testing occurred, and the controls lab where the tags were programmed and signal strengths were observed. There is a variety of equipment used in each lab that will be defined in the following sections.

3.2.1 Composites Lab

- Aluminum plate used as layup tools
- Kiln
- Vacuum pump
- Consumable materials

3.2.2 Materials Lab

- Universal testing machine
- Computer
- Test Fixtures for compression and shear testing

3.2.3 Controls Lab

- Alien 9600+ reader
- Alien ALR-8696-C circular antenna
- Computer using Alien's RFID Gateway v2.23.01 software

Data analysis for the experiments occurred at both Tarleton and at the University of Texas Arlington using Excel, Minitab, and SAS.

Chapter 4

Results

This chapter discusses the analysis performed on the data from the experiments. The first section discuss the simulations that were performed for compression and then evaluates the actual mechanical testing performed on the parts. The second section looks at the simulations and mechanical testing performed for the shear testing. The simulations provided a likely location for the failure in the materials during the tests. The tests defined how the embedded electronics affected the FRP's structure. The third section evaluates the impact that the tags and the materials had on the RFID tags' read distances. The last section discusses the work performed on the Life Cycle Analysis. This research sets up what the flowchart for the supply chain processes look like.

4.1 Mechanical Analysis Simulation

4.1.1 Compression Test

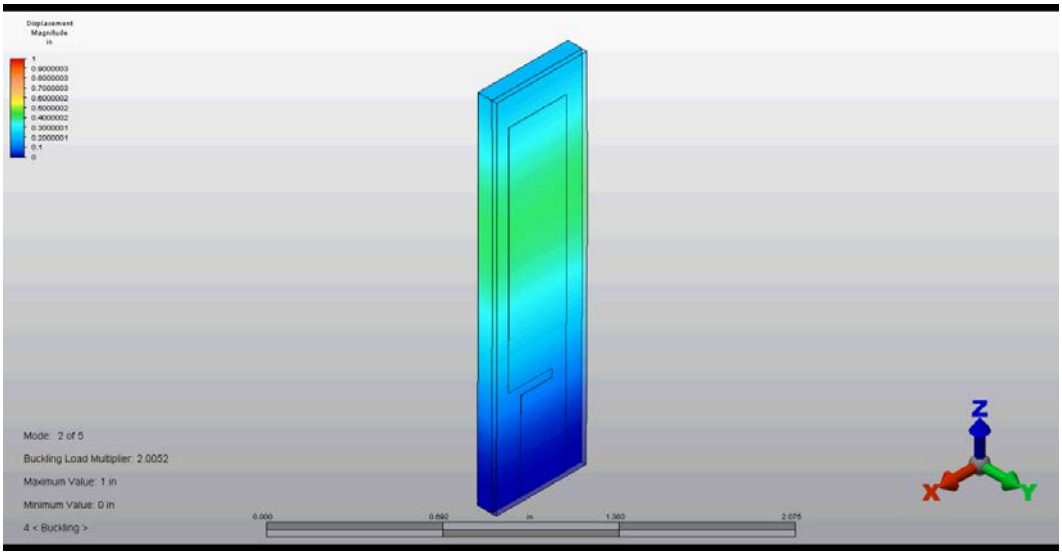

Figure 4-1: Compression Simulation of Glass Reinforced Epoxy

The compression simulation for the glass reinforced epoxy shows the maximum movement of the material. This information signifies where the break in the material can be expected to occur as indicated in this simulation as the green area. The displacement of the material is approximately 0.40 inches at the defined location.

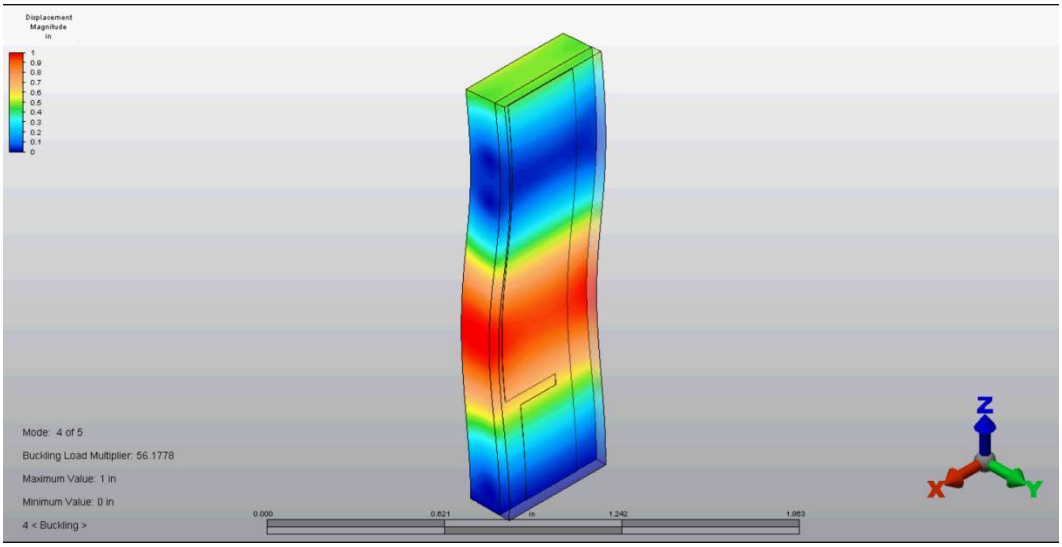

Figure 4-2: Compression Simulation of Kevlar Reinforced Epoxy

The compression simulation for the Kevlar reinforced epoxy also shows the maximum movement of the material. This information signifies where the break in the material can be expected to occur as indicated in this simulation as the red area. Of interest is the amount of movement in the material compared to the glass simulation. The Kevlar under the same load will displace up to 1 inch. Most of this can be explained due to the properties that Kevlar exhibits, specifically the elastic property being better than glass.

Figure 4-3: Glass Test Specimen from Compression Tests

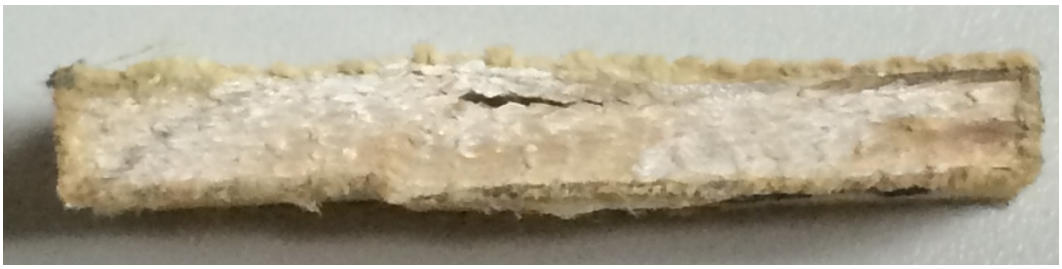

Figure 4-4: Kevlar Test Specimen from Compression Tests

During the compression tests, parts typically failed at the location shown in the simulations. One of the interesting results of the tests that did not show up in the simulations run was that the failure occurred between the RFID tag and the PET backing material on the tag. This leads to the belief that from the compression tests and simulations that the epoxy bond to the RFID tag is not the biggest contributor to failure during the tests.

Compression Testing

Table 4-1: Descriptive Statistics for Glass Fiber Reinforced Epoxy

Variable	Glass Tag Type	Total Count	Mean	Standard Deviation	Coefficient of Variance
Glass Compression (psi)	0	5	15469	487	3.15
	1	5	17857	1099	6.15
	2	5	13429	1228	9.15
	3	5	14732	3183	21.60
	4	5	18508	1779	9.61
	5	5	13092	1410	10.77

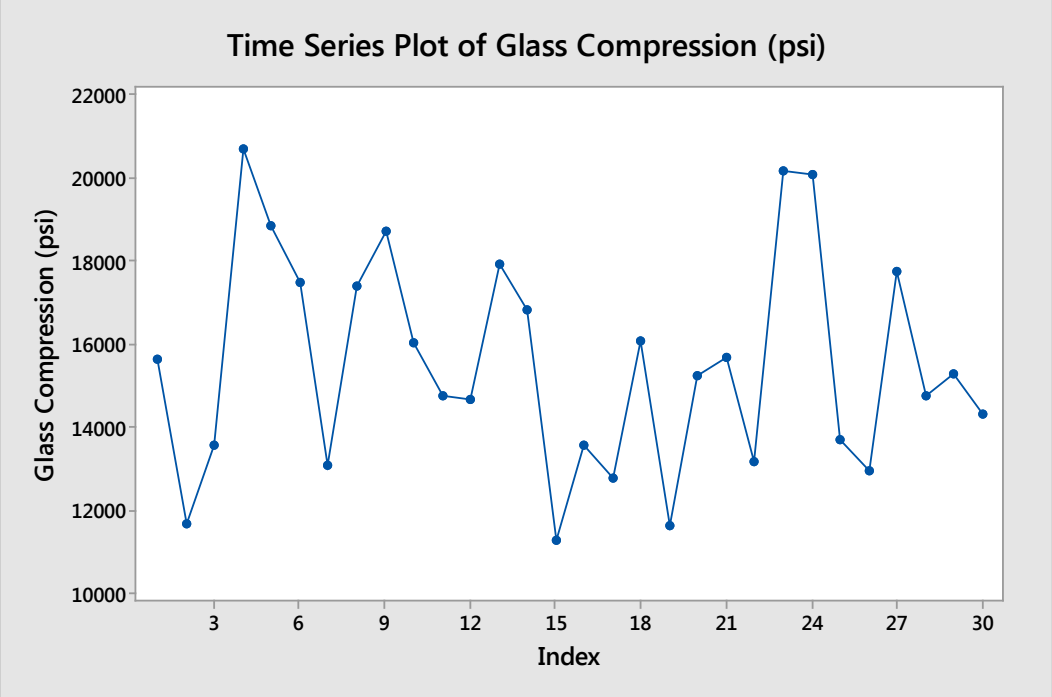

Figure 4-5: Time Series Plot of Glass Fiber Reinforced Epoxy

The random jaggedness of the time series plot shows that there are not trends in the data. This shows that the data is random and that there is not a serial correlation between the data points. The mean data shows that two of the specimen with embedded tags had a higher compression strength than the control. These were the perforated and feathered tags. The control specimen that did not have an embedded tag seemed to test more repeatedly.

One-way ANOVA: Glass Compression (psi) versus Glass Tag Type

Null hypothesis – H_0: All compression strength means are equal

Alternative hypothesis – H_A: At least one mean is different

Significance level $\alpha = 0.05$

Table 4-2: Factor Information for RFID Tags in Glass Fiber Reinforced Epoxy

Factor	Levels	Values
Glass Tag Type	6	0, 1, 2, 3, 4, 5

Table 4-3: Compression Test ANOVA for Glass Fiber Reinforced Epoxy

Source	DF	Adj SS	Adj MS	F-Value	p-Value
Glass Tag Type	5	126398637	25279727	8.32	0.000
Error	24	72934581	3038941		
Total	29	199333217			

Upon evaluating the F-value, the ANOVA yields a value of 8.32. This is larger than the values from the F distribution of 2.62. This results in rejecting the null hypothesis and that at least one of the means is different. The p-value reinforces the rejection of the null hypothesis since the 0.000 in the ANOVA is less than the α of 0.05. This also means that constant variance is not satisfied in the data.

Table 4-4: Model Summary

S	R-sq	R-sq(adj)	R-sq(pred)
1743.26	63.41%	55.79%	42.83%

Table 6identifies the R2 of the model. Because the value is somewhat low, it can be assumed that the derived model does not define the data very well.

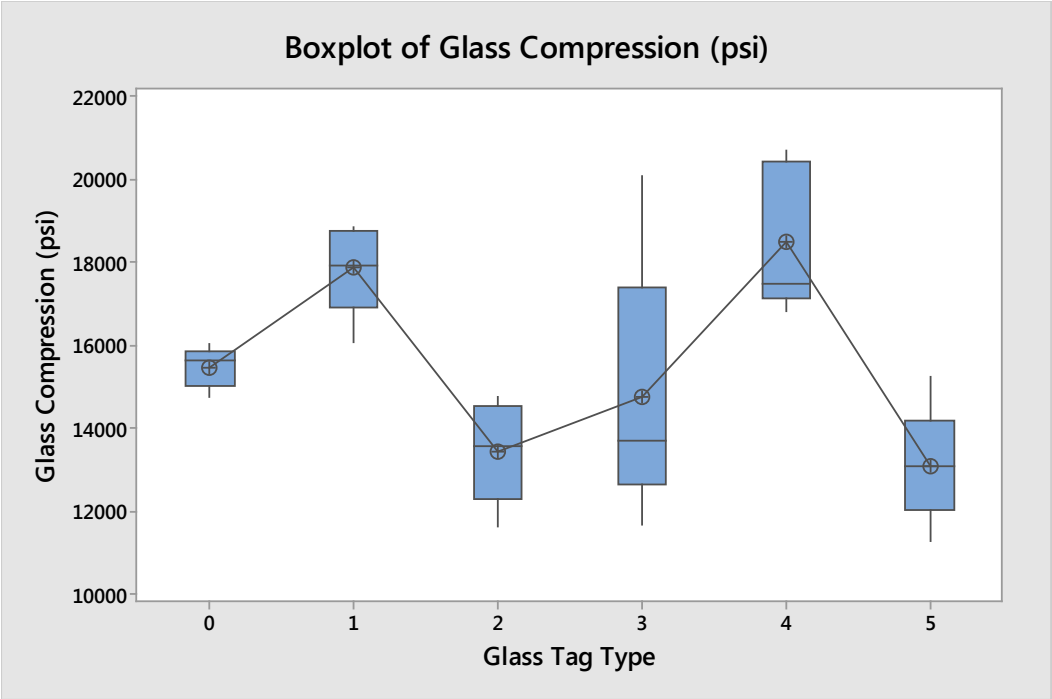

Figure 4-6: Boxplot of Glass Compression Test Data

The boxplot of the data from the compression test is shown in Figure 4-13. The boxplot shows the means and the quartiles of the results for each tag type. Tags 1 and 4 appear to be different than the other three tags and the control.

Table 4-5: Glass Compression Data Means

Glass Tag Type	N	Mean	Standard Deviation	95% CI
0	5	15469	487	(13860, 17078)
1	5	17857	1099	(16248, 19466)
2	5	13429	1228	(11820, 15038)
3	5	14732	3183	(13123, 16341)
4	5	18508	1779	(16899, 20117)
5	5	13092	1410	(11483, 14701)

Tukey Pairwise Comparisons

Table 4-6: Grouping Information Using the Tukey Method at 95% Confidence

Glass Tag Type	N	Mean	Grouping
4	5	18508	A
1	5	17857	AB
0	5	15469	ABC
3	5	14732	BC
2	5	13429	C
5	5	13092	C

Means that do not share a letter are significantly different.

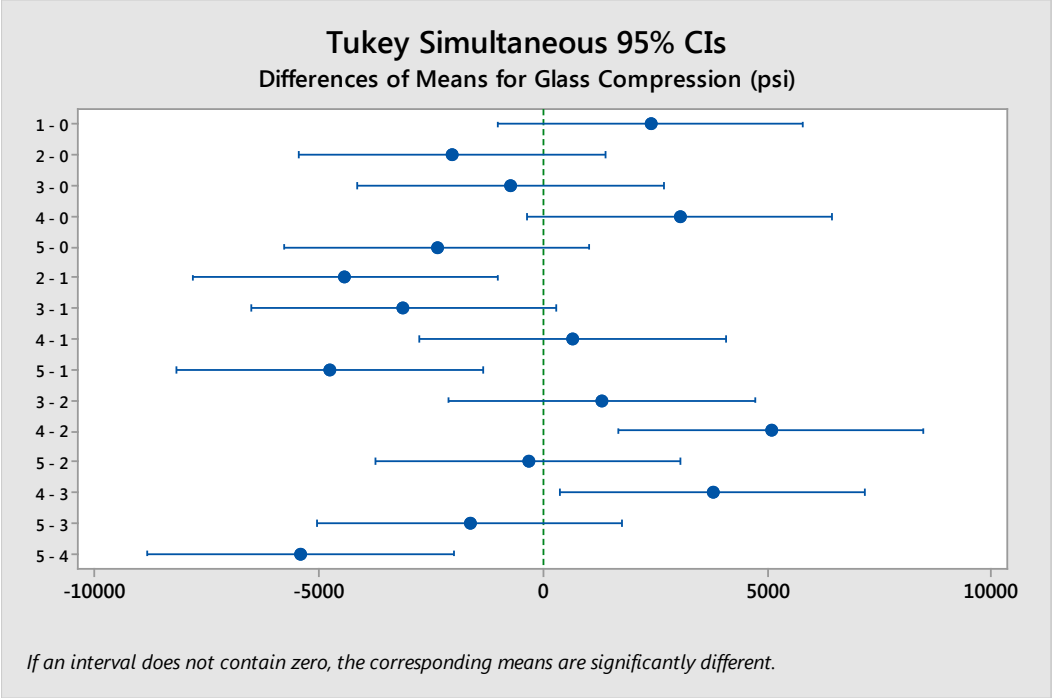

Figure 4-7: Tukey 95% Confidence Interval

The Tukey confidence intervals identify which tag types can be grouped with each other. In this analysis, tags 4, 1, and 0 are similar, tags 1, 0, and 3 are similar, and

tags 0 3, 2, and 5 are similar. This indicates not only that there are different means but which means are the most closely associated with each other.

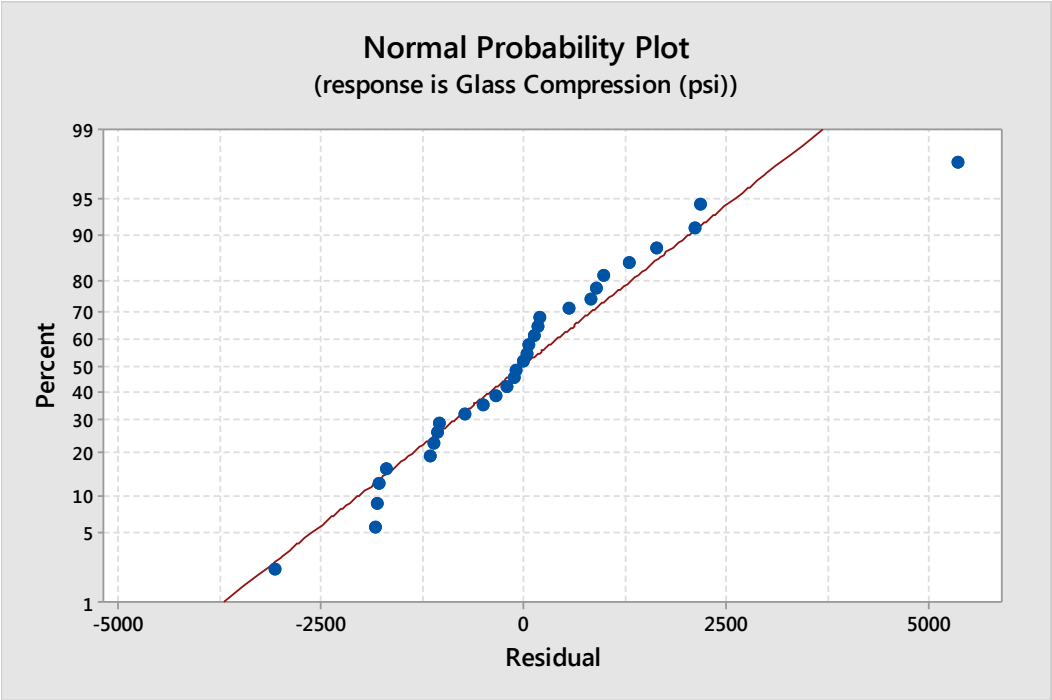

Figure 4-8: Normal Probability Plot for Glass Compression Data

The normal probability plot shows that the data is somewhat normally distributed. There is one data point that appears to be significantly different than the other data points. It will be evaluated as an outlier though it did not register as one during the boxplot.

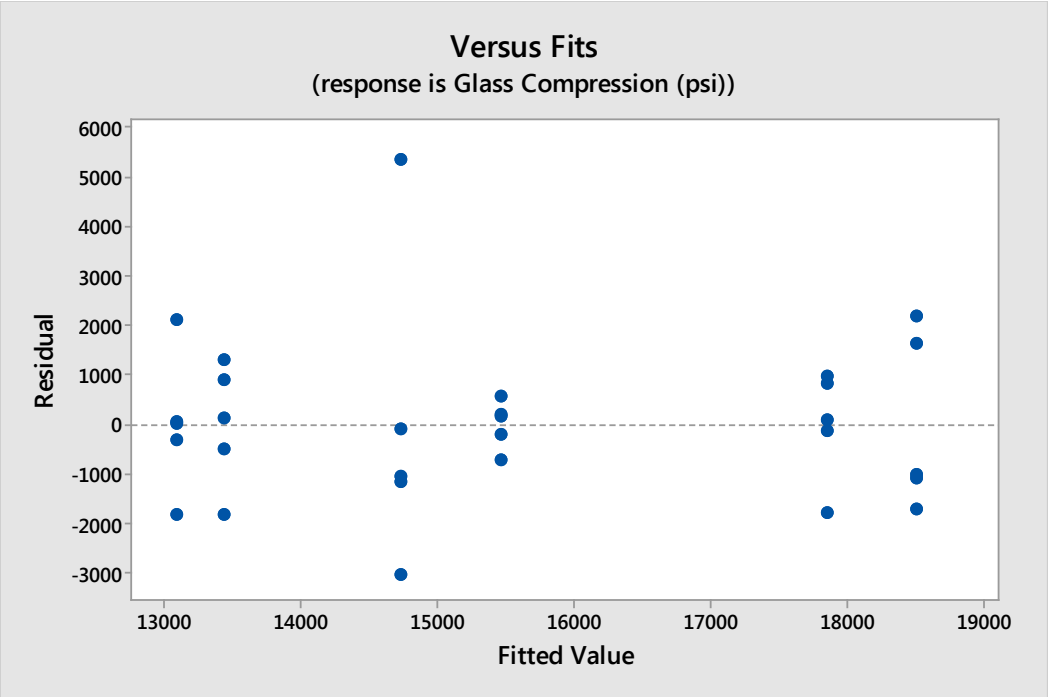

Figure 4-9: Residuals vs. Fitted Values Plot for Glass Compression

The Residuals vs. Fitted Values Plot shows mostly constant variance in the data. One point appears as an outlier and needs to be evaluated further.

Table 4-7: Descriptive Statistics for Kevlar Fiber Reinforced Epoxy

Variable	Glass Tag Type	Total Count	Mean	Standard Deviation	Coefficient of Variance
Kevlar Compression (psi)	0	5	10501	478	4.55
	1	5	12603	288	2.28
	2	5	10128	794	7.84
	3	5	10186	845	8.29
	4	5	12043	584	4.85
	5	5	9812	187	1.91

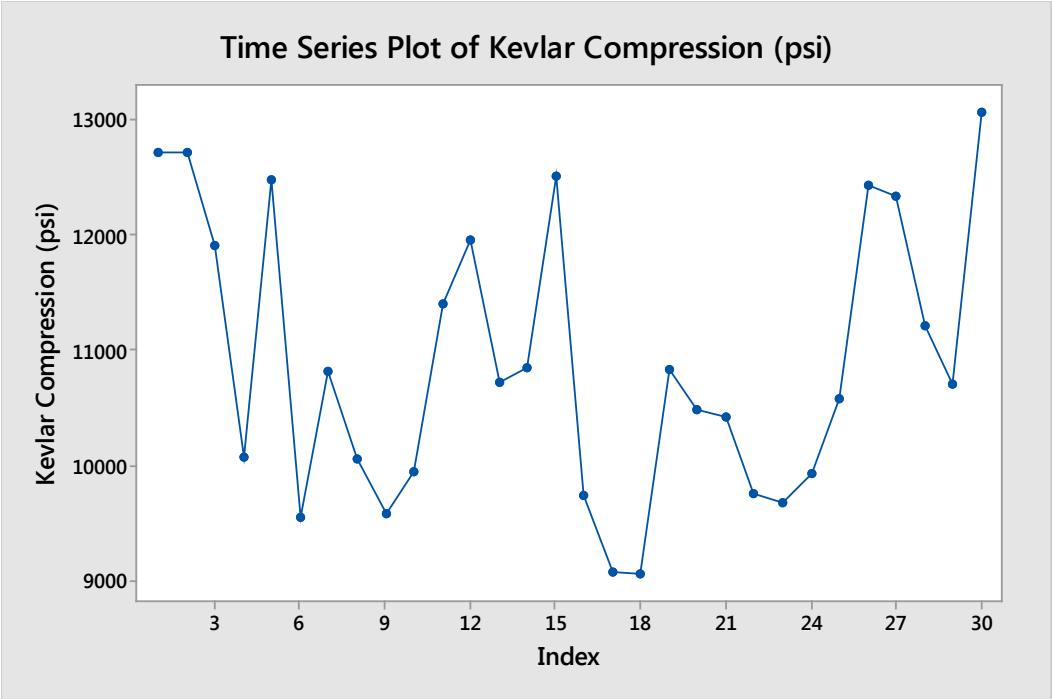

Figure 4-10: Time Series Plot of Kevlar Fiber Reinforced Epoxy

The Kevlar fiber reinforced epoxy also shows random jaggedness and a lack of serial correlation between the data points. The means appear to be somewhat consistent with each other though the means for specimen 1 and 4 are higher.

One-way ANOVA: Kevlar Compression (psi) versus Kevlar Tag Type

Null hypothesis All means are equal

Alternative hypothesis At least one mean is different

Significance level $\alpha = 0.05$

Table 4-8: Factor Information for RFID Tags in Kevlar Fiber Reinforced Epoxy

Factor	Levels	Values
Kevlar Tag Type	6	0, 1, 2, 3, 4, 5

Table 4-9: Compression Test ANOVA for Kevlar Fiber Reinforced Epoxy

Source	DF	Adj SS	Adj MS	F-Value	p-Value
Kevlar Tag Type	5	33268423	6653685	19.66	0.000
Error	24	8123900	338496		
Total	29	41392324			

Evaluating the F-value in the ANOVA yields a value of 19.66. This is larger than the values from the F distribution of 2.62. Because of this the null hypothesis is rejected and at least one of the means is different. The p-value of 0.000 is less than the α of 0.05 so the null hypothesis is again rejected and the constant variance is not satisfied in the data.

Table 4-10: Model Summary

S	R-sq	R-sq (adj)	R-sq(pred)
581.804	80.37%	76.28%	69.33%

The R-sq value for the Kevlar Reinforced data is at 80%. The model is a decent indicator of the data points.

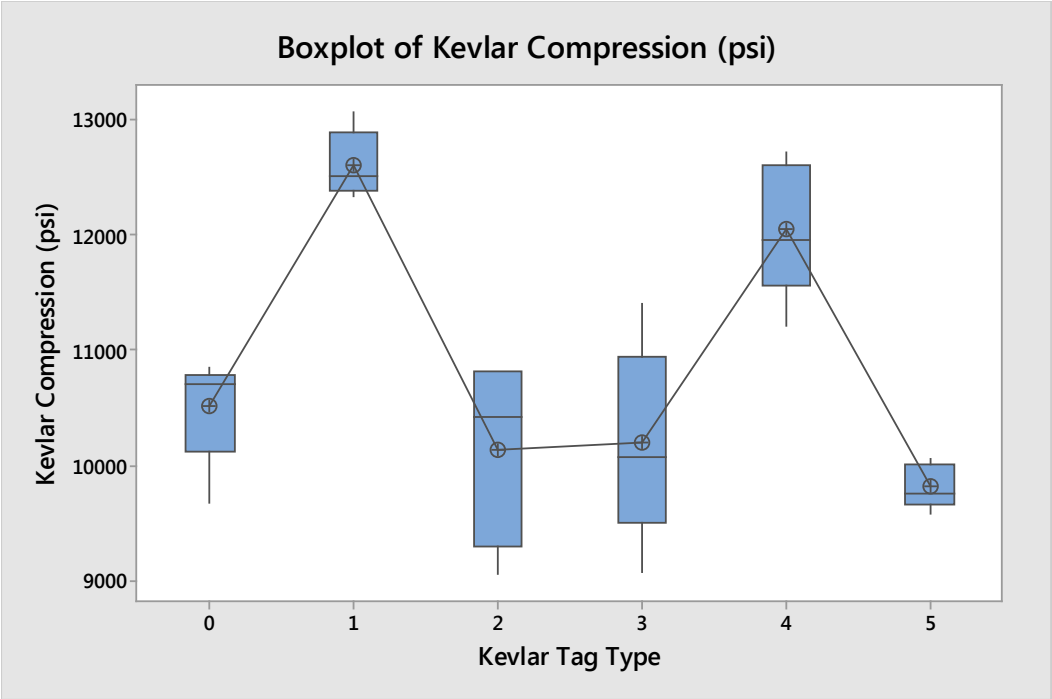

Figure 4-11: Boxplot of Kevlar Fiber Reinforced Epoxy

In Figure 4-11, tags 1 and 4 appear to be considerably different than the other tags. In this case they have a higher compression strength than the control and the other three tag types.

Table 4-11: Kevlar Compression Data Means

Kevlar Tag Type	N	Mean	Standard Deviation	95% CI
0	5	10501	478	(9964, 11038)
1	5	12603	288	(12066, 13140)
2	5	10128	794	(9591, 10665)
3	5	10186	845	(9649, 10723)
4	5	12043	584	(11506, 12580)
5	5	9812	187	(9275, 10349)

Tukey Pairwise Comparisons

Table 4-12: Grouping Information Using the Tukey Method at 95% Confidence

Kevlar Tag Type	N	Mean	Grouping
1	5	12603	A
4	5	12043	A
0	5	10501	B
3	5	10186	B
2	5	10128	B
5	5	9812	B

Means that do not share a letter are significantly different.

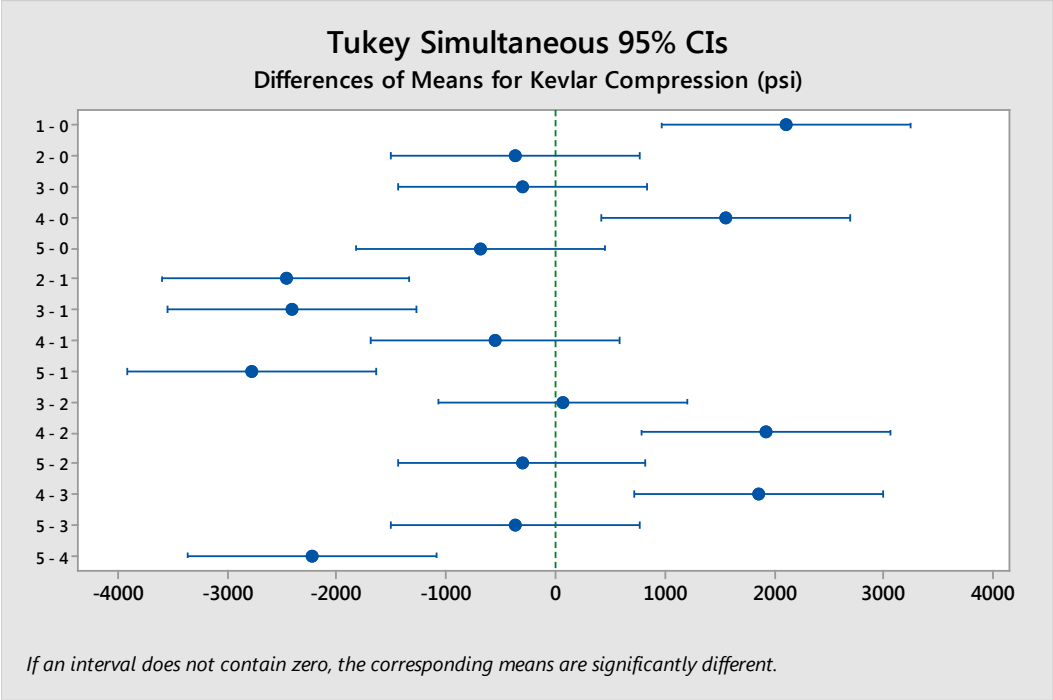

Figure 4-12: Tukey 95% Confidence Interval

In the Kevlar analysis, tags 4 and 1are similar to each other while tags 0, 3, 2, and 5 are similar to one another. This validates what was assumed when the means

were looked at earlier in the results. It is also interesting that tags 0, 3, 2, and 5 were similar in the data analysis for the RFID tags embedded in glass.

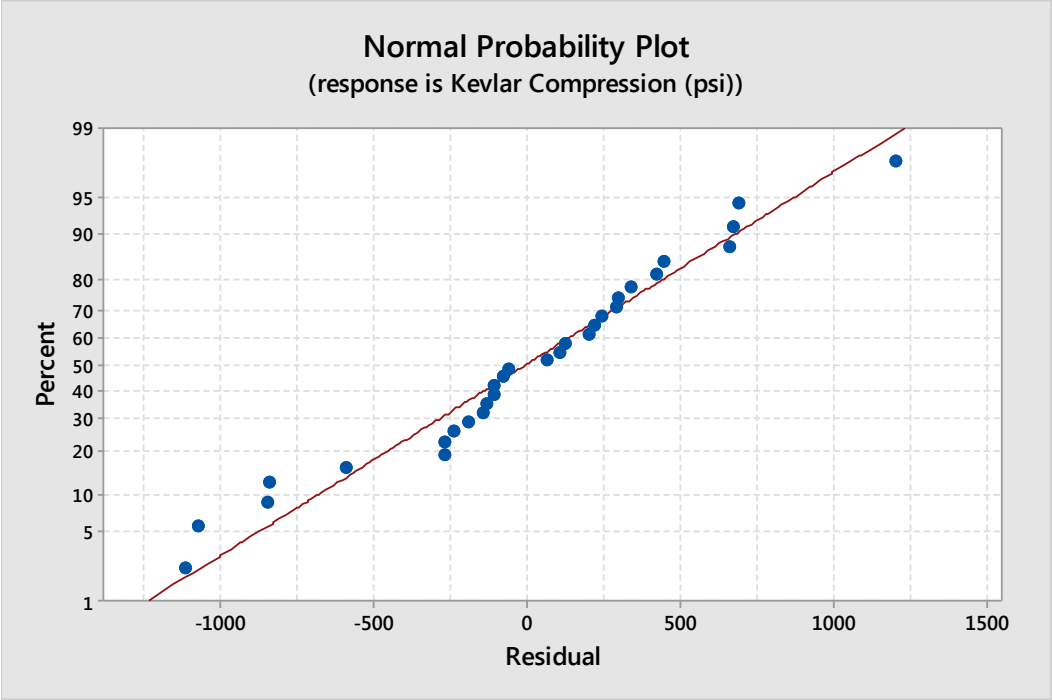

Figure 4-13: Normal Probability Plot for Kevlar Compression Data

The normal probability plot shows that the data is normally distributed. All points lie linearly along the reference line.

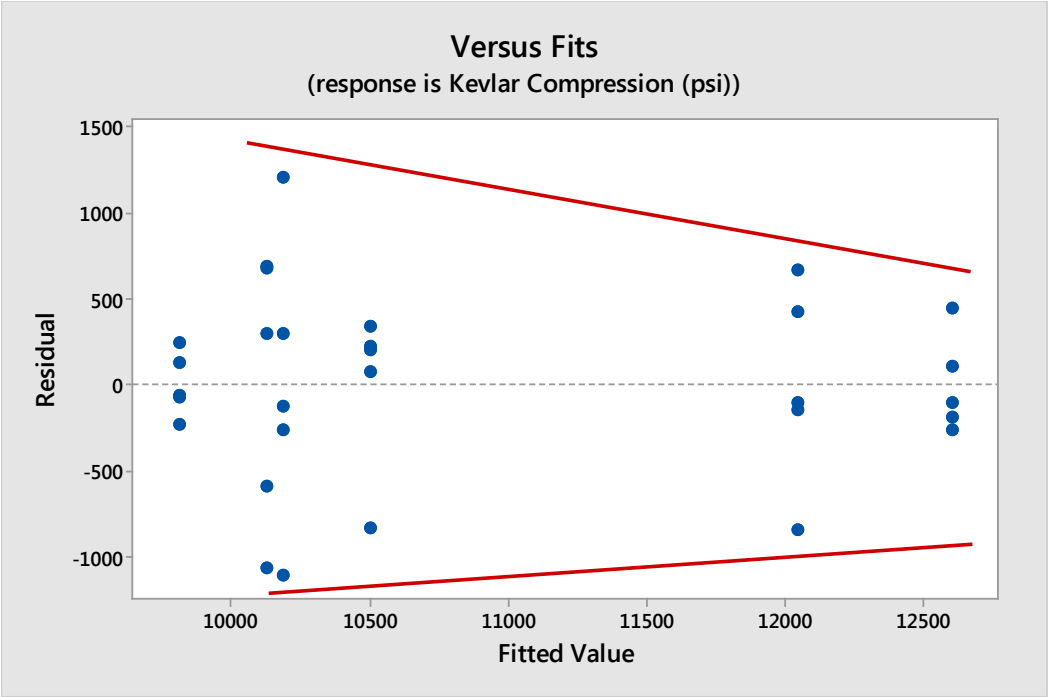

Figure 4-14: Residuals vs. Fitted Values Plot for Kevlar Compression

The Residuals versus Fitted Values Plot appears to show non constant variance in the data. Because of this, the Box-Cox transformation is performed. A $\lambda = 3$ is calculated and yields the graph shown in Figure 4-22. It exhibits a smaller funnel effect than the initial plot but upon evaluation of the transformed ANOVA our F-value is still greater than the 2.62 and the p-value is still less than the α of 0.05. This results in the need to still reject the H_0 and that the means of the Kevlar Tag Types are different.

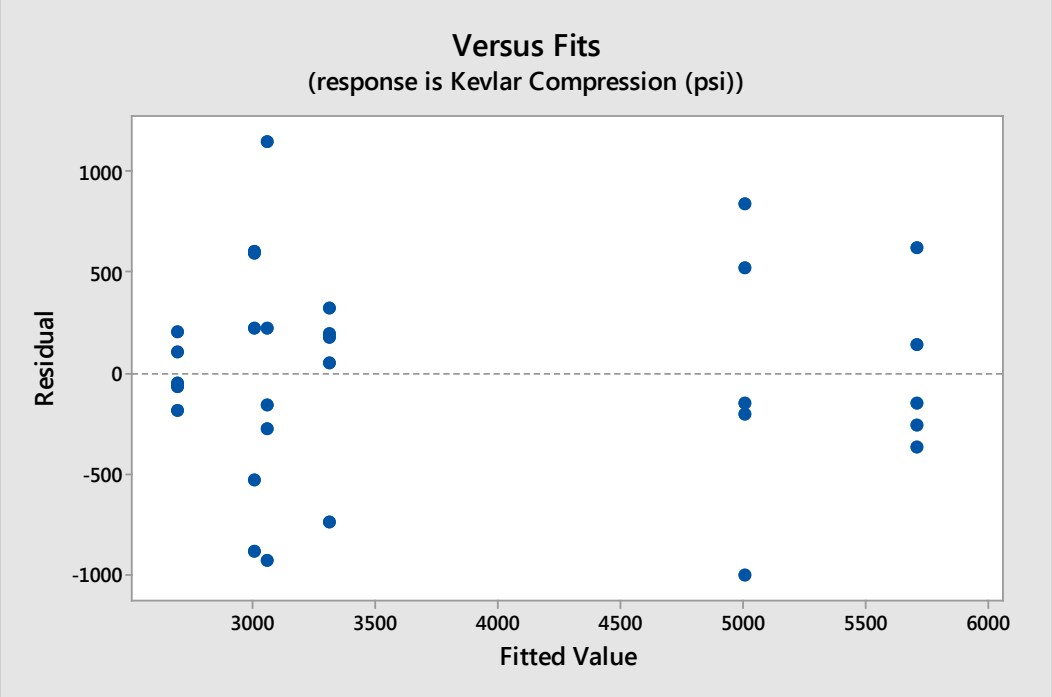

Figure 4-15: Transformed Residuals vs. Fitted Values Plot

Material Type and Tag Type Compression Strengths

Hypothesis:

H_0: There is no significant difference between part i on parameter j.

Where:

i is the material type

j is the compression strength

H_A: There is a significant difference between part i on parameter j.

The hypothesis will be tested at $\alpha = 0.30$

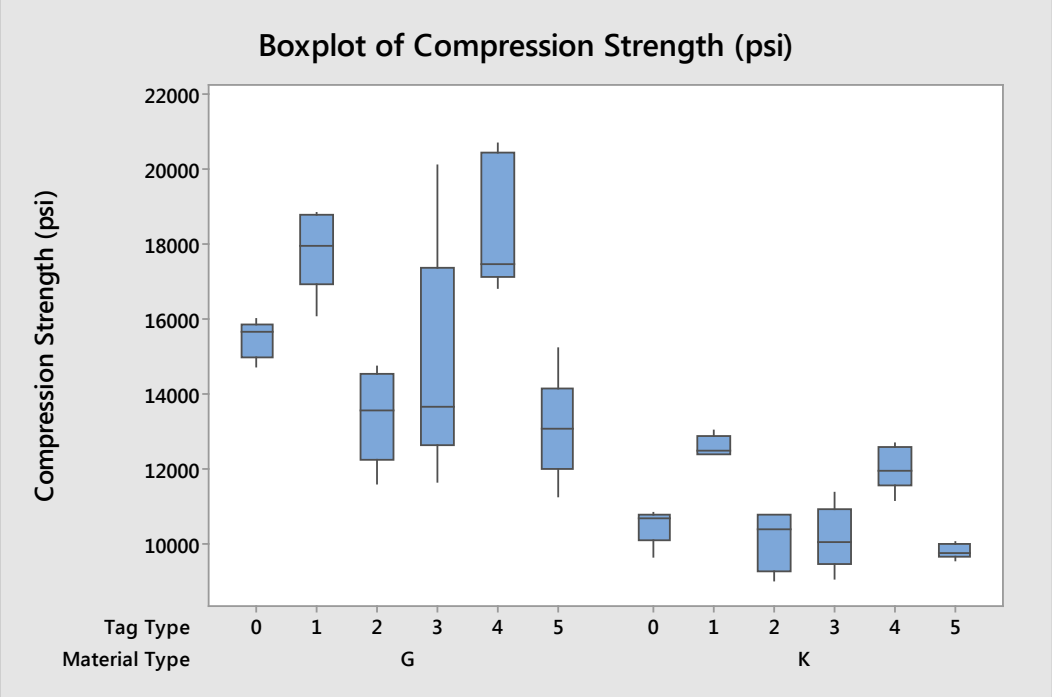

Figure 4-16: Boxplot of Compression Strengths

Categorical predictor coding (-1, 0, +1)

Table 4-13: Analysis of Variance

Source	DF	Adj SS	Adj MS	F-Value	P-Value
Regression	6	463387093	77231182	41.05	0.000
Material Type	1	322381432	322381432	171.34	0.000
Tag Type	5	141005661	28201132	14.99	0.000
Error	53	99719880	1881507		
Lack-of-Fit	5	18661398	3732280	2.21	0.069
Pure Error	48	81058481	1688718		
Total	59	563106973			

Upon evaluating the ANOVA for the compression strengths of material types and the tag types, the F-values are higher than the F distribution value of 1.25. In this instance the null hypothesis is rejected and the alternative hypothesis is used. For these

calculations, there is a significant difference between the material types and at least one of the tag types in the compression tests.

Table 4-14: Model Summary

S	R-sq	R-sq (adj)	R-sq(pred)
1371.68	82.29%	80.29%	77.30%

Table 4-15: Variables Used in Determining Compression Strength from Material and Tag Type

Variable	Coefficient	SE Coefficient	T	p-value
Constant	13197	177	74.52	0.000
Glass	2318	177	13.09	0.000
Kevlar	-809.5	177	13.09	0.000
Tag 0	-212	396	-0.53	0.595
Tag 1	2033	396	5.13	0.000
Tag 2	-1418	396	-3.58	0.001
Tag 3	-738	396	-1.86	0.068
Tag 4	2079	396	5.25	0.000
Tag 5	-1745	99.4	-4.41	0.000

Regression Equation

Compression Strength (PSI) = 13197 + 2318 Glass - 2318 Kevlar - 212 Tag 0 + 2033 Tag 1 - 1418 Tag 2 - 738 Tag 3 + 2079 Tag 4 - 1745 Tag 5

Table 4-16: Fits and Diagnostics for Unusual Observations

Observation	Shear Strength (PSI)	Fit	Residual	Std Residual
4	11676	14777	-3101	-2.41 R
6	20696	17594	3102	2.41 R
49	20090	14777	5313	4.12 R

R Large residual

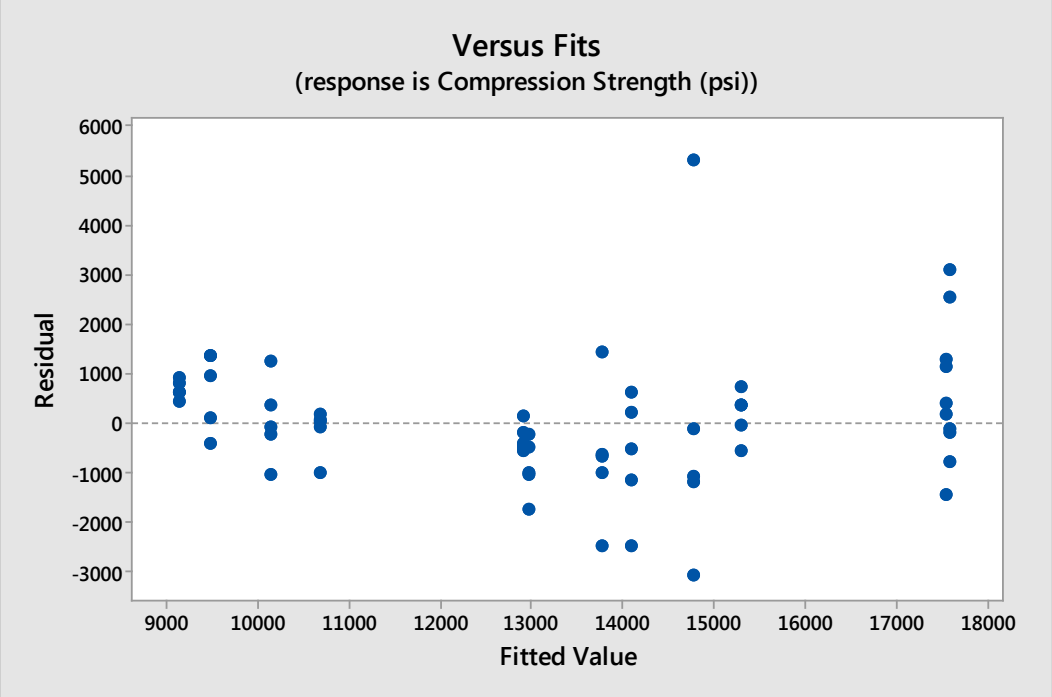

Figure 4-17: Residuals vs. Fitted Values Plot

The residuals versus fitted values plot has some funneling hinting at non constant variance in the data.

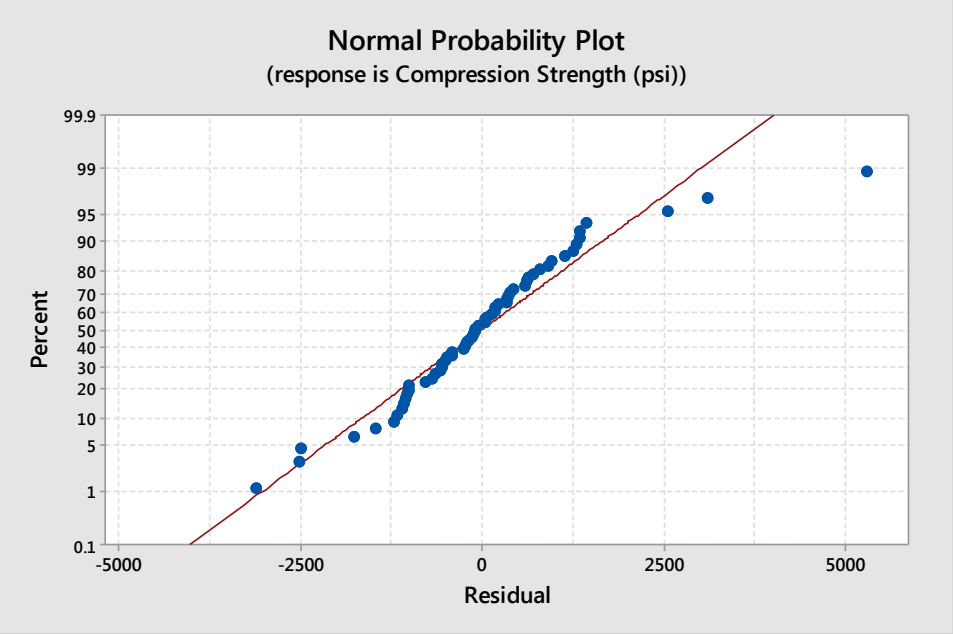

Figure 4-18: Normal Probability Plot

The normal probability plot has a short tail on the right side exhibiting a standard uniform distribution.

4.1.2 Shear Test

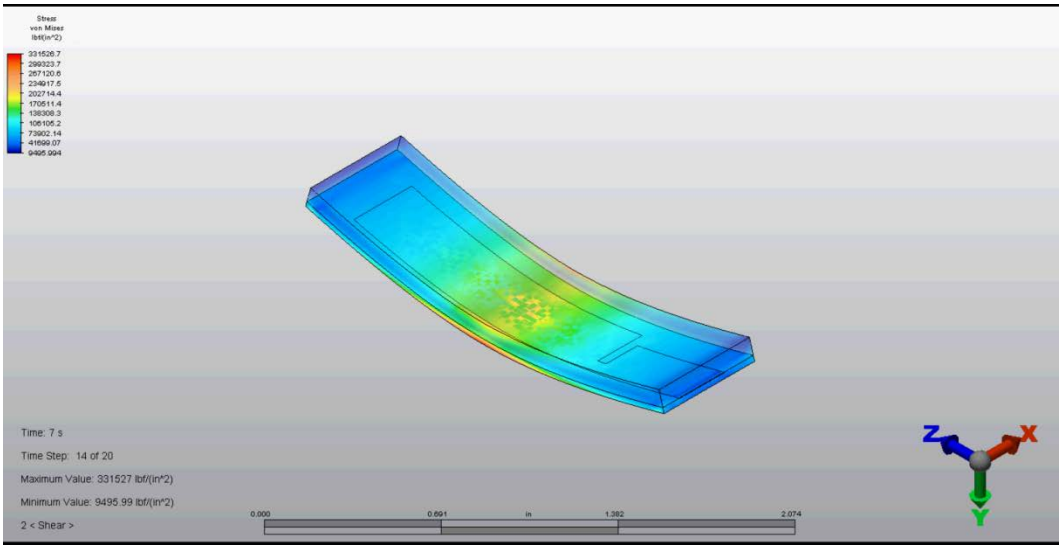

Figure 4-19: Shear Simulation of Glass Reinforced Epoxy

The shear simulation for the glass reinforced epoxy shows the maximum movement of the material and the total forces built up in the part during loading. Again, this information is used to signify where the break in the material can be expected to occur as indicated in this simulation as the yellow and orange areas. Shear applies both tension and compression to the test specimen. Where they are in equilibrium tends to be the location of failure. In this simulation, the 1200 pound load induced a maximum stress of approximately 343,400 psi. The actual test specimen failed at closer to 350 pounds and only saw up to approximately 5100 psi.

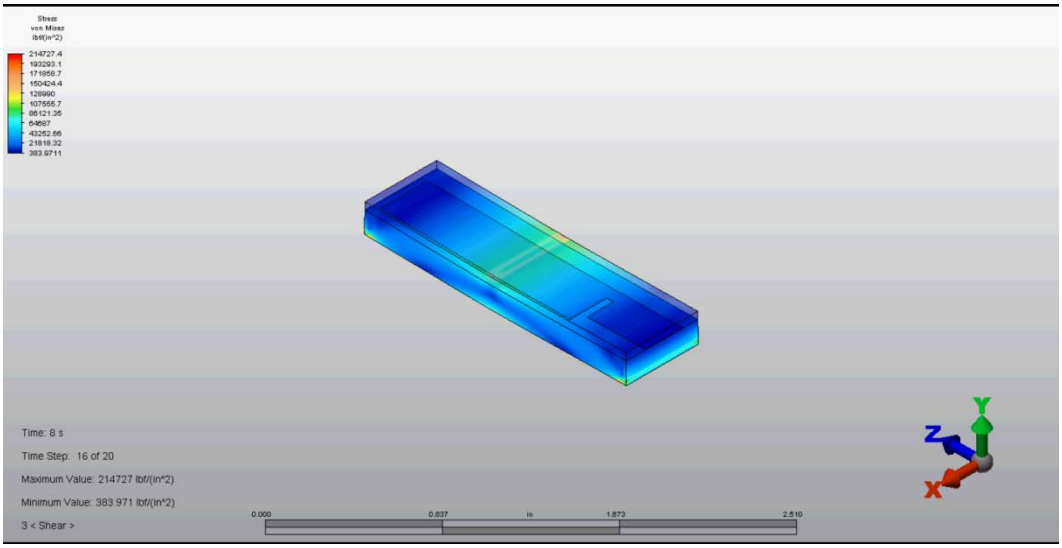

Figure 4-20: Shear Simulation of Kevlar Reinforced Epoxy

The shear simulation for the Kevlar reinforced epoxy shows the maximum movement of the material and the total forces built up in the part during loading. Where the break in the material can be expected to occur is indicated in this simulation as the yellow, orange, and red areas. In this simulation, the 1200 pound load induced a maximum stress of approximately 201,200 psi. The actual test specimen failed at closer to 370 pounds and only saw up to approximately 3000 psi.

The actual tests yield similar failure points. Most failures were flexure failure where the part failed because of tension on the bottom or compression on the top. Because of the speed of the test, most parts exhibited both failures.

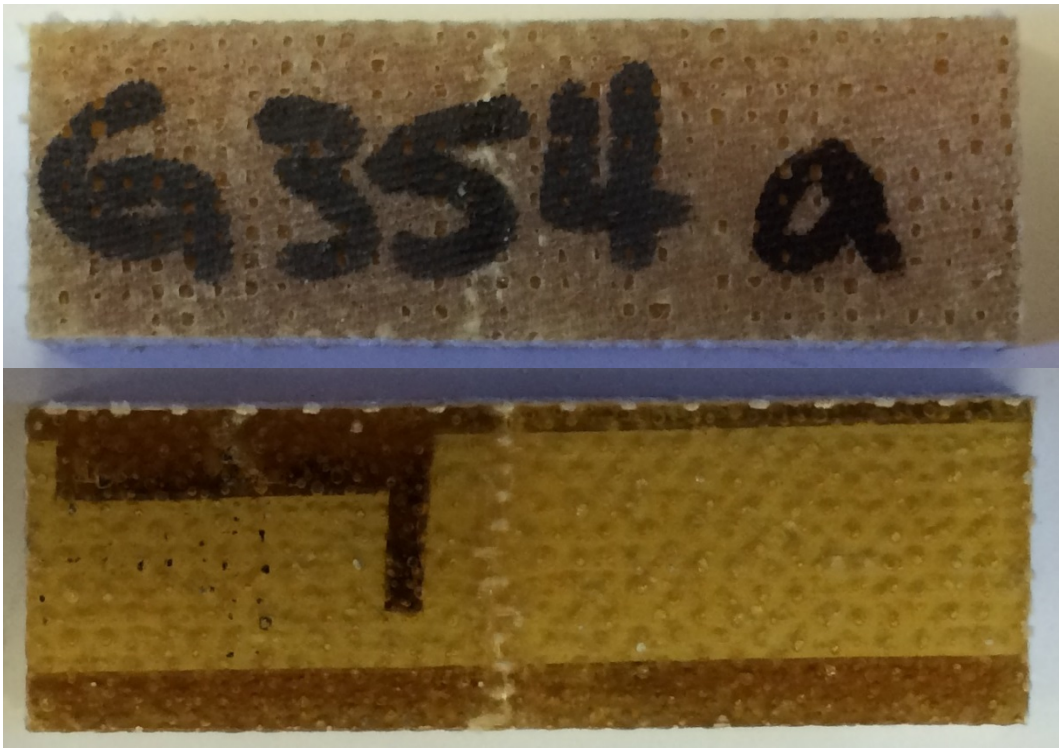

Figure 4-21: Fluxure Failure in Glass Fiber Reinforced Epoxy

There were some parts failures that are classified as interlaminar shear failures. These parts failed between the layers of reinforcement. Upon further evaluation, the interlaminar shear failures occurred within the RFID tag and the PET backing material. This proves that the epoxy to tag bond was not the weakest bond in the material.

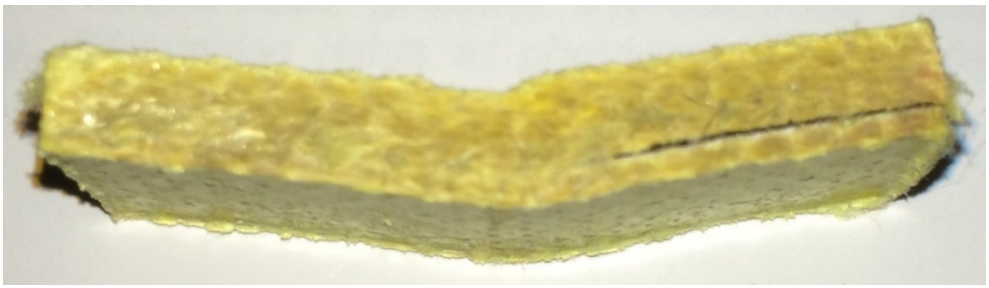

Figure 4-22: Interlaminar Shear Failure in Kevlar Reinforced Epoxy

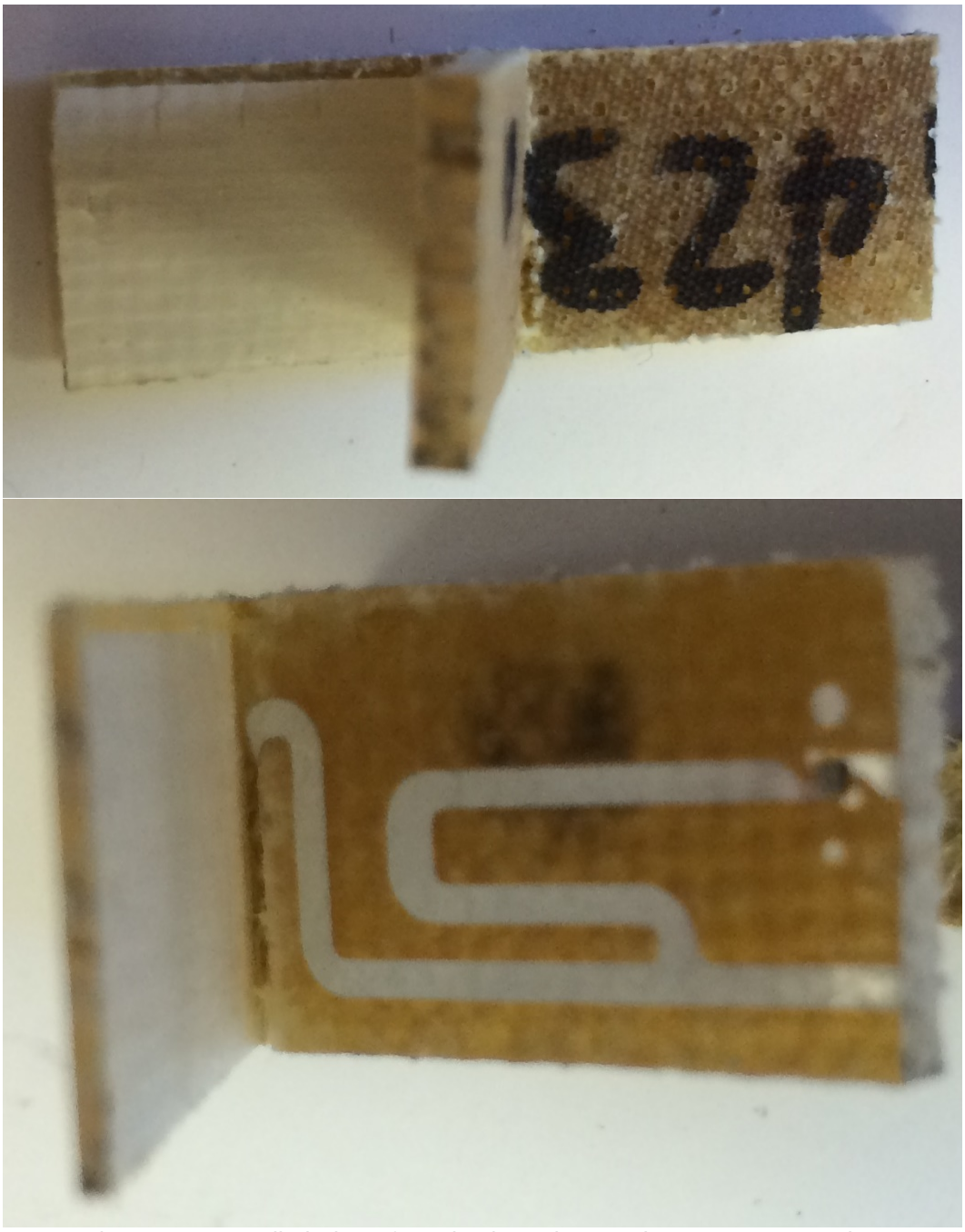

Figure 4-23: Detailed View of Interlaminar Shear at the RFID Tag Location

Table 4-17: Descriptive Statistics for Glass Fiber Reinforced Epoxy

Variable	Glass Tag Type	Total Count	Mean	Standard Deviation	Coefficient of Variance
Glass Shear Strength (psi)	0	5	4996.1	171.5	3.43
	1	5	3564	403	11.32
	2	5	3776	609	16.13
	3	5	3951	558	14.12
	4	5	3816	485	12.71
	5	5	3712	349	9.40

For the glass specimen, the control yielded an average shear strength of 4996.1 psi. This appears to be considerably higher than the test specimen that had the RFID tag included in the material. The standard deviation and the coefficient of variation are also considerably smaller than the other test specimen which leads to the belief that the measurements were more consistent.

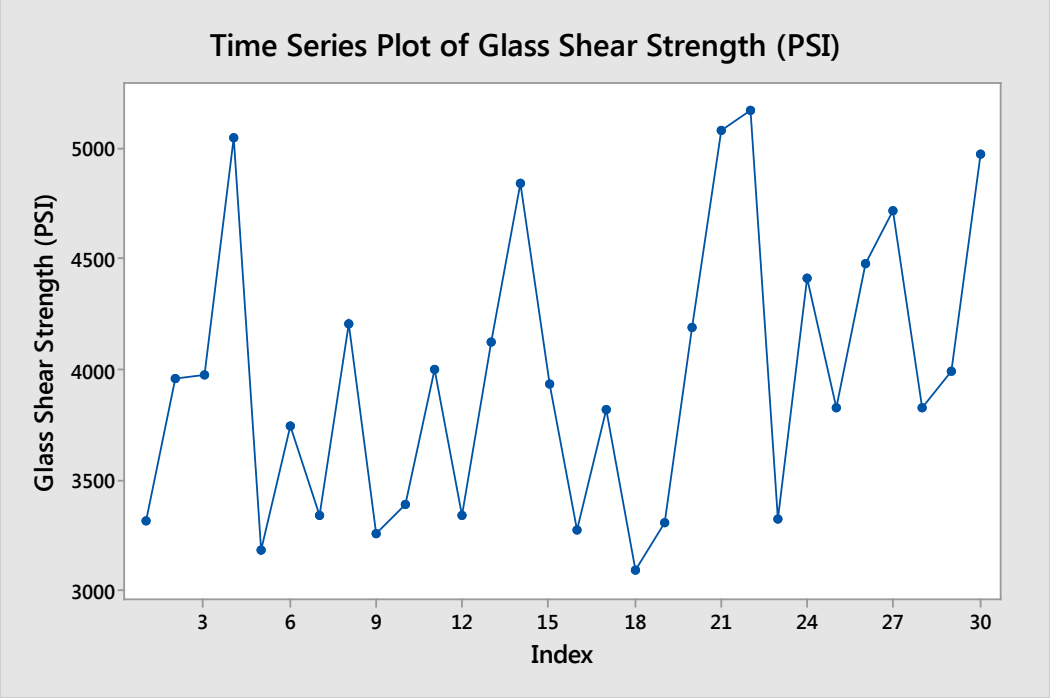

Figure 4-24: Time Series Plot of Glass Fiber Reinforced Epoxy

One-way ANOVA: Glass Shear Strength (PSI) versus Tag Family

Null hypothesis All means are equal

Alternative hypothesis At least one mean is different

Significance level $\alpha = 0.05$

Table 4-18: Factor Information for RFID Tags in Glass Fiber Reinforced Epoxy

Factor	Levels	Values
Glass Tag Type	6	0, 1, 2, 3, 4, 5

Table 4-19: Compression Test ANOVA for Glass Fiber Reinforced Epoxy

Source	DF	Adj SS	Adj MS	F-Value	p-Value
Kevlar Tag Type	5	6729905	1345981	6.56	0.001
Error	24	4924456	205186		
Total	29	11654361			

Table 4-20: Model Summary

S	R-sq	R-sq (adj)	R-sq(pred)
452.974	57.75%	48.94%	33.98%

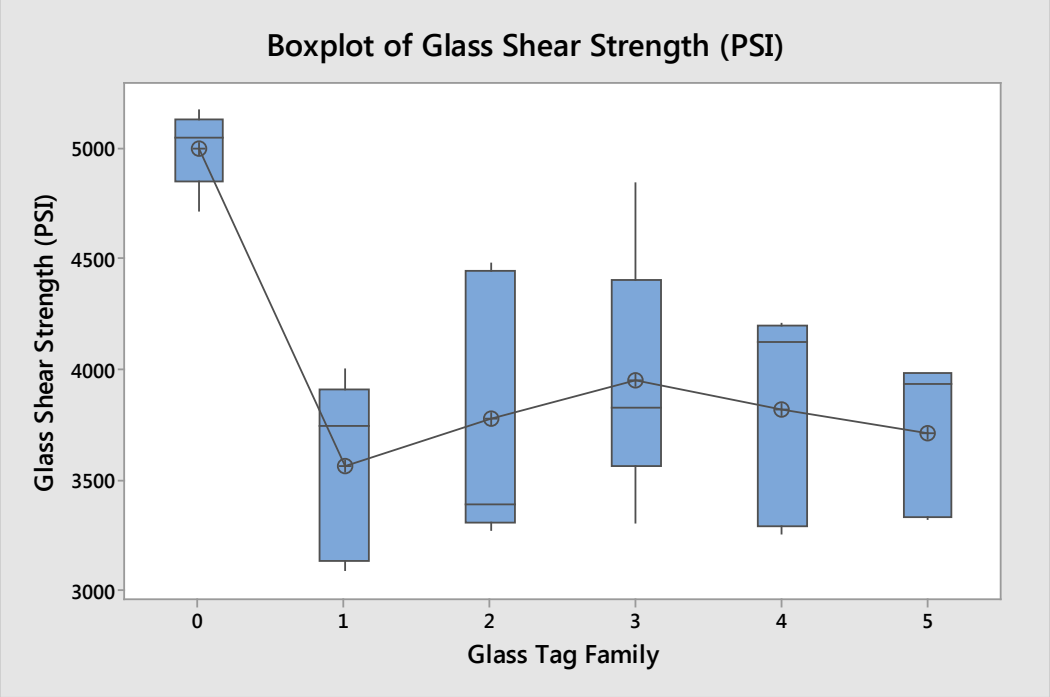

Figure 4-25: Boxplot of Glass Shear Test Data

Table 4-21: Glass Shear Data Means

Tag Type	N	Mean	Standard Deviation	95% CI
0	5	4996	171	(4578, 5414)
1	5	3564	403	(3146, 3982)
2	5	3776	609	(3358, 4194)
3	5	3951	558	(3533, 4369)
4	5	3816	485	(3398, 4234)
5	5	3712	349	(3293, 4130)

Tukey Pairwise Comparisons

Table 4-22: Grouping Information Using the Tukey Method at 95% Confidence

Glass Tag Type	N	Mean	Grouping
0	5	15276	A
3	5	15230	B
4	5	12985	B
2	5	12459	B
5	5	11779	B
1	5	11452	B

Means that do not share a letter are significantly different.

The pairwise comparisons show that the control specimen is statistically different then the specimen with tags. All specimens with tags are statistically the same.

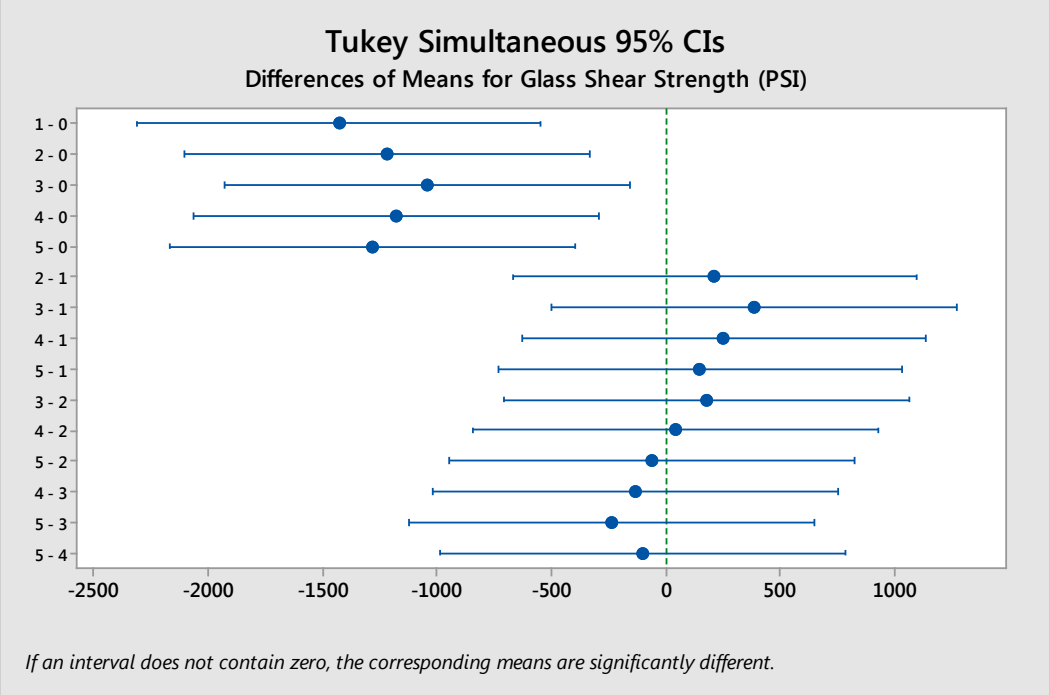

Figure 4-26: Tukey 95% Confidence Interval

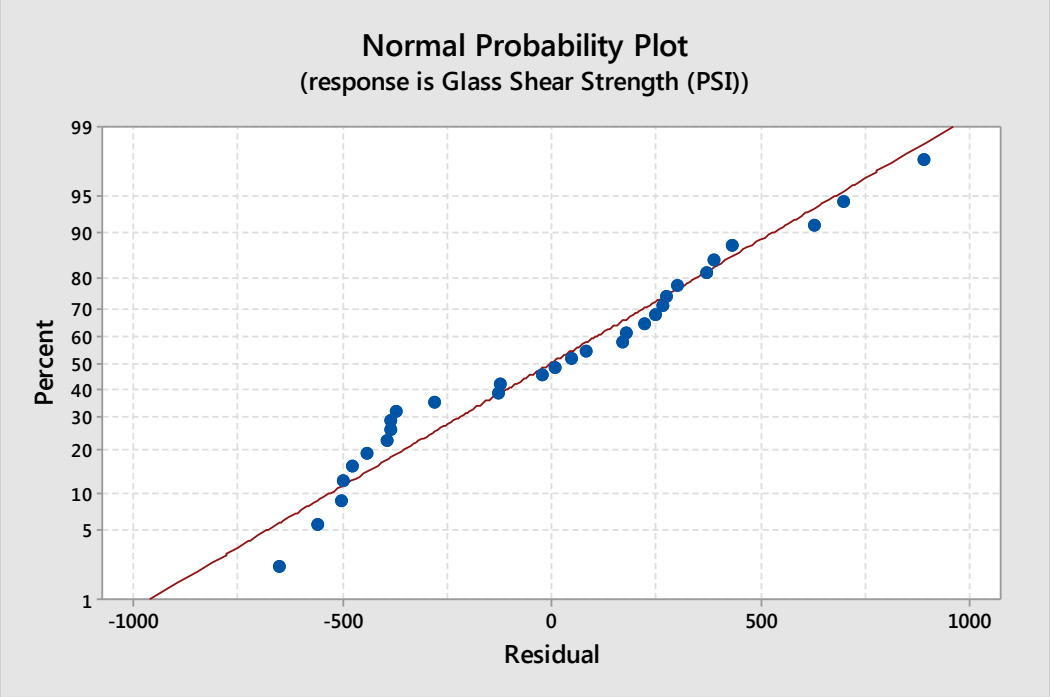

Figure 4-27: Normal Probability Plot for Glass Shear Data

The normal probability plot is somewhat straight hinting at normally distributed data.

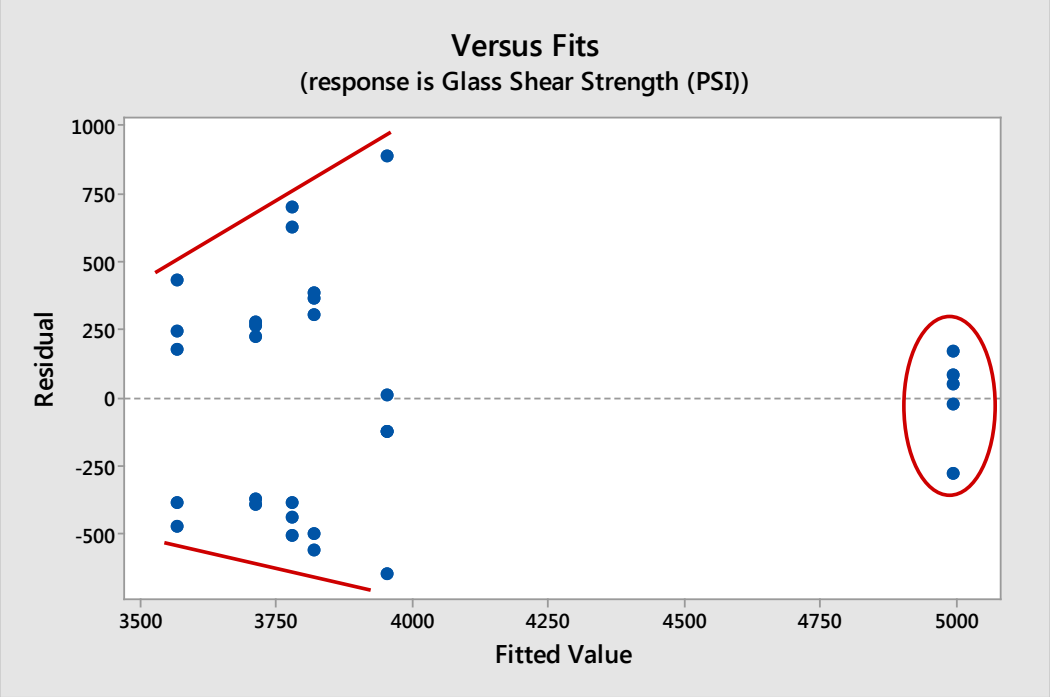

Figure 4-28: Residuals vs. Fitted Values Plot for Glass Shear

The residuals versus fitted values plot shows non constant variance with the fitted values for the control much higher than the data for the parts embedded with RFID tags.

Table 4-23: Descriptive Statistics for Kevlar Fiber Reinforced Epoxy

Variable	Glass Tag Type	Total Count	Mean	Standard Deviation	Coefficient of Variance
Kevlar Shear Strength (psi)	0	5	2968.9	68.5	2.31
	1	5	2164	273	12.60
	2	5	2181.3	204.7	9.38
	3	5	2547.9	155.0	6.08
	4	5	2164.2	85.5	3.95
	5	5	2074.2	148.4	7.16

For the Kevlar specimen, the control yielded an average shear strength of 2968.9 psi. This appears to be somewhat higher than the test specimen that had the RFID tag included in the material. One specimen, specimen 3, though lower strength, is closer to the control than the other specimen types. The standard deviation and the coefficient of variation are also smaller than the other test specimen though some of the test specimens, such as specimen 4, are similar to the control.

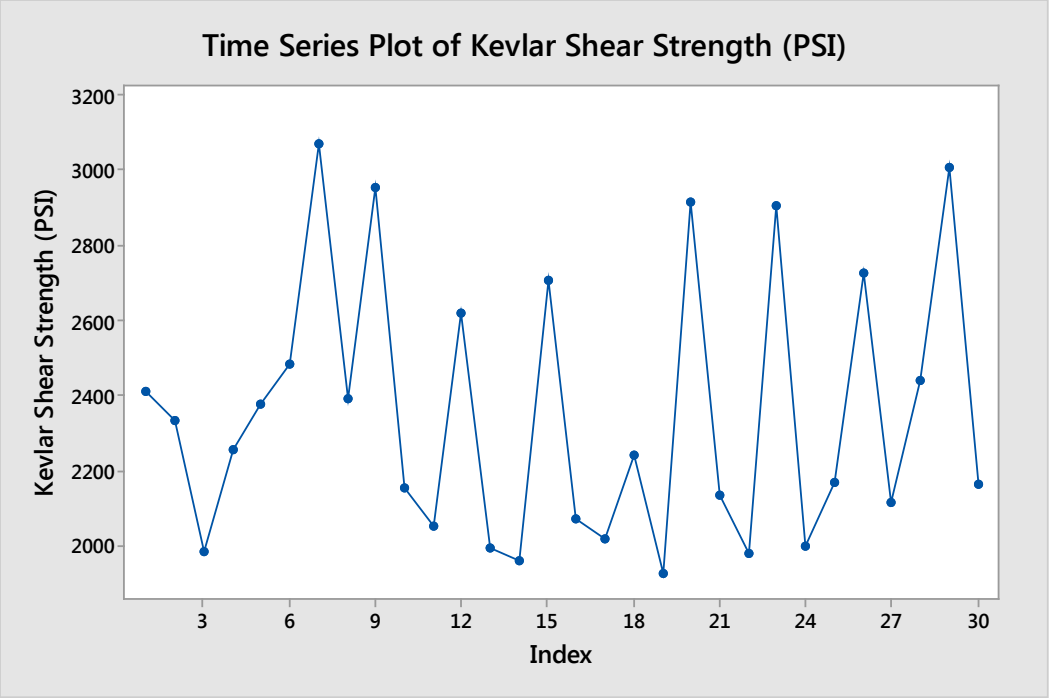

Figure 4-29: Time Series Plot of Kevlar Fiber Reinforced Epoxy

One-way ANOVA: Kevlar Shear Strength (PSI) versus Kevlar Tag Family

Null hypothesis All means are equal

Alternative hypothesis At least one mean is different

Significance level $\alpha = 0.05$

Table 4-24: Factor Information for RFID Tags in Kevlar Fiber Reinforced Epoxy

Factor	Levels	Values
Kevlar Tag Type	6	0, 1, 2, 3, 4, 5

Table 4-25: Shear Test ANOVA for Kevlar Fiber Reinforced Epoxy

Source	DF	Adj SS	Adj MS	F-Value	p-Value
Kevlar Tag Type	5	2979958	595992	20.51	0.000
Error	24	697274	29053		
Total	29	3677232			

Table 4-26: Model Summary

S	R-sq	R-sq (adj)	R-sq(pred)
170.450	81.04%	77.09%	70.37%

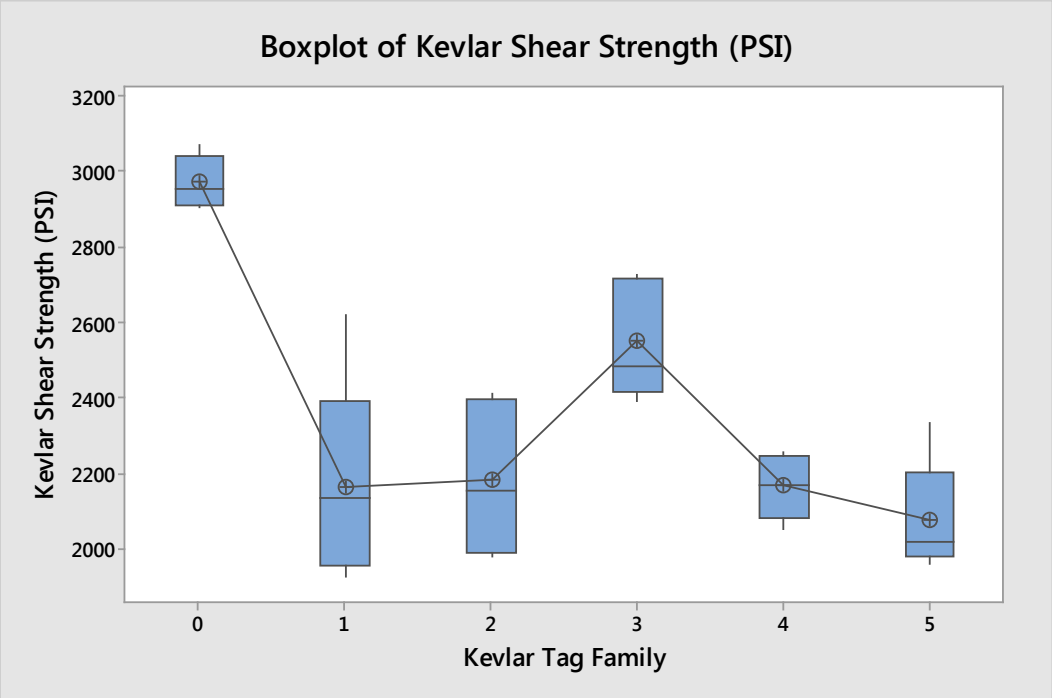

Figure 4-30: Boxplot of Kevlar Shear Test Data

Table 4-27: Kevlar Shear Data Means

Tag Type	N	Mean	Standard Deviation	95% CI
0	5	2969	68	(2812, 3126)
1	5	2164	273	(2006, 2321)
2	5	2181	204	(2024, 2338)
3	5	2547	155	(2390, 2705)
4	5	2164	85	(2007, 2321)
5	5	2074	148	(1917, 2231)

Tukey Pairwise Comparisons

Table 4-28: Grouping Information Using the Tukey Method at 95% Confidence

Kevlar Tag Type	N	Mean	Grouping
0	5	2968.9	A
3	5	2547.9	B
2	5	2181.3	C
4	5	2164.2	C
1	5	2164	C
5	5	2074.2	C

Means that do not share a letter are significantly different.

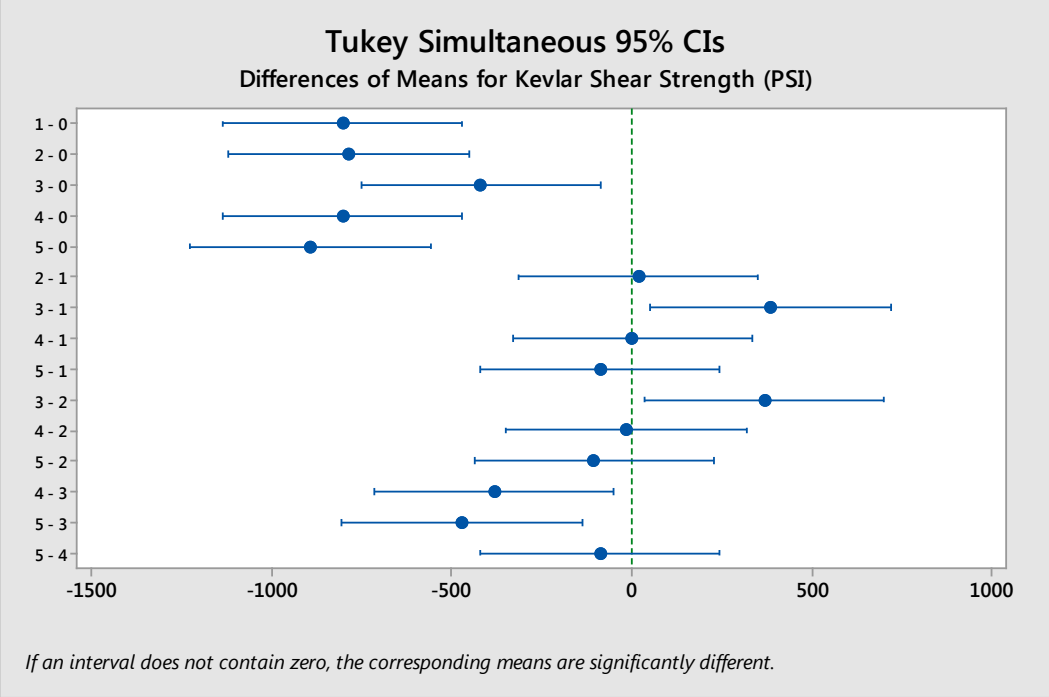

Figure 4-31: Tukey 95% Confidence Interval

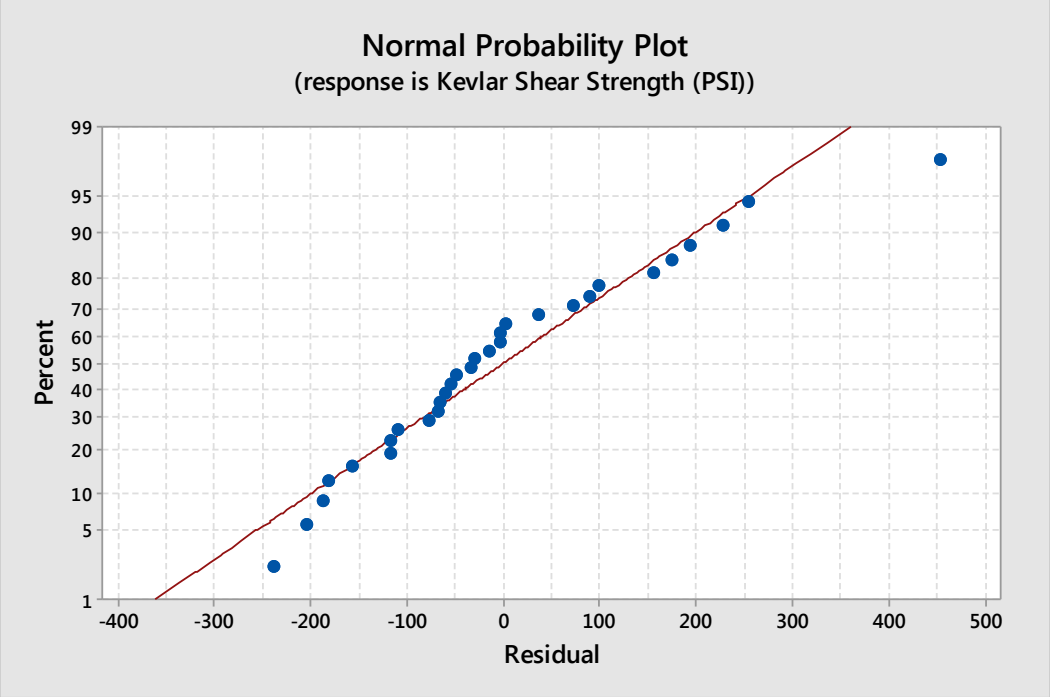

Figure 4-32: Normal Probability Plot for Kevlar Shear Data

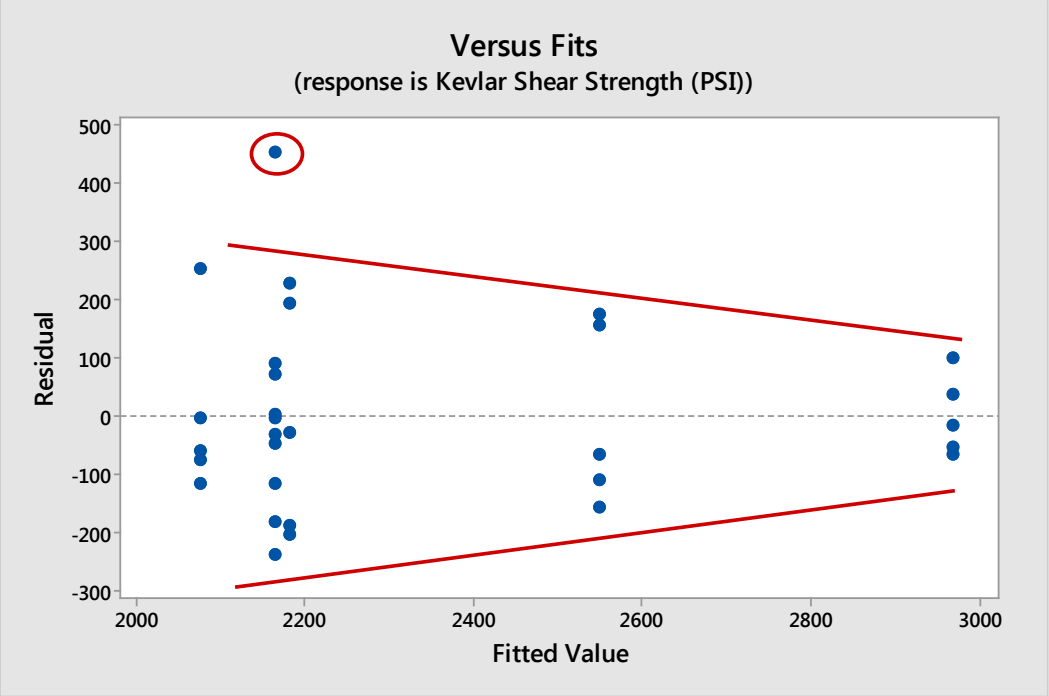

Figure 4-33: Residuals vs. Fitted Values Plot for Kevlar Shear

Material Type and Tag Type Shear Strengths

Hypothesis:

H_0: There is no significant difference between part i on parameter j.

Where:

i is the material type

j is the mechanical property

H_A: There is a significant difference between part i on parameter j.

The hypothesis will be tested at α = 0.30

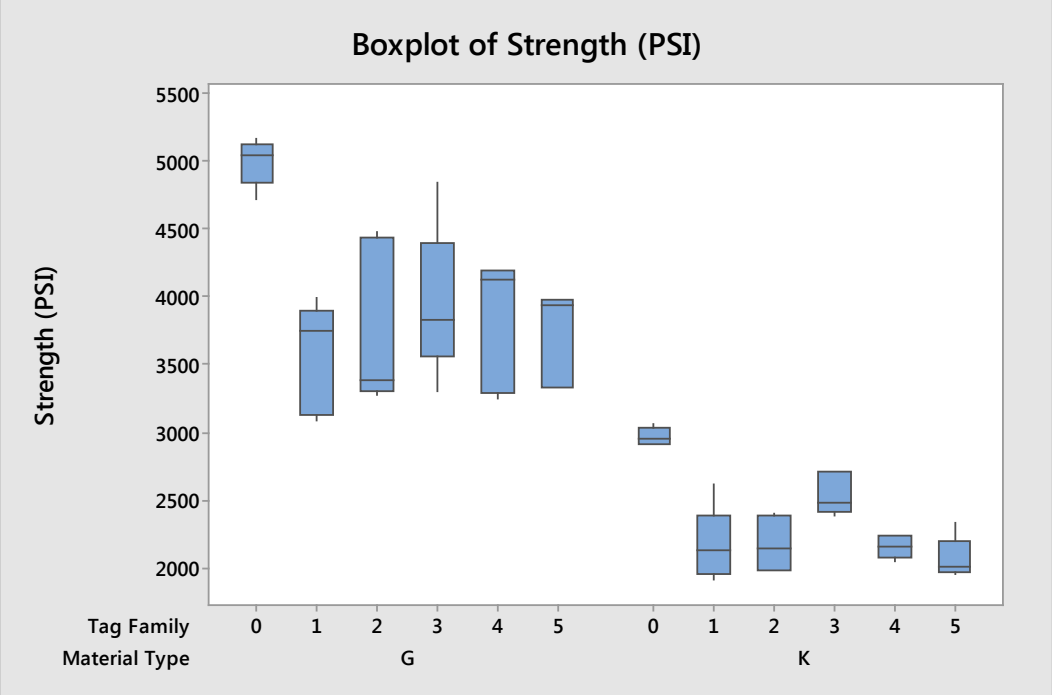

Figure 4-34: Boxplot of Shear Strengths

Categorical predictor coding (-1, 0, +1)

Table 4-29: Analysis of Variance

Source	DF	Adj SS	Adj MS	F-Value	P-Value
Regression	6	48372339	8062056	68.04	0.000
Material Type	1	39320432	39320432	331.86	0.000
Tag Family	5	9051907	1810381	15.28	0.000
Error	53	6279685	118485		
Lack-of-Fit	5	657956	131591	1.12	0.361
Pure Error	48	5621729	117119		
Total	59	54652024			

In the ANOVA for the shear strengths of the material types and the tag types, the F-values are higher than the F distribution value of 1.25. The null hypothesis is rejected and the alternative hypothesis is used. For these calculations, there is a significant difference between the material types and at least one of the tag types in the shear tests.

Table 4-30: Model Summary

S	R-sq	R-sq (adj)	R-sq(pred)
344.216	88.51%	87.21%	85.27%

Table 4-31: Variables Used in Determining Shear Strength from Material and Tag Type

Variable	Coefficient	SE Coefficient	T	p-value
Constant	3159.6	44.4	71.10	0.000
Glass	809.5	44.4	18.22	0.000
Kevlar	-809.5	44.4	-18.22	0.000
Tag 0	822.9	99.4	8.28	0.000
Tag 1	-295.7	99.4	-2.98	0.004
Tag 2	-180.8	99.4	-1.82	0.074
Tag 3	89.7	99.4	0.90	0.371
Tag 4	-169.4	99.4	-1.70	0.094
Tag 5	-266.7	99.4	-2.68	0.010

Regression Equation

Shear Strength (PSI) = 3159.6 + 809.5 Glass – 809.5 Kevlar + 822.9 Tag 0 - 295.7 Tag 1 – 180.8 Tag 2 + 89.7 Tag 3 – 169.4 Tag 4 – 266.7 Tag 5

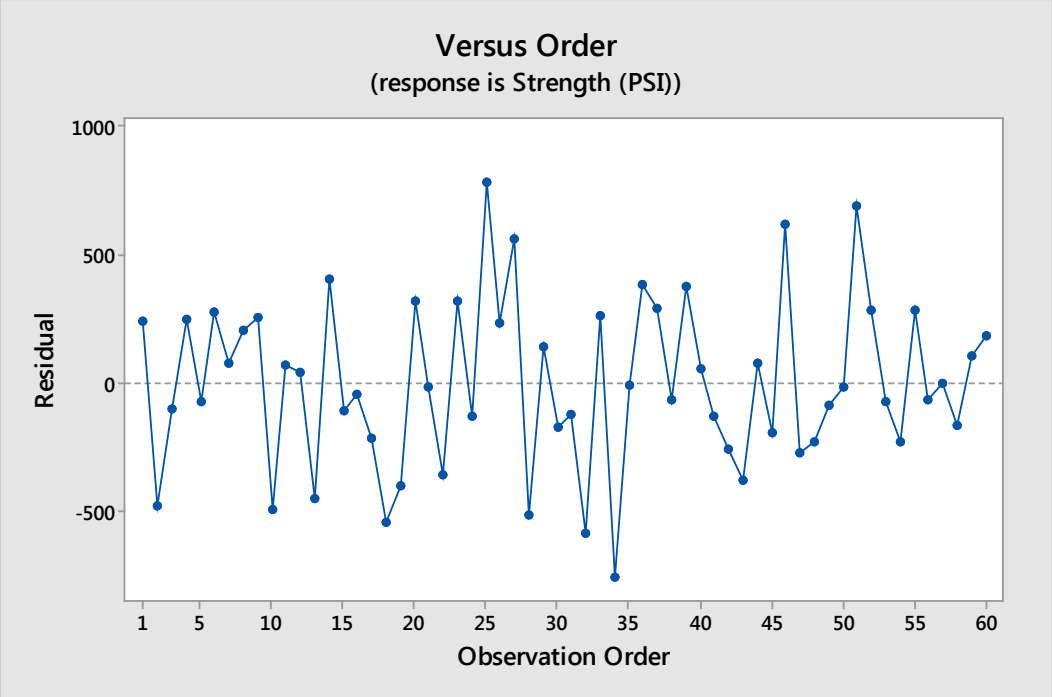

Figure 4-35: Observation Orders

Table 4-32: Fits and Diagnostics for Unusual Observations

Observation	Shear Strength (PSI)	Fit	Residual	Std Residual
25	4841	4059	782	2.42 R
34	3301	4059	-758	-2.34 R
51	4476	3788	688	2.13 R

R Large residual

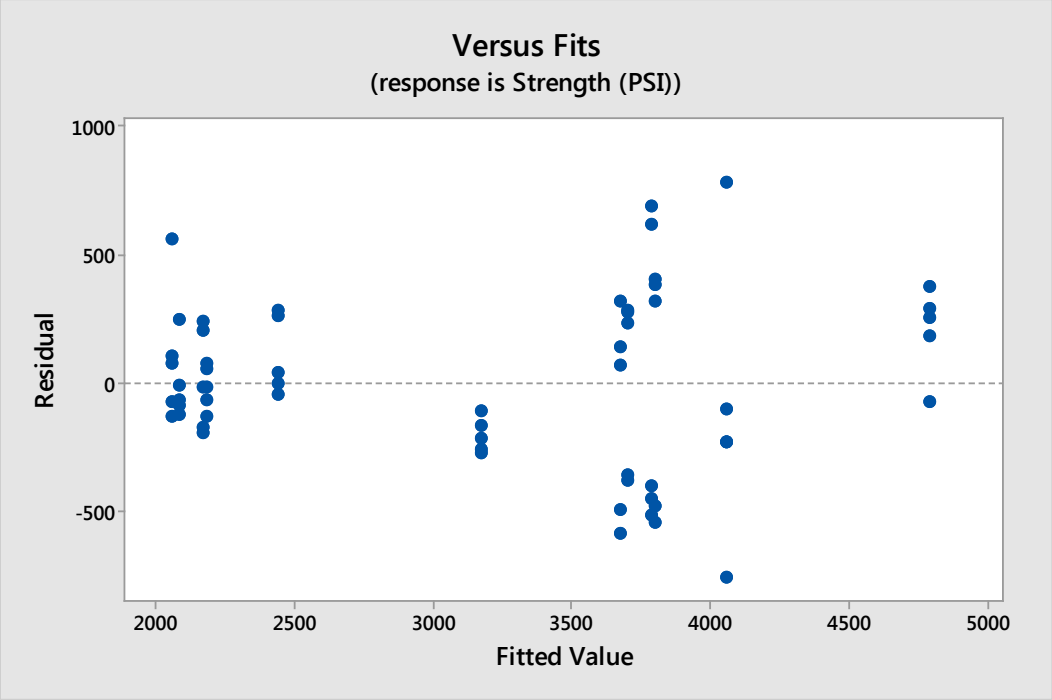

Figure 4-36: Residuals versus Fitted Plot

The residuals versus fitted plot shows some funneling indicating non constant variance.

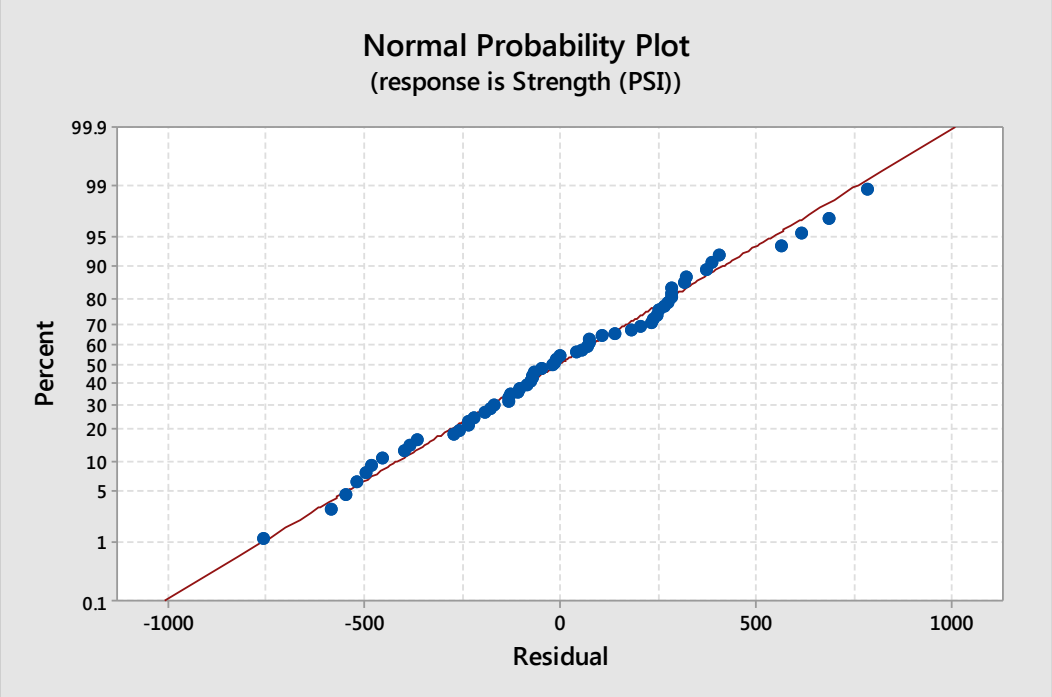

Figure 4-37: Normal Probability Plot

The normal probability plot shows a straight line indicating that the data is normally distributed.

4.2 Read Distance Testing

The read distances occurred in batches of parts. A series of Kevlar parts were run followed by a series of glass parts. There was not a blind series of tests performed on these data sets.

Table 4-33: Descriptive Statistics for Read Distance Testing

Variable	Glass Tag Type	Total Count	Mean	Standard Deviation	Coefficient of Variance
Glass Read Distance (psi)	1	8	100.00	0	0
	2	8	100.00	0	0
	3	8	100.00	0	0
	4	8	85.3	29.9	35.05
	5	8	98.13	3.94	4.02

One-way ANOVA: Glass Distance (ft) versus Glass Tag Type

Null hypothesis All means are equal

Alternative hypothesis At least one mean is different

Significance level $\alpha = 0.05$

Table 4-34: Factor Information for RFID Tags in Glass Fiber Reinforced Epoxy

Factor	Levels	Values
Glass Tag Type	5	1, 2, 3, 4, 5

Table 4-35: Read Distance Test ANOVA for Glass Fiber Reinforced Epoxy

Source	DF	Adj SS	Adj MS	F-Value	p-Value
Glass Tag Type	4	1326	331.6	1.83	0.146
Error	35	6358	181.7		
Total	39	7685			

The F-value from the ANOVA is less than the 2.09 value listed in the F distribution causing a fail to reject scenario for the H_0 that all means are equal. The p-value is also higher than α meaning that the mean is not statistically significant.

Table 4-36: Model Summary

S	R-sq	R-sq (adj)	R-sq(pred)
13.4784	17.26%	7.80%	0.00%

The R-sq value of 17.25% shows that the models do not adequately represent the data points.

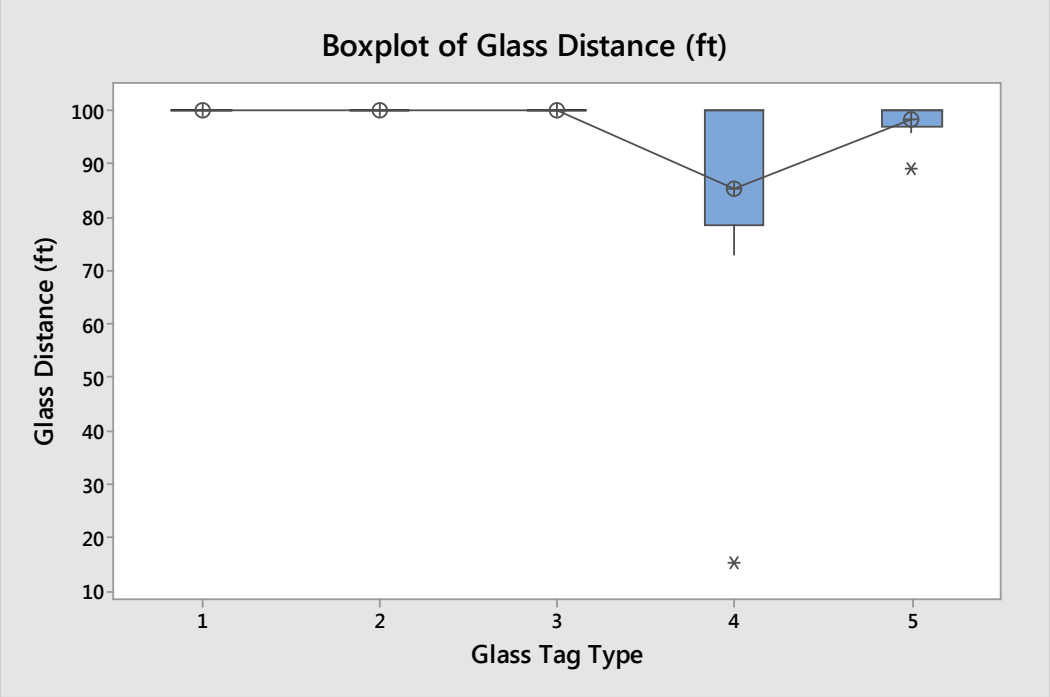

Figure 4-38: Boxplot of Glass Read Distance Test Data

The boxplot shows two outliers in the data for the read distance of the tags embedded in glass fiber. Tag 4 is the feathered tag and was most likely damaged during modification of the tag. This failure point is due to the tag having some limited read range which may be affected by the continuity in the antenna. If the antenna was cut then it would lose much of its effectiveness. The second outlier is in the tag 5 parts. Tag 5 is the abraded tag so the likelihood of damage to the tag through modification is very small. This tag may have had some defect to begin with or was adversely affected by the heat in the cure cycle.

The boxplot does show that tag 4 has a high amount of variability. The outlier and its magnitude are contributing to this non constant variation.

Table 4-37: Glass Read Distance Data Means

Tag Type	N	Mean	Standard Deviation	95% CI
1	8	100.0	0	(90.3, 109.7)
2	8	100.0	0	(90.3, 109.7)
3	8	100.0	0	(90.3, 109.7)
4	8	85.3	29.9	(75.6, 94.9)
5	8	98.13	3.94	(88.45, 107.80)

Tukey Pairwise Comparisons

Table 4-38: Grouping Information Using the Tukey Method at 95% Confidence

Glass Tag Type	N	Mean	Grouping
3	8	100.0	A
2	8	100.0	A
1	8	100.0	A
5	8	98.13	A
4	8	85.3	A

Means that do not share a letter are significantly different.

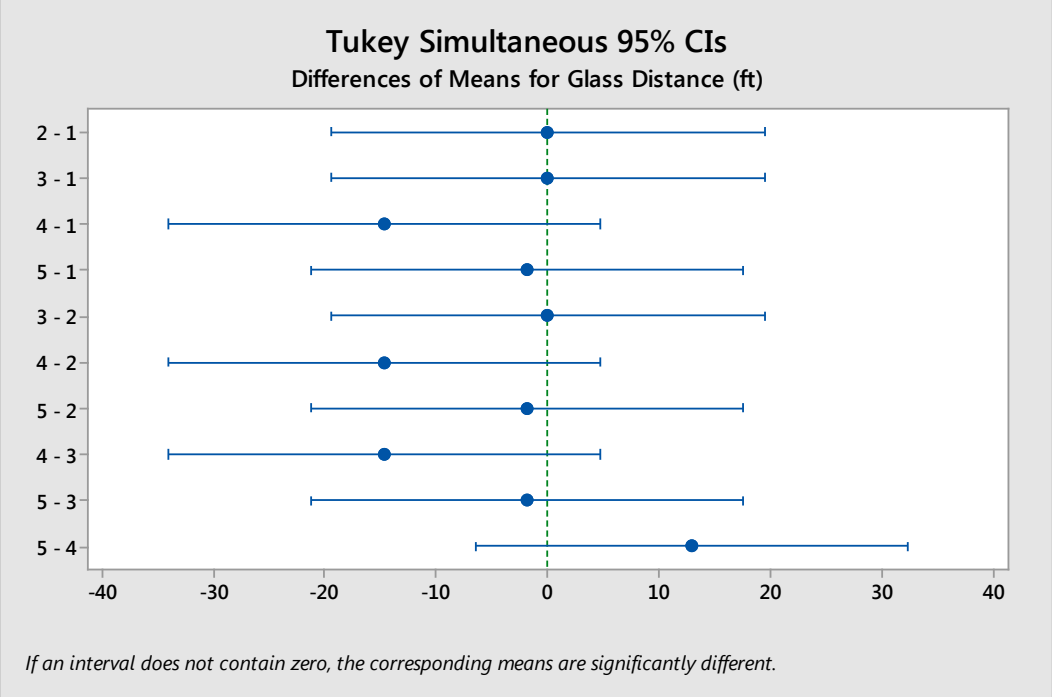

Figure 4-39: Tukey 95% Confidence Interval

For the tags embedded in glass, all tags are similar to each other meaning that the tags all read to approximately the same distances.

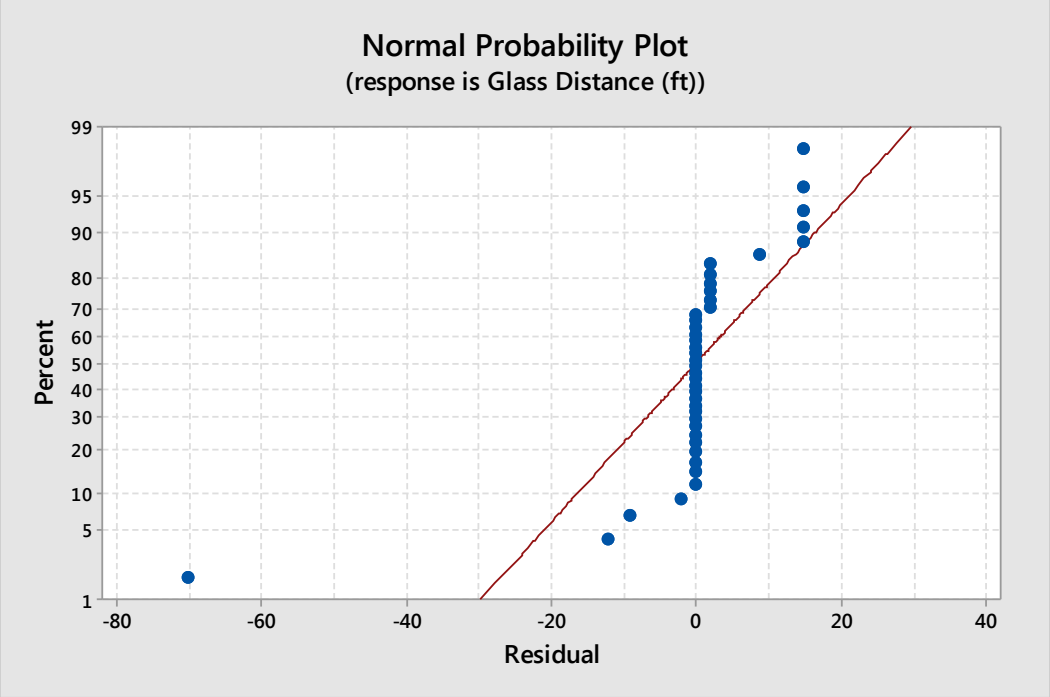

Figure 4-40: Normal Probability Plot for Glass Read Distances Data

The normal probability plot shows an s-curve in the residuals. The abnormality of this plot is caused by the way the data was collected and the large number of samples that read out to 100 feet.

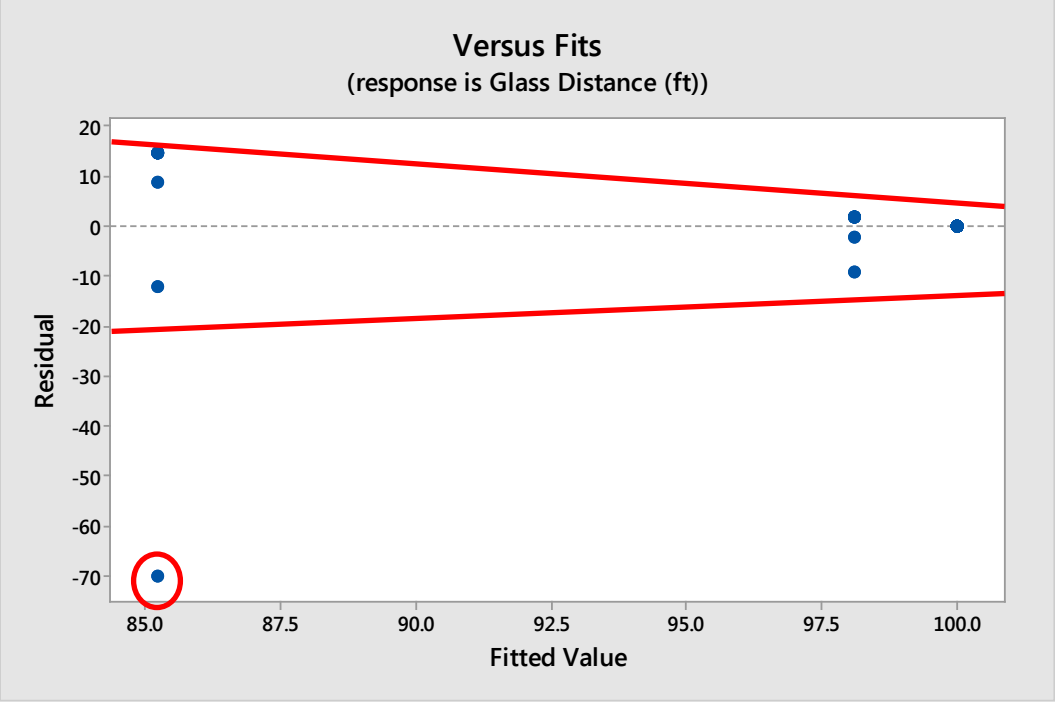

Figure 4-41: Residuals vs. Fitted Values Plot for Glass Read Distances

Once the outlier is removed from the residuals versus fitted values plot, the data exhibits a slight non constant variance. Again, the large number of data points that read at 100 feet have an effect on the plot.

Descriptive Statistics: Kevlar Distance (ft)

Table 4-39: Descriptive Statistics for Kevlar Read Distances

Variable	Glass Tag Type	Total Count	Mean	Standard Deviation	Coefficient of Variance
Kevlar Read Distance (psi)	1	8	69.25	25.71	37.12
	2	8	80.13	18.34	22.89
	3	8	79.88	24.58	30.78
	4	8	71.3	31.5	44.22
	5	8	79.5	36.6	46.08

One-way ANOVA: Kevlar Distance (ft) versus Kevlar Tag Type

Null hypothesis All means are equal

Alternative hypothesis At least one mean is different

Significance level $\alpha = 0.05$

Table 4-40: Factor Information for RFID Tags in Kevlar Fiber Reinforced Epoxy

Factor	Levels	Values
Kevlar Tag Type	5	1, 2, 3, 4, 5

Table 4-41: Read Distance ANOVA for Kevlar Fiber Reinforced Epoxy

Source	DF	Adj SS	Adj MS	F-Value	p-Value
Kevlar Tag Type	4	899.3	224.8	0.29	0.885
Error	35	27556.7	787.3		
Total	39	28456.0			

The F-value from the ANOVA is less than the 2.09 value listed in the F distribution causing a fail to reject scenario for the H_0 that all means are equal. The p-value is also much higher than α resulting in the mean being not statistically significant.

Table 4-42: Model Summary

S	R-sq	R-sq (adj)	R-sq(pred)
28.0595	3.16%	0.00%	0.00%

The R-sq of 3.16% shows that the data is not represented by the model.

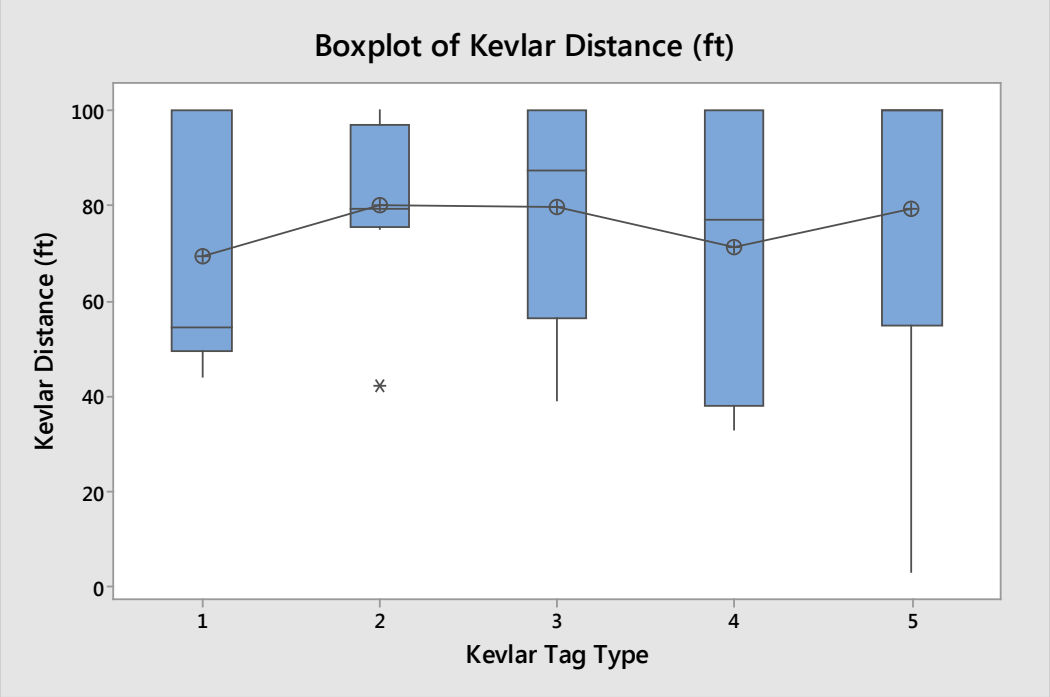

Figure 4-42: Boxplot of Kevlar Read Distance

The boxplot for the Kevlar tags shows one outlier in tag 2. Tag 2 is the unmodified tag. Because this tag read so much shorter than the other tags in the data set, it is assumed that there was a problem with the tag from either the manufacturer or a problem that propagated during the manufacturing of the Kevlar part.

All Kevlar parts had a reduced read range compared to the glass FRP parts. It is postulated that the Kevlar material does have a slight impact on the transmission of RF signals transmitted to and from the RFID tags.

Table 4-43: Kevlar Read Distance Data Means

Tag Type	N	Mean	Standard Deviation	95% CI
1	8	69.25	25.71	(49.11, 89.39)
2	8	80.13	18.34	(59.99, 100.26)
3	8	79.88	24.58	(59.74, 100.01)
4	8	71.3	31.5	(51.1, 91.4)
5	8	79.5	36.6	(59.4, 99.6)

Tukey Pairwise Comparisons

Table 4-44: Grouping Information Using the Tukey Method at 95% Confidence

Kevlar Tag Type	N	Mean	Grouping
2	8	80.13	A
3	8	79.88	A
5	8	79.5	A
4	8	71.3	A
1	8	69.25	A

Means that do not share a letter are significantly different.

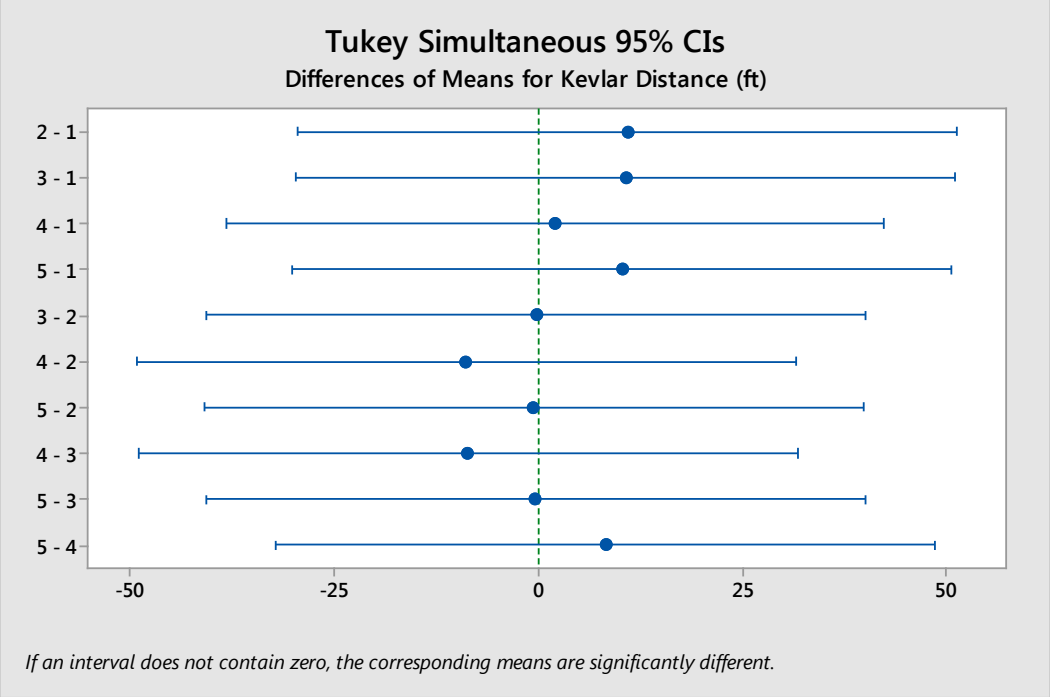

Figure 4-43: Tukey 95% Confidence Interval

In the read distances for the Kevlar, all means for the different tags are statistically the same.

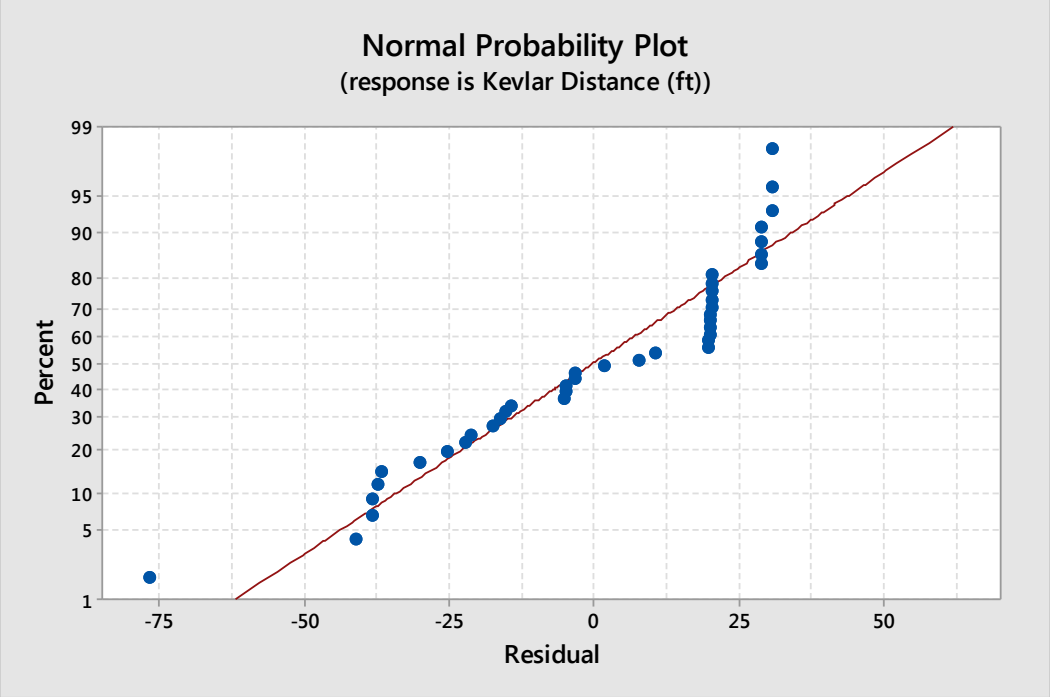

Figure 4-44: Normal Probability Plot for Kevlar Read Distances

The normal probability plot shows upper tail on the right side. This points to a more exponential distribution of the data instead of normally distributed.

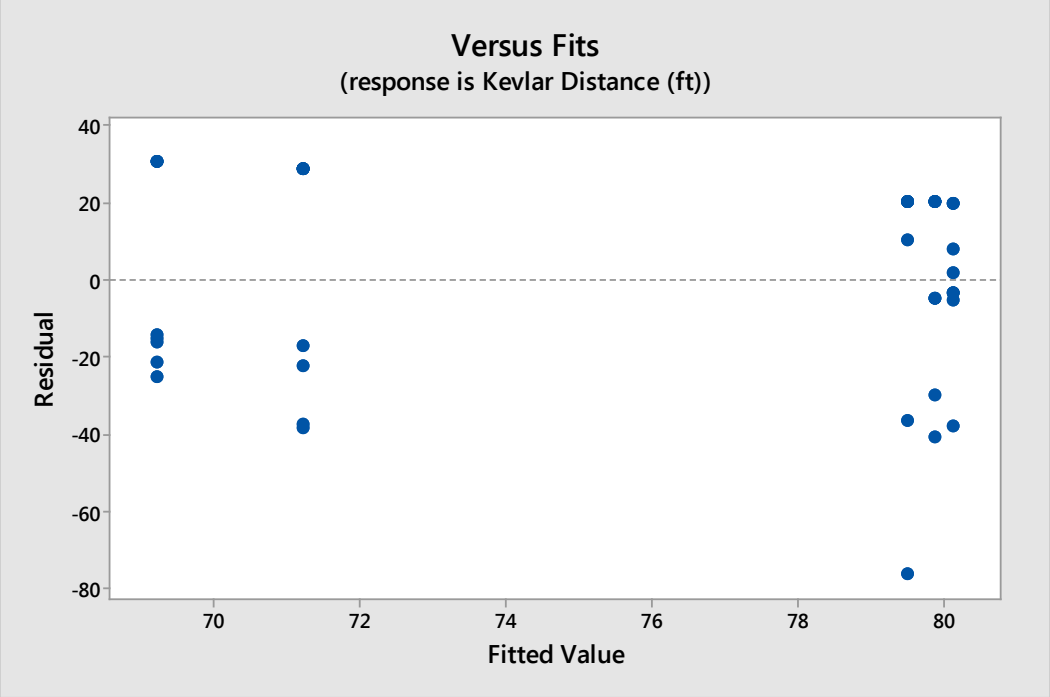

Figure 4-45: Residuals vs. Fitted Values Plot for Kevlar Read Distances

The residuals versus fitted values plot is mostly constant and does not exhibit any funneling in the data.

Material Type and Tag Type Read Distances

Hypothesis

H_0: There is no significant difference between part i and the electronic transmission readability performance factor K.

Where

i is the material type

K is the electronic transmission readability performance factor

H_A: There is a significant difference between part i and the electronic transmission readability performance factor K.

An $\alpha = 0.30$ will be used

Categorical predictor coding (-1, 0, +1)

Table 4-45: Analysis of Variance

Source	DF	Adj SS	Adj MS	F-Value	P-Value
Regression	5	10169.9	2034.0	4.36	0.002
Material Type	1	8549.1	8549.1	11.33	0.000
Tag Family	4	1620.8	405.2	0.87	0.487
Error	74	34519.9	466.5		
Lack-of-Fit	4	604.8	151.2	0.31	0.869
Pure Error	70	33915.1	484.5		
Total	79	44689.9			

In the ANOVA for the read distances, the F-value for the material type is higher than the F distribution value of 1.25 while the F- value for the tag family is lower than the F distribution value of 1.09. The null hypothesis is rejected for the material type and the alternative hypothesis is used. For these calculations, there is a significant difference between the material types in the read distances. We fail to reject the null hypothesis for the tag family which is interpreted as there is not a significant difference on the read distances from the tag types.

Table 4-46: Model Summary

S	R-sq	R-sq (adj)	R-sq(pred)
21.5983	22.76%	17.54%	9.72%

Table 4-47: Variables Used in Determining Shear Strength from Material and Tag Type

Variable	Coefficient	SE Coefficient	T	p-value
Constant	86.34	2.41	35.75	0.000
Glass	10.34	2.41	4.28	0.000
Kevlar	-10.34	2.41	-4.28	0.000
Tag 1	-1.71	4.83	-0.35	0.724
Tag 2	3.72	4.83	0.77	0.443
Tag 3	3.60	4.83	0.75	0.458
Tag 4	-8.09	4.83	-1.65	0.098
Tag 5	2.47	4.83	0.51	0.610

Regression Equation

Distance (ft) = 86.34 + 10.34 Glass – 10.34 Kevlar – 1.71 Tag 1 + 3.72 Tag 2 + 3.60 Tag 3 – 8.09 Tag 4 + 2.47 Tag 5

Table 4-48: Fits and Diagnostics for Unusual Observations

Observation	Shear Strength (PSI)	Fit	Residual	Std Residual
12	3.00	78.47	-75.47	-3.63 R
75	15.00	88.59	-73.59	-3.54 R

R Large residual

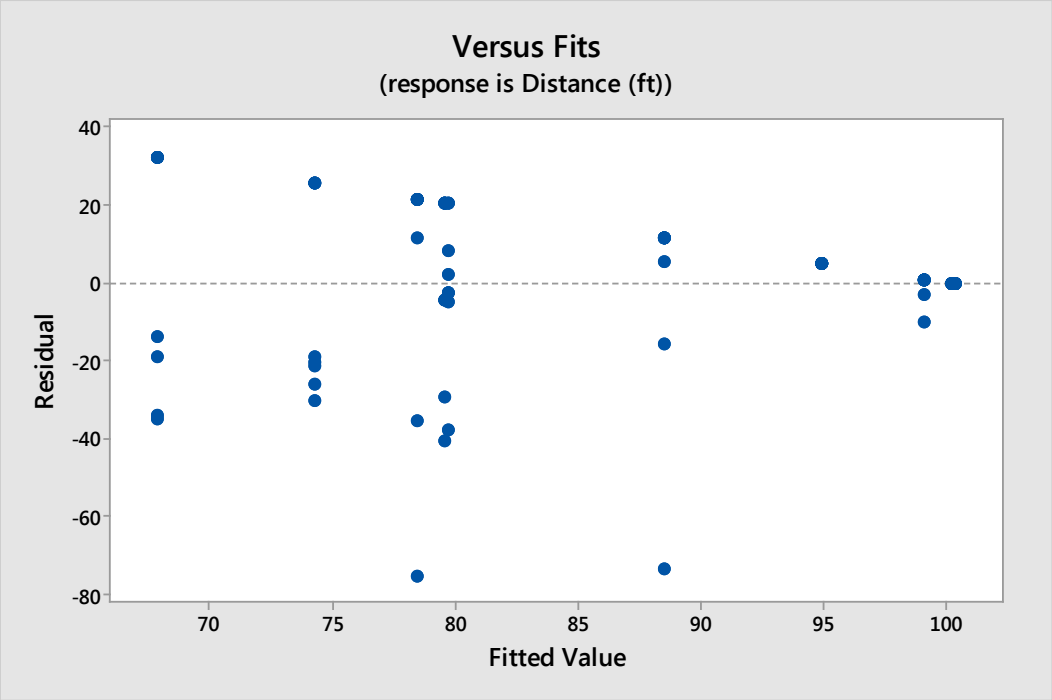

Figure 4-46: Residuals vs. Fitted Values Plot

The residuals versus fitted plot shows non constant variance due to the funneling effect of the data.

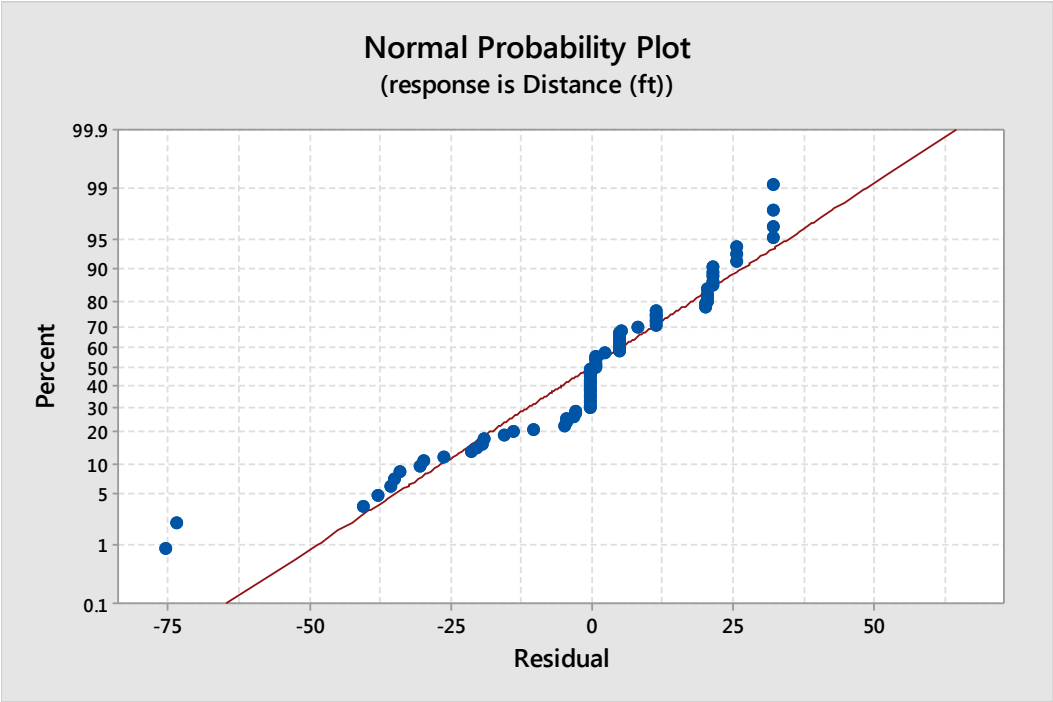

Figure 4-47: Normal Probability Plot

The normal probability plot Exhibits some curvature in the data. There may be a slight exponential distribution in the data.

4.3 Life Cycle Analysis

Hypotheses

H_0: There is not a significant difference between part i and the life cycle analysis parameter L.

Where

i is the material type

L is the LCA parameter

H_A: There is a significant difference between part i and the life cycle analysis parameter L.

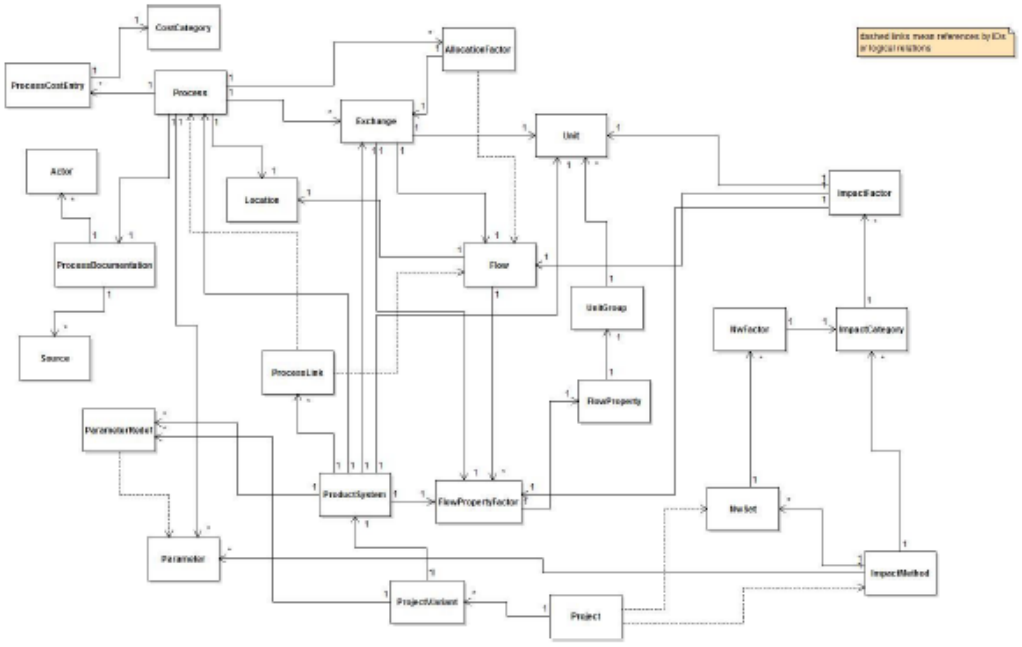

Table 4-49: Flowchart of Life Cycle Analysis (Winters, 2015)

One expected outcome from the Life Cycle Analysis is the creation of a flowchart that shows how energy and products interact. In the example shown from Winters' (2005) work, complexity of the LCA grows rapidly depending on the product. This flowchart is of a water bottle. Due to restrictions in the data, the method for performing the LCA for the fiber reinforced polymers and the fiber reinforced polymers with embedded electronics is only defined in the methodology.

Chapter 5

Conclusions and Discussions

The conclusion describes the outcomes of the research based on the results along with which recommendations are made based on those results. The discussion in the conclusion lists out the limitations of the research and defines what the future work will include. Figure 5-1 shows where this work applies and where future work will contribute.

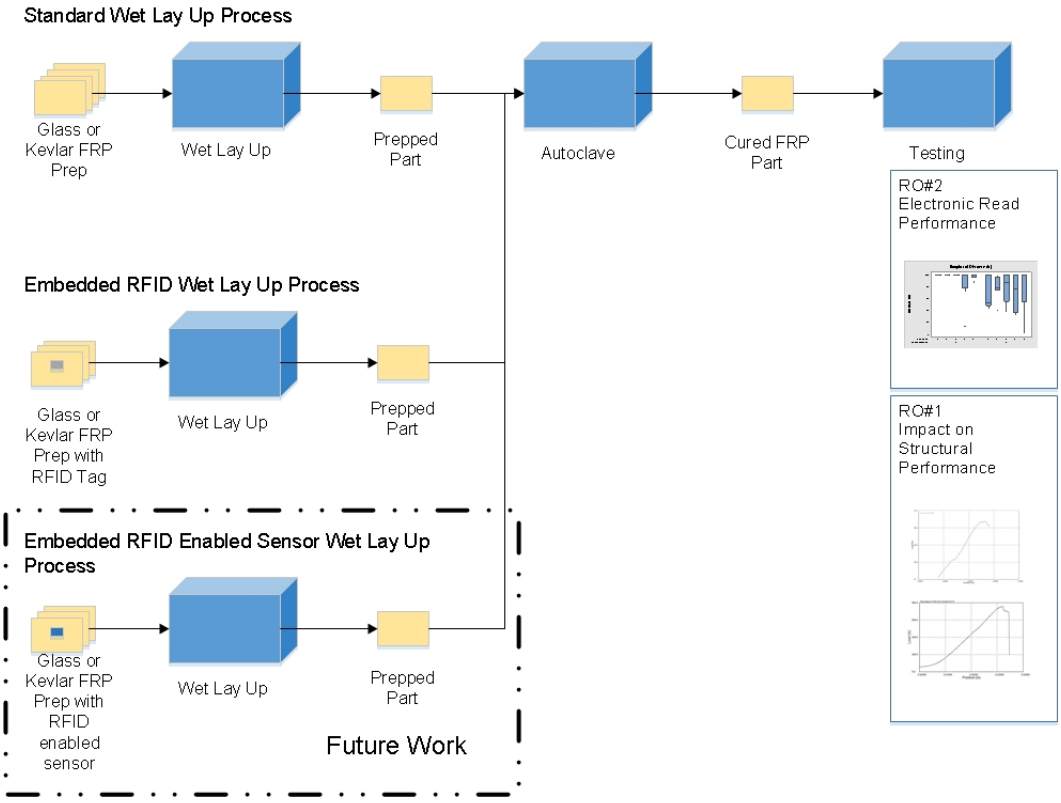

Figure 5-1: RFID Enabled Sensing In Fiber Reinforced Polymers

5.1 Conclusions

Simulation Testing

The FEM simulations can be successful once additional information is known from actual testing. The location identified in the simulations as movement in the part was very near the actual breaks in the mechanical tests. The stresses encountered in this research were not always very close to the simulated stresses. We believe that although the correct materials in the simulations were used, the values for these materials may need to be redefined. We also know that the simulations will only show the stress build up in the simulated part and that they will not simulate the actual break.

Mechanical Testing

The compression tests showed where the breaking point of the material is and allowed identification of the failure mode. In the compression test, the typical failure occurred in a region that contained the tag. All of these failures occurred on the tag side of the laminations and never between two layers of fabric. Upon evaluating the hypothesis that there is no significant difference in the compression strength between the materials and the tags, it was found that there are differences between the materials and there are differences between the tags.

The shear tests also showed the failure points in the materials and are much more interesting and somewhat more relevant to actual use. The shear tests did not always fail because of the tag causing delamination in the part. Some of the failures were in the materials themselves. Fortunately, the failures in the materials were at a higher load than the failures of the tag. Upon dissecting the failures of the parts with delamination, the failure did not occur between the tag and the resin. All of these failures occurred in the tag where the antenna was pulled from the inlay. This indicated that the tag used in the experiments caused the failure because of its construction, not

necessarily because of the RFID tag being a defect in the layers of the FRP. In fact the epoxy seemed to bond well with both the PET inlay and with the antenna. The mechanical testing also showed that there may be something to reducing the footprint of the tag in the FRP though more testing needs to take place. Evaluating the hypothesis it was found that there is a significant difference between the material types and there is a significant difference between the tags.

Electrical Testing

The readability of the tags is influenced by embedding the tag into the FRP. The glass FRP did not greatly affect the read distances as most of the tags would read out to 100 feet. Tag 4, the feathered tag, had the worst performance of the tags embedded in glass. All of the Kevlar FRP parts influenced the read distance as the read distances ranged from 3 feet out to 100 feet. On average the read distances of the Kevlar are only 75% of the read distances seen in the glass. This suggests that the Kevlar, though still able to pass RF, does negatively affect the transmission of RF. The possibility of the manufacturing process affecting the Kevlar tags is ruled out since both the glass and Kevlar parts are manufactured in the same manner. It would have made more sense that the glass would have been affected more by the heat since it is thinner than the Kevlar. When the hypothesis is evaluated it was found that there is a significant difference in the read distances in the materials but the tags do not exhibit a significant difference in the read distances.

Life Cycle Analysis

The LCA proved much more difficult to obtain than originally thought. The environmental and energy costs for the various points of manufacturing and transport are much more in depth and difficult to obtain. The flowchart of the processes does indicate a

complicated energy usage problem regardless of whether the RFID tag is embedded or not.

5.2 Limitations

One of the biggest limitations to the research has been the costs associated with the life cycle analysis. The literature does a good job of discussing these issues but there is a big hole in data, especially when trying to dig down at the chemical component level.

From the testing standpoint, there needs to be a more precise method of placing the tags into the FRP's. All tags are placed in the FRP but there is a margin of error as to the orientation that the tag. This can be alleviated some with the use of the pre-preg materials but it will remain a problem to some extent.

5.3 Contribution to the Body of Knowledge

This work has helped by showing how RFID affects the strength of a composite material when it is embedded into that material. It has also shown that RFID can transmit through the FRP materials and depending on the set up of the RFID tag, RFID may be able to be used as an energy source to power small sensors attached to it. The biggest impact that this research has had on the body of knowledge is the mechanical testing of the materials with the tag embedded into the material. In this research an off the shelf tag was used and though it did not work entirely as planned it still showed that the tag construction, or the bond between the antenna and the inlay, is weaker than the bond between the epoxy resin and the tag.

5.4 Future Work

There is more work to be done. The next step is to go forward with the tensile tests to ensure that there is not an effect on the fibers due to the inclusion of the RFID tag. This will require a better manufacturing method in order to precisely lay the tag into the FRP layers. Another step is to reevaluate the tag used in the testing and replace the

current tag with one that does not have an inlay. An alternative to this is to print an RFID tag onto a different material such as tefzel or onto glass or Kevlar fiber so that it becomes more of the structure of the part.

Another step in the future work is to expand into other manufacturing processes such as working with pre-preg materials, working with resin infusion transfer, and working with the pultrusion process. This would expand the usability of the tool and increase the likelihood of adoption. It would also be interesting to see how the RFID tag would affect those structures since they are mechanically different.

The third future work area would be to include RFID into shaped structures that do not have flat faces. Curved parts or irregularly shaped parts would be needed to be tested since there are a large number of FRP parts that are not square.

The fourth area for future work is the integration of sensors into the RFID tags. There are existing strain enabled RFID tags but more work needs to be done in the area with these tags.

5.5 Related Coursework

There are several courses taken at the University of Texas at Arlington (UTA) and taught at Tarleton State University that have contributed to this dissertation.

At UTA many of the courses required factored into this dissertation. The first is IE 5300 RFID and Logistics. From this course, the main topic of RFID played heavily into the research as the embedded electronics used are RFID tags. A second class is IE 6302 Facility Planning. From this course, the use of standard practices helped with the manufacture of parts but the logistics of how people and items move through the supply chain helped more with the life cycle analysis piece of the research. IE 5339 and IE 5346 helped with determining how to implement new technology as well as determining and resolving problems related to manufacturing, reliability, and testing of these new

technologies. IE 5304 Engineering Economy helped with justifying different options during the research. It was especially helpful with the life cycle costs and determining economic feasibility.

At Tarleton, being thrust into teaching ENGT 3325 Thermoset Manufacturing contributed to the knowledge needed to build and manipulate the reinforcement fibers used in this research. The class also provided valuable manpower and the ability to validate the manufacturing processes with students before working on the actual parts and performing the tests.

References

. ISO 14040:2006 - Environmental management - Life cycle assessment - Principles and framework (2006): International Standards Organization.

. ASTM D695-10, Standard Test Method for Compressive Properties of Rigid Plastics. (2010). West Conshohocken, PA: ASTM International.

. ASTM D2344 / D2344M-13, Standard Test Method for Short-Beam Strength of Polymer Matrix Composite Materials and Their Laminates. (2013). West Conshohocken, PA: ASTM International.

. ASTM D638-14, Standard Test Method for Tensile Properties of Plastics. (2014). West Conshoshoken, PA: ASTM International.

. Fiber Reinforced Polymer Composite Manufacturing Workshop: Summary Report (E. E. a. R. E. A. M. Office, Trans.). (2014) (pp. 25): Department of Energy.

Al-Salem, S., Lettieri, P., & Baeyens, J. (2009). Recycling and recovery routes of plastic solid waste (PSW): A review. *Waste management, 29*(10), 2625-2643.

Al-Salem, S., Lettieri, P., & Baeyens, J. (2010). The valorization of plastic solid waste (PSW) by primary to quaternary routes: from re-use to energy and chemicals. *Progress in Energy and Combustion Science, 36*(1), 103-129.

Andræ, A., & Liu, J. (2002). Development of a generic model for life cycle inventory (LCI) of upstream processes in life cycle assessment (LCA) of electronic products. *Proceedings of the Design and Manufacture for Sustainable Development, Liverpool*, 241-253.

Andrae, A. S. (2009). *Global life cycle impact assessments of material shifts: the example of a lead-free electronics industry*: Springer Science & Business Media.

Andrae, A. S., & Andersen, O. (2011). Life cycle assessment of integrated circuit packaging technologies. *The International Journal of Life Cycle Assessment, 16*(3), 258-267.

Andrae, A. S., Zou, G., & Liu, J. (2004). LCA of electronic products. *The International Journal of Life Cycle Assessment, 9*(1), 45-52.

Arronche, L., La Saponara, V., Yesil, S., & Bayram, G. (2013). Impact damage sensing of multiscale composites through epoxy matrix containing carbon nanotubes. *Journal of Applied Polymer Science, 128*(5), 2797-2806.

Ashby, M. F. (2011). *Materials selection in mechanical design* (4th ed.). Burlington, MA: Butterworth-Heinemann.

Azapagic, A. (1999). Life cycle assessment and its application to process selection, design and optimisation. *Chemical engineering journal, 73*(1), 1-21.

Bernhard, J., Dräger, T., Grabowski, C., Sotriffer, I., & Philipp, T. (2011). *Integrating RFID in fibre-reinforced plastics.* Paper presented at the RFID SysTech 2011; 7th European Workshop on Smart Objects: Systems, Technologies and Applications; Proceedings of.

Braungart, M., McDonough, W., & Bollinger, A. (2007). Cradle-to-cradle design: creating healthy emissions–a strategy for eco-effective product and system design. *Journal of Cleaner Production, 15*(13), 1337-1348.

Cai, H., Miyano, Y., Nakada, M., & Ha, S. K. (2008). Long-term fatigue strength prediction of CFRP structure based on micromechanics of failure. Journal of composite materials, 42(8), 825-844.

Castella, P. S., Blanc, I., Ferrer, M. G., Ecabert, B., Wakeman, M., Manson, J.-A., . . . Jolliet, O. (2009). Integrating life cycle costs and environmental impacts of composite rail car-bodies for a Korean train. *The International Journal of Life Cycle Assessment, 14*(5), 429-442.

Corbiere-Nicollier, T., Laban, B. G., Lundquist, L., Leterrier, Y., Månson, J.-A., & Jolliet, O. (2001). Life cycle assessment of biofibres replacing glass fibres as reinforcement in plastics. *Resources, Conservation and Recycling, 33*(4), 267-287.

Corporation, S. A. I., & Curran, M. A. (2006). *Life-cycle assessment: principles and practice*: National Risk Management Research Laboratory, Office of Research and Development, US Environmental Protection Agency.

Das, S. (2011). Life cycle assessment of carbon fiber-reinforced polymer composites. *The International Journal of Life Cycle Assessment, 16*(3), 268-282.

Dean, A., & Voss, D. (1999). *Design and analysis of experiments*. New York: Springer.

Donaldson, J., & Francis, D. (1996). Selection of industry specific burdens for life cycle inventories. *The International Journal of Life Cycle Assessment, 1*(2), 105-109.

Dumstorff, G., Paul, S., & Lang, W. (2014). Integration without Disruption: The Basic Challenge of Sensor Integration. *Sensors Journal, IEEE, 14*(7), 2102-2111.

Haes, H. A. U., Heijungs, R., Suh, S., & Huppes, G. (2004). Three strategies to overcome the limitations of life-cycle assessment. *Journal of Industrial Ecology, 8*(3), 19-32.

Hunt, R. G., Franklin, W. E., & Hunt, R. (1996). LCA—How it came about. *The International Journal of Life Cycle Assessment, 1*(1), 4-7.

Jensen, A. A. (1998). *Life cycle assessment (LCA): a guide to approaches, experiences and information sources*: European Communities.

Jeon, J., Muliana, A., & La Saponara, V. (2014). Thermal stress and deformation analyses in fiber reinforced polymer composites undergoing heat conduction and mechanical loading. *Composite Structures, 111*, 31-44.

Jones, E. C. (2014). *Quality Management for Organizations Using Lean Six Sigma Techniques*: CRC Press.

Jones, E. C., & Chung, C. A. (2011). *RFID and auto-ID in planning and logistics a practical guide for military UID applications* (pp. 1 online resource (xxix, 392 pages)). Retrieved from http://lib-ezproxy.tamu.edu:2048/login?url=http://proquest.safaribooksonline.com/?uiCode=tamucollst&xmlId=9781420094282

Joshi, S. (1999). Product environmental life-cycle assessment using input-output techniques. *Journal of Industrial Ecology, 3*(2-3), 95-120.

Joshi, S. V., Drzal, L., Mohanty, A., & Arora, S. (2004). Are natural fiber composites environmentally superior to glass fiber reinforced composites? *Composites Part A: Applied Science and Manufacturing, 35*(3), 371-376.

Kendall, A., Keoleian, G. A., & Lepech, M. D. (2008). Materials design for sustainability through life cycle modeling of engineered cementitious composites. *Materials and Structures, 41*(6), 1117-1131.

Keoleian, G., Kendall, A. M., Lepech, M. D., & Li, V. C. (2005). *Guiding the design and application of new materials for enhancing sustainability performance: Framework and infrastructure application.* Paper presented at the MRS Proceedings.

Kumar, S., & Putnam, V. (2008). Cradle to cradle: Reverse logistics strategies and opportunities across three industry sectors. *International Journal of Production Economics, 115*(2), 305-315.

La Saponara, V., Horsley, D. A., & Lestari, W. (2011). Structural health monitoring of glass/epoxy composite plates using PZT and PMN-PT transducers. *Journal of Engineering Materials and Technology, 133*(1), 011011.

Lazarevic, D., Aoustin, E., Buclet, N., & Brandt, N. (2010). Plastic waste management in the context of a European recycling society: comparing results and uncertainties in a life cycle perspective. *Resources, Conservation and Recycling, 55*(2), 246-259.

Loyola, B. R., Briggs, T. M., Arronche, L., Loh, K. J., La Saponara, V., O'Bryan, G., & Skinner, J. L. (2013). Detection of spatially distributed damage in fiber-reinforced polymer composites. *Structural Health Monitoring, 12*(3), 225-239.

Loyola, B. R., Zhao, Y., Loh, K. J., & La Saponara, V. (2013). The electrical response of carbon nanotube-based thin film sensors subjected to mechanical and environmental effects. *Smart Materials and Structures, 22*(2), 025010.

Merilampi, S., Björninen, T., Ukkonen, L., Ruuskanen, P., & Sydänheimo, L. (2011). Embedded wireless strain sensors based on printed RFID tag. *Sensor Review, 31*(1), 32-40.

Miyano, Y., Nakada, M., & Cai, H. (2008). Formulation of long-term creep and fatigue strengths of polymer composites based on accelerated testing methodology. Journal of composite materials.

Nakada, M., & Miyano, Y. (2009). Accelerated testing for long-term fatigue strength of various FRP laminates for marine use. *Composites Science and Technology, 69*(6), 805-813.

Panda, A. K., Singh, R., & Mishra, D. (2010). Thermolysis of waste plastics to liquid fuel: A suitable method for plastic waste management and manufacture of value added products—A world prospective. *Renewable and Sustainable Energy Reviews, 14*(1), 233-248.

Patlolla, V. R., & Asmatulu, R. (2013). RECYCLING AND REUSING FIBER-REINFORCED COMPOSITES. *Environmental Research Journal, 7*(2), 145-160.

Perugini, F., Mastellone, M. L., & Arena, U. (2005). A life cycle assessment of mechanical and feedstock recycling options for management of plastic packaging wastes. *Environmental Progress, 24*(2), 137-154.

Philipp, T. R., Winkler, T., & Reinhart, G. (2013). Enhanced Production Control for Prepreg Manufacturing. *Procedia CIRP, 7*, 467-472.

Pille, C. (2010). In-Process Embedding of Piezo Sensors and Rfid Transponders into Cast Parts for Autonomous Manufacturing Logistics. *Smart Systems Integration*, 1-10.

Reap, J., Roman, F., Duncan, S., & Bras, B. (2008). A survey of unresolved problems in life cycle assessment. *The International Journal of Life Cycle Assessment, 13*(5), 374-388.

Rebitzer, G., Ekvall, T., Frischknecht, R., Hunkeler, D., Norris, G., Rydberg, T., . . . Pennington, D. (2004). Life cycle assessment: Part 1: Framework, goal and scope definition, inventory analysis, and applications. *Environment international, 30*(5), 701-720.

Schaaf, K., Cook, B., Ghezzo, F., Starr, A., & Nemat-Nasser, S. (2005). *Mechanical properties of composite materials with integrated embedded sensor networks.* Paper presented at the Smart structures and materials.

Schaaf, K., & Nemat-Nasser, S. (2008). *Optimization of sensor introduction into laminated composite materials.* Paper presented at the The 15th International Symposium on: Smart Structures and Materials & Nondestructive Evaluation and Health Monitoring.

Schaaf, K., Rye, P., & Nemat-Nasser, S. (2007). *Optimization of sensor introduction into laminated composites.* Paper presented at the Proceedings of the 2007 SEM Annual Conference and Exposition on Experimental and Applied Mechanics.

Schaaf, K. L. (2008). Composite materials with integrated embedded sensing networks.

Shim, D.-J., & Lagacé, P. A. (2005). An analytical method for interlaminar stresses due to global effects of ply drop-offs. *Mechanics of Advanced Materials and Structures, 12*(1), 21-32.

Song, Y. S., Youn, J. R., & Gutowski, T. G. (2009). Life cycle energy analysis of fiber-reinforced composites. *Composites Part A: Applied Science and Manufacturing, 40*(8), 1257-1265.

Subramanian, P. (2000). Plastics recycling and waste management in the US. *Resources, Conservation and Recycling, 28*(3), 253-263.

Suh, S. (2006). Reply: Downstream cut-offs in integrated hybrid life-cycle assessment. *Ecological Economics, 59*(1), 7-12.

Suh, S., & Huppes, G. (2005). Methods for life cycle inventory of a product. *Journal of Cleaner Production, 13*(7), 687-697.

Tang, H.-Y., Winkelmann, C., Lestari, W., & La Saponara, V. (2011). Composite structural health monitoring through use of embedded PZT sensors. *Journal of Intelligent Material Systems and Structures*, 1045389X11406303.

Timmis, A. J., Hodzic, A., Koh, L., Bonner, M., Soutis, C., Schäfer, A. W., & Dray, L. (2014). Environmental impact assessment of aviation emission reduction through the implementation of composite materials. *The International Journal of Life Cycle Assessment, 20*(2), 233-243.

Vink, E. T., Rabago, K. R., Glassner, D. A., & Gruber, P. R. (2003). Applications of life cycle assessment to NatureWorks™ polylactide (PLA) production. *Polymer Degradation and stability, 80*(3), 403-419.

Winter, S., Emara, Y., Ciroth, A., Su, C., Srocka, M. (2015). OpenLCA 1.4: Comprehensive User Manual.

Williams, E. (2004). Energy intensity of computer manufacturing: Hybrid assessment combining process and economic input-output methods. *Environmental science & technology, 38*(22), 6166-6174.

Zamagni, A., Pesonen, H.-L., & Swarr, T. (2013). From LCA to Life Cycle Sustainability Assessment: concept, practice and future directions. *The International Journal of Life Cycle Assessment, 18*(9), 1637-1641.

Biographical Information

Billy Gray was born in Dallas, Texas. During his youth he enjoyed hunting, fishing, and taking things apart. After high school, Billy learned how to weld and worked his way through his baccalaureate degree at Tarleton State University in Manufacturing Engineering Technology, graduating in 2001. While working in the aerospace industry as a manufacturing engineer, Billy attended Texas Tech University and graduated with his masters in Systems and Engineering Management through the industrial engineering department in 2006. He continued to work in aerospace eventually becoming employed as the director of operations at the age of 30. In 2011, Billy switched careers and hired on at Tarleton State University teaching in the Engineering Technology Department. He was then admitted to the University of Texas Arlington to pursue his doctorate in Industrial Engineering. His research has dealt primarily with the employment of RFID technologies and how to make the technology a viable solution in numerous problems.